UNIVERSITA' DEGLI STUDI DI MILANO

PhD School in Integrative Biomedical Research

Department of Pharmacological and Biomolecular Sciences

Curriculum: Neuroscience

New signaling pathways regulating Schwann cells of the peripheral nervous system: implications in peripheral neuropathies.

Simona Melfi

R10937

PhD School Coordinator: Prof. Chiarella Sforza

PhD Supervisor: Prof. Valerio Magnaghi

Academic Year 2016/2017

Index

Abbreviation list:

17α-HSD: 17α-hydroxysteroid-dehydrogenase
3α-HSD: 3α-hydroxysteroid-dehydrogenase
3β-HSD: 3β- hydroxysteroid-dehydrogenase
5α-R: 5α-reductase
AC: adenylate cyclase
AGO: argonaute
AKT: serine/threonine kinase 1
ALLO: allopregnanolone, 5α-pregnan-3α-ol-20-one, also named tetrahydroprogesterone
AMOTL2: angiomotin like-2
AREG: amphiregulin
AXL: AXL receptor tyrosine kinase
BDNF: brain derived neurotrophic factor
BP: biological process
BPE: bovine pituitary extract
BRN2/POU3F2: POU domain, class 3, transcription factor 2
BSA: bovine serum albumin
C-JUN: jun proto-oncogene
CA: cytosolic carbonic anhydrase
cAMP: cyclic adenosine monophosphate
Caspr: contactin associated protein
CC: cellular compartment
CCL2 or MCP-1: chemokine ligand 2
CCR: coiled-coil region
CDC42: cell division cycle
CGRP: calcitonin gene-related peptide
CMT: Charcot-Marie-tooth
CNP: 2',3'-cyclic nucleotide 3' phosphodiesterase
CNS: central nervous system
CRB: crumbs homolog
CREB-2: transcription factor 2
CTGF: connective tissue growth factor
CX32: connexin 32
CYR61: cysteine rich protein
DAPI: 40,6-diamidino-2-phenylindole
DCHS: dachsous protein
DHH: Dicer
DMEM: Dulbecco modified eagle medium
DP: dehydroprogesterone
DRG: dorsal root ganglia
EAAC1: excitatory amino acid transporter 1

E_{Cl}: equilibrium potential of Cl^- anions
EDTA: ethylendiaminetetraacetic acid
EGF: epidermal like growth factor
EMF: electromagnetic field
ERBB: tyrosine kinase epidermal growth factor receptors
ERK: RAS/RAF/MEK/ERK
ERK/MAPK: extracellular regulated MAPK/mitogen-activated protein kinase 1
FAK: focal adhesion kinase
FAT: transmembrane cadherine proteins
FBS: fetal bovine serum
FERM: 4.1 ezrin, radixin, moesin domain
GABA-A R: GABA-A receptor
GABA-B R: GABA-B receptor
GABA-T: GABA transaminase enzyme
GABA: γ-aminobutyric acid
GAD: glutamic acid decarboxylase
GDNF: glialcell line derived neurotrophic factor
GFAP: glial fibrillary acidic protein
GLI2: GLI-Kruppel family member
GO: gene ontology
GPCRs: G-protein coupled receptors
GPR126: g protein coupled receptor G6
HMN: motor neuropathies
HMSN: hereditary motor and sensory neuropathies
HPN: hereditary peripheral neuropathies
HPO: Hippo
HRS: hepatocyte growth factor-regulated tyrosine kinase substrate
HSN: sensory neuropathies
IFL: immunofluorescence
IGF-1: insulin growth factor-1
IGF-2: insulin-like growth factor 2
IL-1α and β: interleukin 1α and β
KCC2: K^+/Cl^- cotransporter
KCTD: potassium channel tetramerization domain
KO: knock out
KROX20: myelin transcription factor Egr2
L1: L1 cell adhesion molecule
LATS1/2: large tumor suppressor
LIF: leukemia inhibitory factor
LOH: loss of heterozygosity
MAG: myelin-associated glycoprotein
MAP4Ks: mitogen-activated protein kinase

MATS: mob as tumor suppressor
MBP: myelin basic protein
Merlin-1: Merlin isoform 1
Merlin-2: Merlin isofrom 2
MF: molecular fucntion
miRNAs: microRNAs
MOB1a/b: MOB kinase activator
mPR: putative membrane progesterone receptor
MRI: magnetic resonance imaging
MST1/2: serine/threonine kinase ½
mTOR: mechanistic target of rapamycin
NCAM: neural cell adhesion molecule
NF: neurofilament
NF1: neurofibromatosis type 1
NF2: neurofibromatosis type 2
Nf2: neurofibromin 2
NGF: nerve growth factor
NHERF: the solute carrier family 9, sodium/hydrogen exchanger, member 3 regulator 1
NICD: Notch intracellular domain
NKCCl: $Na^+/K^+/Cl^-$ cotransporter
NOTCH: neurogenic locus notch homolog protein
NRG1: neuregulin 1
NT3: neurotrophin 3
OCT6/POU3F: POU domain, class 3, transcription factor 1
OLs: oligodendrocytes
OPCs: OL-precursors cell
P: progesterone
P0: myelin protein zero
P450SCC: P450 cholesterol side-chain cleavage enzyme
p75NTR: nerve growth factor receptor
PAK: p-21 activated kinase
PBS: phosphate buffer saline
PDGF-B: platelet derived growth factor, b polypeptide
PDK1: 3-phosphoinositide dependent protein kianse-1
PI3K: phosphoinositide-3-kinase regulatory subunit 1
PIP2: phosphatidylinositol diphosphate
PIP3: phosphatidylinositol triphosphate
PKA: protein kinase A
PKC: protein kinase C
PLP: proteolipid protein
PMP22: peripheral myelin protein 22
PN: peripheral neuropathies

pNF: plexiform neurofibroma
PNS: peripheral nervous system
PP2: 4-amino-5-(4-chlorophenyl)-7-(dimethylethyl)-pyrazolil-[3,4-*d*]pyrimidine
RISC: RNA-induced silencing complex
SAV: salvador
SAV1: salvador family WW domain containing protein 1
SCHIP1: schwannomin interacting protein 1
SCPs: SC-precursors
SCs: schwann cells
SKP1/ASK1: E3 Ubiquitin ligase SCF complex subunit
SOX10: SRY-Box10
SOX2: SRY-Box2
SRC: non-receptor tyrosine kinase Src
SSADH: succinate semi-aldehyde dehydrogenase enzyme
TAOK1/2/3: TAO kinases
TEAD: TEA domain transcription factor
TERT: telomerase reverse transcriptase
TGF-β: transforming growth factor-β
TNF-α: tumor necrosis factor-β
VEGF: vascular endothelial growth factor
VGATs: vescicular GABA transporters
VGLL4: vestigial like family member 4
$\mathbf{V_m}$: resting membrane potential of the neuron
VS: vestibular schwannoma
Wnt: wingless
Wnt1: proto-oncogene protein 1
Wts: warts
YAP/TAZ: yes associated protein/tafazzin
Yki: Yorkie
Zeb2: zinc-finger E-box binding homeobox 2

List of figures

List of Tables

Abstract

The origin, development and maturation of Schwann cells (SCs), the main glial cells of the peripheral nervous system (PNS), are a set of complicated and intriguing processes. These multifactorial processes take place following a precise and unique coordination between different molecules and intracellular signaling, that interact with a complex of endogenous and exogenous signals. Among these, there are integrins, neuregulins, growth factors, hormones, neurotransmitters and intracellular pathway, including protein kinase A and protein kinase C (PKA and PKC), serine/threonine kinase 1 (AKT), extracellular regulated MAPK/mitogen-activated protein kinase 1 (ERK/MAPK), Hippo, mechanistic target of rapamycin (mTOR), etc.

This thesis is focused on some novel intracellular signaling pathways involved in the SCs development and maturation, from their origin to the acquisition of the myelinating or repairing phenotype.

The first part of the thesis focuses on a proto-oncogene, the non-receptor tyrosine kinase SRC (*SRC*), and the focal adhesion kinase (FAK), which are intermediate pathways known to play a role in the control of adhesion, motility, and migration of SCs. It has been investigated whether these pathways are regulated by allopregnanolone (ALLO), a neuroactive steroid of peculiar interest for the control of SCs maturation.

The second part of this thesis focuses on the study of the Hippo signaling pathway, known to be a key regulator of proliferation, apoptosis, control of organ size and crucial for cancer proliferation. Hippo pathway has been studied in SCs, where it is linked to Merlin (an oncosuppressor protein) and Yes associated protein/tafazzin (YAP/TAZ) factors. Interestingly, these mechanisms were responsive to physical and environmental challenges.

Lastly, the third part of this thesis move on studying the role of the γ-aminobutyric acid (GABA) system in the control of peripheral myelination. In particular, the whole expression profile was investigated in conditional *knock out* mice for the B1 subunit of the GABA-B receptor (GABA-B R), with a specific deletion in SCs. By the use of microarray technology, several genes resulted up- or downregulated in SCs, opening new perspectives on the possible targets downstream GABA-B R in SCs.

Overall, these results highlight new aspects of the SCs biology, shedding light on unraveled mechanisms and underlying their importance in the development and maturation of these specialized cells of the PNS. This may be of pharmacological and therapeutically interest, in order to identify reliable approaches for the treatment of PNS diseases.

Introduction

Peripheral nervous system (PNS)

The nervous system is the morpho-functional unit deputed to process internal and external stimuli and elaborate a response. It is formed by neuronal and glial cells, blood vessels and connective tissue. From an anatomically point of view the nervous system can be divided in central and PNS.

The central nervous system (CNS) is subdivided in encephalon and spinal cord. The role of the CNS is to control physiological functions, like analysis and coordination of sensory input and motor output, learning, memory and emotions. CNS cooperates with the PNS for the implementation of these functions, indeed the two systems are anatomically and functionally linked.

The most important function of the PNS is the correlation of the CNS with the periphery. PNS is able to collect the input data from the internal and external parts of the body and conduct them to the CNS through the sensitive fibers. When the information reaches the CNS, is elaborated and the response is forwarded to the periphery through the efferent (Marieb and Hoehn, 2007).

From a physiological point of view, the PNS can be divided into somatic and autonomous. The somatic PNS controls the voluntary movements, originates from the spinal cord gray matter and make contact with the skeletal muscles. The autonomous PNS, indeed, controls involuntary body responses, making contact with heart, visceral smooth muscles, blood vessels and glands. The autonomous PNS is subdivided in sympathetic and parasympathetic, both originating from the spinal cord. More in detail, the sympathetic portion originates from the turaco-lumbar tract of the spinal cord, whereas the parasympathetic originates from the cervical and sacral portions. Fundamentally, these systems exert opposite actions. The

sympathetic branches is activated under stressful conditions (the “fight or flight” response), while the parasympathetic is prevalent in resting situations (Marieb and Hoehn, 2007; Monk et al., 2015).

Peripheral nerves and dorsal root ganglia (DRG) neurons

Nerves are the anatomical structure responsible for signal conduction and are formed by fascicles of nerve fibers in the PNS. Nerves are subdivided in sensitive, motor and mixed nerves, which are the most common in the PNS. Nerve fibers are formed by two components, the axon (the cellular process originating from the neuronal soma) and the myelin sheath formed by SCs, the glial cells of the PNS, that wrap the nerves in a 1:1 ratio (Figure 1). These are myelinated fibers, characterized by a significant fast conductance. Fibers that do not present the myelin sheath are named unmyelinated fibers, and are organized in structures known as Remak bundles, in which a single SC embraces multiple axons, without myelin formation (Monk et al., 2015).

Macroscopically, a nerve appears like a white cordlike structure with a thickness between 0.2 μM and 1 cm. Peripheral nerves are formed by myelinated and unmyelinated fibers grouped to form fascicles, separated by connective laminae that also contain arterial, venous and lymphatic vessels. Single fascicles may be formed only by myelinated or unmyelinated fibers, or have both type. There are three different connective sheaths in a nerve. Single fibers are wrapped by a sheath called endoneurium; group of fibers are enveloped by the perineurium, while the epineurium ensheaths the whole nerve (Marieb and Hoehn, 2007).

In adult nerve the endoneurium is linked to the basal lamina and surround the axon-SC unit, forming a stable structure where nerve fibers are sustained and protected by collagen and vascularized extracellular matrix. Moreover, the perineurium, is a

multilayer cellular tube that protect the endoneurium and the nerve fibers from exogenous cells and molecules (Marieb and Hoehn, 2007). Around E16 in rat (E14 in mouse), the compact structure changes fast, the extracellular spaces containing collagen appear within the nerve and fibroblast and blood vessels appear; SCs basal lamina starts its formation, and it becomes evident the perineurial sheath (Peltonen et al., 2013). Contacts between axons and glia at the nodes of Ranvier are established by SCs microvilli, which are enriched in F-actin (Oguievetskaia and Goutebroze, 2006).

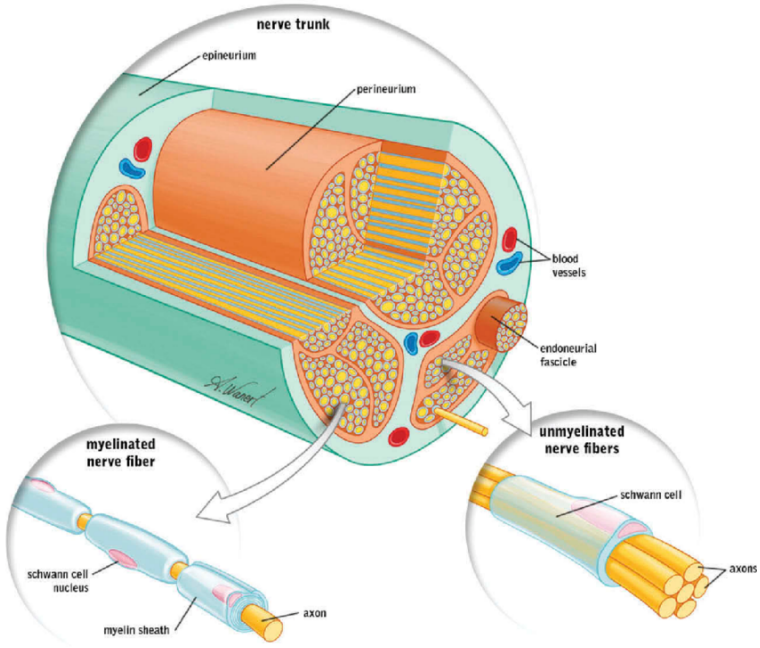

Figure 1 Nerve anatomy.

The cell bodies of neurons forming the motor/effector nerves are located in the ventral horns of the spinal cord. Sensitive nerves cell bodies, indeed, are grouped in anatomical structures called DRG, located outside the spinal cord, paravertebral to the spinal column (Figure 2).

DRG are formed by pseudounipolar neurons, presenting a single axon originating from the soma that divides in a "T" shape, respectively in a peripheral and central branch.

The peripheral branch represents the afferent fiber, which collect information from the periphery, while the central branch projects to the dorsal horn of the spinal cord. In the DRG the neuronal soma is surrounded by satellite cells, a particular type of glial cells. They are homologous to SCs and their function is to give structural and biochemical support to DRG neurons (Hanani, 2005).

As better detailed below, SCs in the PNS are deputed to the formation of the myelin sheath, and are fundamental in the development of the PNS (Feltri et al., 2016), SCs are important for the complex cross-talk with neurons (Faroni et al., 2014b; Salzer, 2015; Taveggia, 2016), and address the nerve regeneration process following an injury (Glenn and Talbot, 2013; Faroni et al., 2015).

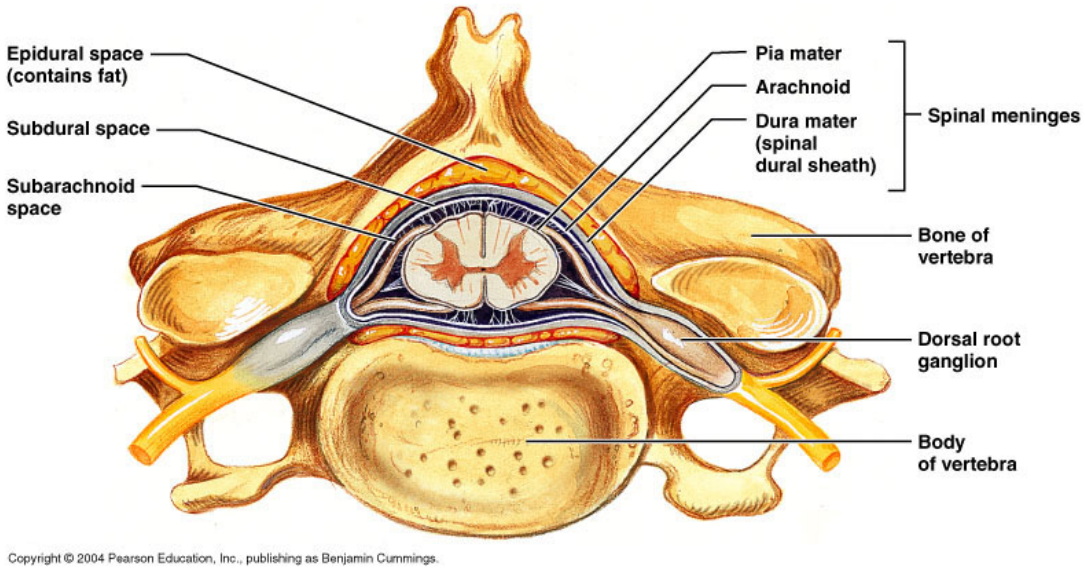

Figure 2 Cross-sectional anatomy of the spinal cord.

Schwann cell origin, development and myelination

SCs derive from the migratory cells of the neural crest in a well-defined sequence of events (Figure 3). During early vertebrate development, neural crest cells delaminate from the dorsal-most region of the neural tube and these progenitor cells are migratory and proliferative. They migrate throughout the embryo to originate to different cell types, including cardiac cells, melanocytes, skeletal and connective tissue components of the head, neurons and glia of the PNS (Monk et al., 2015). SCs derive from ventrally migrating neural crest cells, like sympathetic neurons and DRG neurons (Le Douarin and Teillet, 1973).

Most SCs arise from neural crest derived SC precursors (SCPs), these, like neural crest cells, are migratory and proliferative. SCPs co-migrate with axons in the developing PNS and are dependent upon axonal signals for survival (Dong et al., 1995). SCPs are the cells representing the first stage of the SC lineage (Jessen et al., 2015).

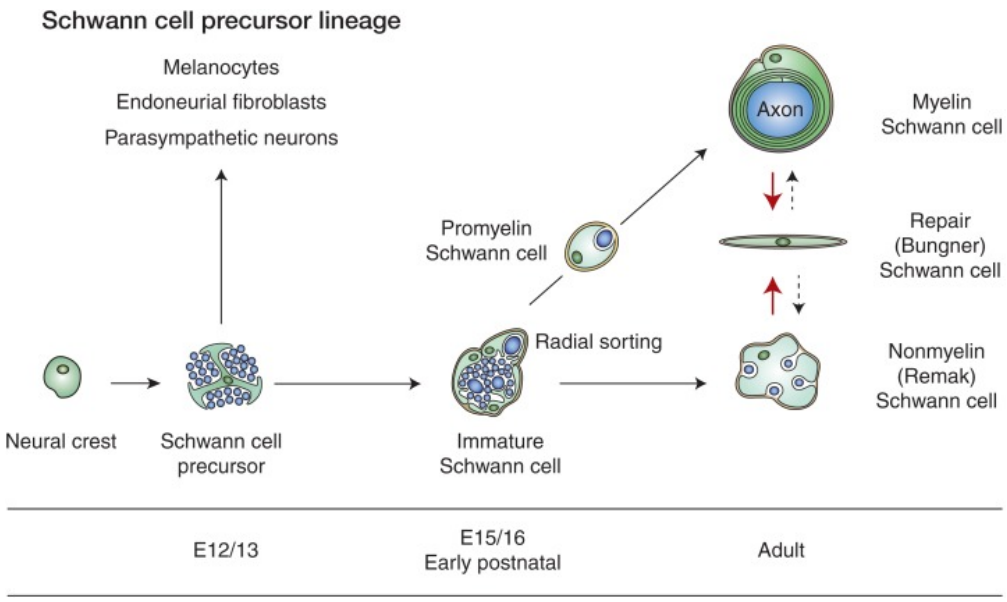

Figure 3 Schwann cell lineage – *"Schwann Cells: Development and Role in Nerve Repair" Jessen KR, Mirsky R, Lloyd AC - Cold Spring Harb Perspect Biol. 2015.*

At E16, SCPs differentiate to immature SCs. By E18 in rat (E16 in mouse), nerves are formed of axon-SCs bundles embedded in extracellular matrix containing collagen and blood vessels. SCPs disappear from developing nerves when immature SCs and fibroblast appear (Wanner et al., 2006). SCPs show different phenotype from neural crest cells and immature SCs, because they express glial differentiation markers and other factors and respond differently to survival, proliferation and differentiation signals (Jessen and Mirsky, 2005; Woodhoo and Sommer, 2008). Furthermore, SCPs and immature SCs are different also in term of molecular expression, since the increase in S100 (a specific marker of SCs) mRNA levels is the characteristic of the immature SCs. Moreover, also the survival regulation is different. In fact, SCPs are acutely dependent on the axon-associated survival signal neuregulin 1 (NRG1) type III. NRG1 is neuronal epidermal like growth factor (EGF), interacting with its tyrosine kinase epidermal growth factor (ERBB) receptors, that are key regulators of myelination (Chen et al., 2003, 2006; Michailov et al., 2004; Taveggia et al., 2005). NRG1/ERBB signaling is the main determinant of SC development, mediating the activation of the phosphoinositide-3-kinase regulatory subunit 1 (PI3K) pathway and leading to the phosphorylation of 3-phosphoinositide dependent protein kinase-1(PDK1), which in turn converts phosphatidylinositol diphosphate (PIP2) to phosphatidylinositol triphosphate (PIP3), then activating AKT (Castelnovo et al., 2017). NRG1 is also expressed on axons, embryonic DRG and motor neurons, suggesting that either the survival of SCPs, the generation of SCs or the myelination are crucially dependent on axonal NRG1. Moreover, other factors like the neurogenic locus notch homolog protein (NOTCH) are important for SCs. Notch is a transmembrane receptor which is activated from ligand, is cleaved and form an intracellular domain (NICD), that acts like a

transcriptional regulator (Boerboom et al., 2017). Notch controls SC proliferation and promotes the generation of immature SCs from SCPs *in vivo* but can acts also as a negative regulator of myelination. NOTCH activation and/or over-activation leads to premature or delayed myelin formation, respectively. The inhibition of NOTCH signaling in adult mice delayed myelin breakdown following a nerve lesion (Woodhoo et al., 2009). NOTCH, and JAGGED 1 (an activator of NOTCH), are expressed on embryonic axons and also present in SCPs. In mice with genetic ablation of *Notch*1, SC generation from precursors is delayed, whereas SCs appear more rapidly in mice where NOTCH signaling is enhanced (Woodhoo et al., 2009). Moreover, *Notch*, in rat nerves after injury improves nerve regeneration and functional recovery (Wang et al., 2015).

SCPs may also control nerve fasciculation and are implicated in the survival of developing DRG and motor neurons (Jessen et al., 2015). Glial cells are determinant on establishing nerve architecture, indeed they confer to the axons the capability to elongate correctly for long distances, creating group of axons that originate nerve fibers. From E15/16 or E17/18, respectively in mice and rats, SCPs start to differentiate in SCs. SCs envelop groups of axons, forming irregular axon/SCs columns, which are covered by the basal lamina and surrounded by extracellular matrix (Webster et al., 1973). Some days later (E19/20 in mice and E21 in rats), the process of radial sorting starts and single axons become individually ensheathed by SCs. This event is a prerequisite for the myelination process, that takes place in case of large axons (Jessen et al., 2015).

By the radial sorting process, SCs separate axons destined to become myelinated from those that will remain in non-myelinated Remak bundles. Moreover, SCs send signal to perineurial cells and other nerve components to promote their differentiation. These

events lead to the formation of the mature final nerve (myelinated fibers and Remak bundles), surrounded by extracellular matrix and blood vessels (Monk et al., 2015).

During the embryogenesis, the conversion from SCPs and immature SCs is accompanied by an increase in proliferation, which in turn is correlated to an intracellular cyclic adenosine monophosphate (cAMP) level increase (Stewart et al., 1993; Chernousov et al., 2008). The increase in cAMP levels is due to the interaction between G-protein coupled receptors ($GPCR_s$) and specific agonist; the activation of a $G\alpha_s$ protein (stimulatory), activates the adenylate cyclase (AC), determining a signal transduction cascade which increase cAMP levels (Arthur-Farraj et al., 2011; Mogha et al., 2013).

SCs proliferation *in vivo* is driven by axon-associated signals, for example NOTCH and NRG1, soluble signals, such as transforming growth factor-β (TGF-β) and signals derived from the basal lamina, such as laminin. In particular, laminin is the principal component of the basal lamina, linking SCs through an interaction with dystroglycan and β1 integrin receptor. Laminin promotes SC proliferation *in vivo*, indeed the lack of the cell division cycle 42 (CDC42), the downstream effector of the β1 integrin, reduces proliferation of immature SCs (Feltri et al., 2008).

SCs possess NOTCH receptors and axons show the presence of NOTCH ligands. Interestingly, NOTCH is a potent inducer of SCs division *in vitro*, indeed, in neonatal nerve, NOTCH signaling inactivation results in a substantial reduction in DNA synthesis and SCs numbers (Woodhoo et al., 2009). These findings demonstrate that NOTCH signaling, drives SCs proliferation in developing nerves (Woodhoo et al., 2009). TGF-β is another important factor that regulates SCs proliferation. TGF-β stimulates SCs proliferation in culture, even though, in some other conditions induces apoptosis (Ridley et al., 1989; Einheber et al., 1995; Parkinson et al., 2001). TGF-β is

able to drive SC division in perinatal nerves (D'Antonio et al., 2006). The function of TGF-β may be to amplify the proliferation of cells with tight axonal contact, or to suppress supernumerary cells with less effective axonal affiliation (D'Antonio et al., 2006).

SC survival changes rapidly when SCs modify their phenotype from SCPs to SCs. Survival of SCPs depends on axon-associated signals (Dong et al., 1995), whereas immature SCs, even in embryonic nerves, bypass this strict axon dependence by the intervention of autocrine survival circuits, including insulin-like growth factor 2 (IGF-2), neurotrophin 3 (NT3), platelet derived growth factor, b polypeptide (PDGF-B), leukemia inhibitory factor (LIF), and lysophosphatidic acid (Jessen and Mirsky, 2005). *In vitro*, cell survival is density dependent, and SCs population survives upon the loss of axonal contact in damaged nerves.

Notably, injury increases SC apoptosis in neonatal nerves but also in the adult (Grinspan et al., 1996; Syroid et al., 2000), suggesting a persistent but decreasing contribution of axonal signals to SC survival. After longer periods, however, most of the SCs not in contact with injured nerves die (Höke, 2006; Sulaiman and Gordon, 2009).

There are different types of peripheral nerve injury. The axonotmesis where the axons are disrupted but the connective tissue and the SCs containing basal lamina tubes remain intact. The neurotmesis, in which axons, connective sheaths and basal lamina tubes are interrupted (Figure 4). Functional recovery after nerve cut is generally incomplete, especially in human. The reason is ascribed to targeting errors made by regenerating axons between the proximal and distal nerve stumps, leading to incorrect target innervation (Witzel et al., 2005; Höke, 2006). Distal to the injury the axons die, triggering a series of events involving SCs, macrophages, and other cells. This

process, called “Wallerian degeneration”, is complex and build up a specific environment to support the survival of injured neurons, axon regrowth and guidance (Chen et al., 2007; Allodi et al., 2012).

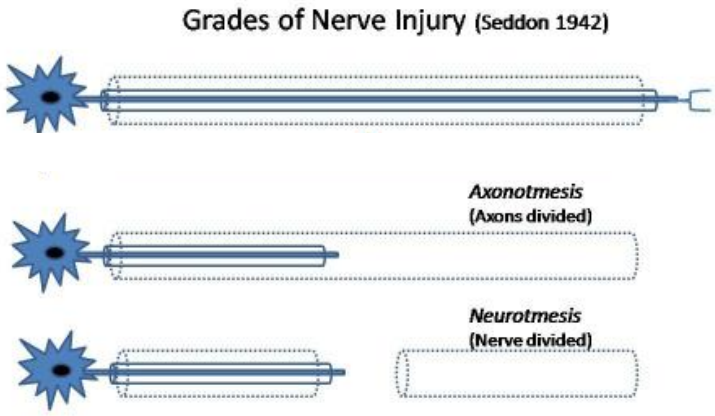

Figure 4 Types of peripheral nerve injury. *From the top to the bottom, a peripheral nerve without damage, the axonotmesis, where only the axon is disrupted, and the neurotmesis where the axon, connective sheath and basal lamina tube are interrupted. (Seddon, 1942).*

The regeneration process depends on SCs plasticity during the repair process. The injury-induced changes in SCs during Wallerian degeneration has been characterized as a kind of dedifferentiation (Chen et al., 2007), although they are commonly described as a kind of activation (Armstrong et al., 2007; Campana, 2007; Webber and Zochodne, 2010; Allodi et al., 2012). Early after the injury, SCs response to the axonal interruption and rapidly develop radical phenotypic changes. This suggest that injured axons alert SCs of axon death, even though the mechanism behind this process should be further elucidated (D’Antonio et al., 2006; Martini et al., 2008). The first step consists of the reversion of the myelin differentiation process. In fact, molecules like L1 cell adhesion molecule (L1), neural cell adhesion molecule (NCAM), nerve growth factor receptor (p75NTR), glial fibrillary acidic protein (GFAP), that characterize SCs before

myelination, are down-regulated. Also other myelin associated genes are decreased, for example the key myelin transcription factor *Egr*2 (KROX20), enzymes of cholesterol sysnthesis, structural proteins such as myelin protein zero (P0), myelin basic protein (MBP), and membrane-associated proteins like myelin-associated glycoprotein (MAG) and periaxin (Jessen and Mirsky, 2008). In this context, the SCs present an increased expression of some neurotrophic factors such as glial cell line derived neurotrophic factor (GDNF), artemin, brain derived neurotrophic factor (BDNF), Nt3, nerve growth factor (NGF), vascular endothelial growth factor (VEGF), and pleiotrophin, that promote the survival of injured neurons and axonal elongation (Fontana et al., 2012; Brushart et al., 2013). Moreover, in the distal stump, the SCs upregulate the expression of cytokines including tumor necrosis factor (TNF)-α, LIF, interleukin (IL)-1α and β, and chemokine ligand 2 (CCL2 or MCP-1), which need to recruit macrophages. Furthermore, SCs activate a myelin breakdown through an autophagic process. All together, these events promote the nerve repair through the activation of different pathways.

The formation of regeneration tracks is an important component of the SCs-activated injury response. The SCs flattened around axons and adopt an elongated bipolar morphology, allowing them to align and constitute a SCs column, that forms track from the injury site to the nerve target areas. Recently it was proposed that the repairing program originate a novel SCs phenotype, specifically committed to participate to the nerve repair, the so-called “repair SCs”. This conversion, from immature SCs to repair SCs is regulated by the transcription factor c-jun, activated in SCs of injured nerves (Arthur-Farraj et al., 2012).

The GABA-ergic system in the PNS

GABA is the main inhibitory neurotransmitter in the mature nervous system. GABA is synthesized from glutamate by two glutamic acid decarboxylase (GAD) enzymes of different molecular weight: GAD67 and GAD65 (Pinal and Tobin, 1998). GAD67 is localized in the cytoplasm, mostly in the neuronal soma, and it provides basal level of GABA synthesis. Conversely, GAD65 is preferentially located in the axonal terminal and it provides additional supply of GABA in condition of metabolic need (Asada et al., 1997; Kash et al., 1997; Namchuk et al., 1997). When GABA is synthesized, vescicular GABA transporters (VGATs) are embedded in presynaptic vescicular membranes and use the electrochemical gradient to shuffle and pack GABA into small synaptic vesicles (Roth and Draguhn, 2012). Upon fusion of the synaptic vesicles to the cell membrane, due to incoming action potentials, GABA is released in the synaptic cleft where it interacts with ionotropic GABA-A, GABA-C, or metabotropic GABA-B Rs. Finally, the catabolism of GABA depends on GABA transaminase enzyme (GABA-T) and succinate semi-aldehyde dehydrogenase enzyme (SSADH), which convert GABA into intermediates of the Krebs cycle and substrates for new glutamate synthesis. Like other neurotransmitters in the CNS, GABA is produced and released also by glial cells, mainly astrocytes. In the hippocampus, for example, GABA released by astrocytes regulates neuronal activity and tonic inhibition (Jow et al.; Liu et al., 2000). Furthermore, in the developing CNS, mechanism involving the activation of GABA receptors influence different processes such as neuronal or glial precursor proliferation, differentiation, and migration (Barres et al., 1990; al-Dahan and Thalmann, 1996; Ben-Ari, 2002; McCarthy et al., 2002; Owens and Kriegstein, 2002).

Recently, SCs were shown to express a functional GABAergic system that can participate in the control of SC development and myelination (Magnaghi et al., 2004b, 2006a), but also in the regulation of the sensory and nociceptive functions (Procacci et al., 2012; Faroni et al., 2014a).

The GABA-A and GABA-B Rs

GABA-A ionotropic R (GABA-A R) is a ligand-gated ion channel. In the adult CNS, upon activation, the GABA-A receptor selectively produce an inward flux of Cl^- resulting in the hyperpolarization of the neuron. This causes an inhibitory effect on the neurotransmission, diminishing the chance of a successful action potential occurrence. The reversal potential of the GABA-A-mediated inhibitory postsynaptic potential (IPSP) is -70 mV. The magnitude and direction of the ionic current through GABA-A Rs depends on its driving force, defined as the difference between the electrochemical equilibrium potential of Cl^- anions. Depending by a positive or negative difference, a flux of Cl^- anions through the plasma membrane may occur. This determines a change in the membrane potential of the neuron.

In neurons, two main chloride cotransporters are responsible for setting intracellular Cl^- concentration $[Cl^-]_i$. The $Na^+/K^+/Cl^-$ cotransporter NKCCl (Blaesse et al., 2009), which imports Cl^- into the neuron, and the K^+/Cl^- cotransporter KCC2, which exports Cl^- out (Rivera et al., 1999; Sernagor et al., 2010; Kahle et al., 2013). When the equilibrium potential of Cl^- anions (E_{Cl}) is close to the resting membrane potential of the neuron (V_m), GABA will exert its inhibitory action by a shunting inhibitory mechanism. Indeed, the local increase in membrane GABA-A Rs conductance will "hold" the neuron at the E_{Cl}, reducing the amplitude of subsequent excitatory

postsynaptic potentials (following Ohm's law) and thus shunting any excitatory input (Gonzalez-Burgos et al., 2011).

The Cl^--extruding K^+-Cl^- cotransporter KCC2, and the cytosolic carbonic anhydrase (CA) isoform CAVII control the efficacy and qualitative nature of GABAergic transmission during development (Rivera et al., 1999). In rat hippocampal pyramidal neurons, a step up-regulation of KCC2 accounts for the "developmental switch", which converts depolarizing and excitatory GABA responses of immature neurons to classical hyperpolarizing inhibition, by the end of the second postnatal week. Around postnatal day 12 (P12), a consistent increase in intrapyramidal CAVII expression takes place, promoting excitatory responses evoked by intense GABAergic activity (Rivera et al., 1999).

GABA-A R present binding sites for GABA and other specific molecules such as muscimol (GABA-A R agonist), gaboxadol (GABA-A R agonist), and bicuculline (GABA-A R antagonist). However the receptor contains a number of different allosteric binding sites, which indirectly modulate the activity of the receptor. The allosteric sites are targets of various other drugs including, benzodiazepines, neuroactive steroids (discussed below), barbiturates, ethanol, anesthetics and picrotoxin (Figure 5).

Nineteen genes encoding for different GABA-A subunits have been identified: α1–α6, β1–β3, γ1–γ3, δ, ε, π, θ, ρ1–ρ3. The subunit composition of major GABA-A Rs is 2α/2β/ϒ (the last being sometimes substituted by δ or ε) (Boileau et al., 2005), although also the existence of other receptor combination was expected (Jones and Henderson, 2007). Functional GABA-A Rs, with the pharmacological profile of native receptors, are formed by pentameric assembly of $2\alpha/2\beta/\Upsilon_2$, where the α and β subunits can be either identical or different. The Υ_2 subunit can be substituted by ϒ1 or ϒ3 subunits

(present et low levels and/or with a restricted expression pattern) or by δ, and possibly ε, subunits (Fritschy and Panzanelli, 2014).

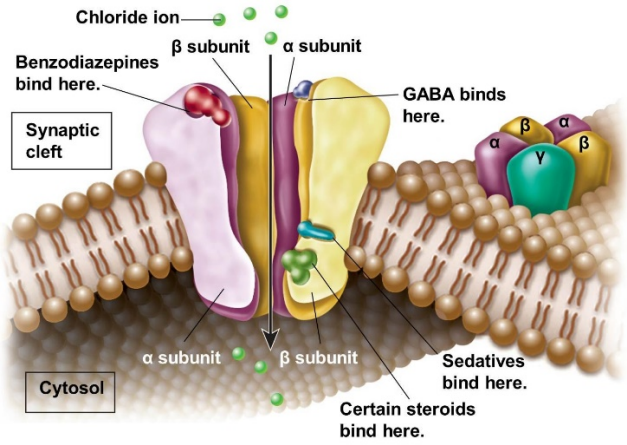

Figure 5 GABA-A R structure - https://www.organicnewsroom.com/gaba-supplement/

GABA-A Rs can be distinguished in classical 'phasic' GABA-A Rs (responsible for synaptic current) and 'tonic' GABA-A Rs, usually extra-synaptic receptors activated by low concentrations of local GABA. Extra-synaptic GABA-A Rs are composed of receptor subunits that generate persistent inhibition, and are pharmacologically and functionally distinct from their synaptic counterparts (Belelli et al., 2009).

Therefore, GABA-A Rs are classified in synaptic and extra-synaptic (depending on their cellular localization). The synaptic one is located at the post-synaptic terminals and mediate the classic phasic inhibition upon GABA release from pre-synaptic terminals. The post-synaptic one is localized beside synaptic position, and are responsible for tonic GABA-A inhibition (Belelli et al., 2009; Reddy, 2011).

In general, α1, α2, α3 and γ2 subunits typically form synaptic receptors, while α4, α5, α6 are typical extra-synaptic receptor subunits, with the γ2 subunit often substituted by δ (Fritschy and Panzanelli, 2014). The β subunits composition is not particularly

indicative of the synaptic or extra-synaptic nature of the receptor. Although that GABA-A R with δ subunit is mostly extra-synaptic, not all extra-synaptic receptors present the δ subunit (Belelli et al., 2009).

The GABA-B R was initially identified by Bowery and colleagues in the 80's. It is a transmembrane metabotropic receptor for GABA that is not responsive to the GABA-A R antagonist bicuculline, evidencing a different structure. GABA-B R is specifically activated by GABA and baclofen but it is not coupled to Cl^- channels, or responsive to barbiturates or benzodiazepines. The GABA-B R is a GPCR, which activation induces the activation of a G_i/G_0 protein, generally linked to the AC enzyme, therefore its activation induces an inhibition and the reduction of cAMP levels, with decrease of PKA activity. As a consequence, the GABA-B may give a reduction of the phosphorylation levels of PKA-dependent transcription factors (Steiger et al., 2004) and kinases (Gassmann and Bettler, 2012). It can also stimulates the opening of the K+ channels which brings the neuron closer to the equilibrium potential of K+. This reduces the frequencies of action potentials, in turn reducing neurotransmitter release. Moreover, GABA-B R can also reduce cell Ca^{2+} conductance.

GABA-B Rs are present at pre- and post-synaptic level. At the pre-synaptic level play an important role in the regulation of the release of other neurotransmitters, including GABA itself, therefore are called auto-receptors; when localized on other terminals they are called hetero-receptors (Gassmann and Bettler, 2012). Two subtypes of GABA-B R, called GABA-B1 and GABA-B2 have been identified (Jones et al., 1998; Kaupmann et al., 1998; White et al., 1998; Kuner et al., 1999) (Figure 6). The B1 has been characterized in 3 different isoforms, B1 a,b and c (Kaupmann et al., 1997; Gassmann and Bettler, 2012) by different groups. Different studies demonstrated that the

heterodimer GABA-B1/GABA-B2, within the two subunits in a 1:1 stoichiometric ratio, is the active form (Charles et al., 2003). The GABA-B1 subunit is responsible for binding GABA and other specific ligands, while GABA-B2 is responsible for the receptor functions, for the co-regulation of some transcription factors [eg. activating transcription factor 2 (CREB-2)] and for the interaction with auxillary subunits belonging to the potassium channel tetramerization domain (KCTD) family, which bind to GABA-B2 on the cell surface (Charles et al., 2003; Gassmann and Bettler, 2012). The interaction of the two subunits takes place at the carboxyl-terminal domains, leading to the formation of a α-helix coiled coin structure.

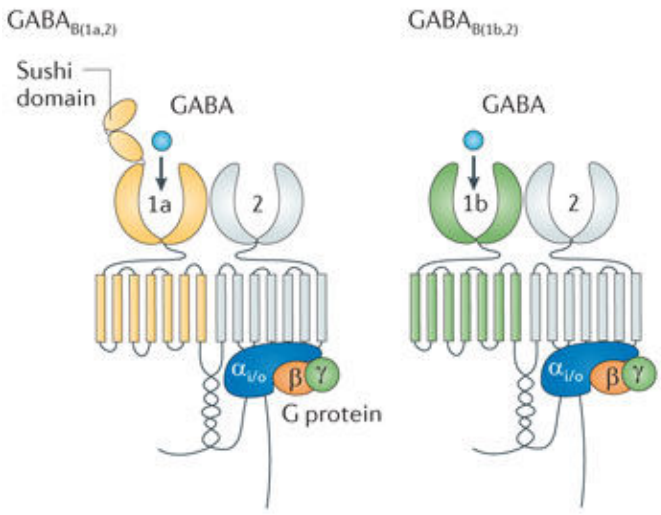

Figure 6 GABA-B R structure "Regulation of neuronal GABA-B receptor functions by subunit composition" *Gassmann M, Bettler B - Nature Reviews Neuroscience 2012*

GABA-B Rs are present in the neuronal compartment of the spinal cord white matter (Margeta-Mitrovic et al., 1999; Charles et al., 2001) and their expression is higher in the laminae I–IV of the dorsal horn (Price et al., 1987; Towers et al., 2000), where it co-localize with GAD enzymes and primary afferent fibers (Barber et al., 1978; Todd and Lochhead, 1990; Waldvogel et al., 1990). GABA-B R isoforms were also found

in pig nodose ganglion cells, in autonomic nerve terminals, in peripheral axons and in rat DRG (Bowery et al., 1981; Towers et al., 2000; Zagorodnyuk et al., 2002). Different studies confirmed the presence of GABA-B R not only in the neuronal, but also in the glial compartment (Kuhn et al., 2004; Kozlov et al., 2006; Serrano et al., 2006; Luyt et al., 2007).

The role of the GABA Rs in the PNS

First observations in the 80's demonstrated that in the PNS, myelinated and unmyelinated fibers, possess GABA Rs and GABA carriers (Brown and Marsh, 1978; Brown et al., 1979; Morris et al., 1983; Olsen et al., 1984). In the 1984, Gavrilovic and colleagues, demonstrated the uptake of GABA by high-affinity mechanism, in purified SCs maintained in cell culture *in vitro* for up to six months (Gavrilovic et al., 1984).

Recently, the presence of GABA-A and B Rs has been shown in PNS, particularly in the SCs, which possess the functional receptors and are able to synthesize GABA (Magnaghi et al., 2010). In the sciatic nerve of adult male rats were α2, α3, β1, β2 and β3 and SCs showed similar expression levels. The mRNA studies were confirmed with immunohistochemical analysis on rat SCs. The presence of GABA-B isoforms 1a, 1b, 1c and 2 mRNAs, was demonstrated not only in the brain (Margeta-Mitrovic et al., 1999; Towers et al., 2000; Charles et al., 2001) but also in the sciatic nerve and in the SCs (Magnaghi et al., 2004b, 2008a).

The GABAergic system is implicated in the regulation of the myelination process. It has a physiological role in SCs, influencing the expression of myelin protein. For example, peripheral myelin protein 22 (PMP22), which is one of the most important proteins required for the maintenance of the multilamellar structure of the peripheral myelin (Quarles, 1997; Bronstein, 2000). May be under the control of the GABA-A R.

In fact, it has been demonstrated that a prolonged exposure of SCs to the GABA-A agonist muscimol, in the range of micromolar concentration, exerted a stimulatory effect on the mRNA level of PMP22 (Magnaghi et al., 2001; Melcangi et al., 2005). This might be of pharmacological interest, since alterations in the gene encoding for the PMP22 are associated with a set of hereditary peripheral neuropathies, for example the Charcot-Marie-Tooth type – 1A (see below) (Naef and Suter, 1998)

SCs cultures, the GABA-B R is negatively coupled to the AC system (Magnaghi et al., 2004a), in fact baclofen (GABA-B R specific agonist) counteracted the forskolin (a cAMP- inducing agent) -induced proliferation of SCs *in vitro* and control the mRNA levels of specific peripheral myelin proteins, such as glycoprotein P0, PMP22, myelin MAG and Connexin32 (CX32) (Magnaghi et al., 2004a).

The importance of the GABAergic system in the peripheral myelination emerges also from *in vivo* studies. Mice with an ablation of the B1 subunit of the GABA-B R show an increase in the P0 and PMP22 levels, nerve with smaller fibers and thinner myelin sheaths with and increased number of fibers with small axons and irregular profiles. These mice have an increased number of calcitonin gene-related peptide (CGRP)-positive fibers and decreased number of neurofilament (NF)-200-positive fibers in peripheral nerves. Moreover, the nerve cell bodies of lumbar DRG are smaller in GABA-B1 -/- mice. The total *knock out* mice show also a gait alterations and signs of hyperalgesia, without allodynia (Magnaghi et al., 2008b).

Interestingly, GABA-B Rs may regulate myelination and nociception in the PNS, through the important contribution of the glial compartment. In fact *conditional knock out* mice, bearing the deletion of the B1 subunit of the GABA-B R, only in SCs, present signs of SCs degeneration, tomacula, fractured myelin and partial uncompaction of

myelin. These mice present also an increase in the number of irregular fibers, suggesting a SCs-autonomous modulatory action of GABA-B1 (Faroni et al., 2014a). The deletion of the receptor in SCs can affect also the neuronal compartment demonstrating also signs of SCs non-autonomous mechanism. Indeed, number and size of small fibers were changed with an increase in small unmyelinated axons. These mice also shown an altered pain sensitivity with signs of hyperalgesia and allodynia (Faroni et al., 2014a).

Neuroactive steroids

The first observation on the existence of neuroactive steroids comes from the 80's, when the novel concept that hormonal steroids may be synthesized *de novo* or metabolized in the nervous system, was introduced. In the 1997, Baulieu and colleagues coined the term "neurosteroids" in order to define these molecule (Baulieu, 1997). The central and peripheral glial cells, which are fundamental for the regulation of neuronal activity, are also able to synthesize neurosteroids (Celotti et al., 1992; Melcangi et al., 2001). Glial cells possess the complex machinery required for the production of steroids: the P450 cholesterol side-chain cleavage enzyme (P450SCC), the 17α-hydroxysteroid-dehydrogenase (17α-HSD), the 3β- hydroxysteroid-dehydrogenase (3β-HSD) and some others. These cells also convert them into neuroactive metabolites (Mellon et al., 2001). Indeed, the enzymatic complex formed by the 5α-reductase (5α-R) and the 3α-hydroxysteroid-dehydrogenase (3α-HSD) enzymes deputed to convert the native steroids into the 5α3α active metabolites, has been characterized in several areas of the mammalian brain (Steckelbroeck et al., 2001) and in the PNS (Melcangi et al., 1990, 1992, 1999; Celotti et al., 1992)

Evidences from the literature show that the metabolism of neuroactive steroids may be relevant for the differentiation of glial cells (Gago et al., 2004). The presence of 5α-R-3α-HSD enzymatic complex in oligodendrocytes (OLs) and SCs suggests that the locally formed neuroactive steroids might play a crucial role in the process of myelination (Melcangi et al., 1988, 2001; Martini et al., 2003)

The 5α-pregnan-3α-ol-20-one, also named tetrahydroprogesterone or ALLO is the main hormonal steroid that was originally shown to act as neurosteroids. It is synthesized through the action of the 5αR-3α-HSD, which converts progesterone (P) into dehydroprogesterone (DHP) and subsequently, via a bidirectional reaction, into ALLO. The ALLO actions on the neuronal compartment were demonstrated, although other observations suggested important roles for ALLO also in glial cells.

ALLO is a potent modulator of the GABA-A R (Lambert et al., 1995). In fact, the most important "non-classic", non-genomic action of neuroactive steroids is represented by ALLO's activation of GABA-A R (Lambert et al., 2003). The mechanism of action on GABA-A receptor is concentration dependent. In a low nanomolar concentration ALLO acts allosterically, enhancing the action of the natural ligand GABA, while at higher concentration (micromolar range) ALLO directly gates the GABA-A R channel complex (Puia et al., 1990). Interestingly, neuroactive steroids might also influence the activation of the GABA-A R acting indirectly, for example, on the regulation of its subunits (Maguire and Mody, 2009). ALLO is also able to interact with protein kinase or phosphatases, which in turn act on GABA-A subunits altering the entire receptor functions (Belelli and Lambert, 2005). Furthermore, the phosphorylation of GABA-A R by PKC influences the sensitivity to neuroactive steroids (Vergnano et al., 2007).

Neuroactive steroids proved particularly active in the PNS. Progestagens stimulate the expression of specific peripheral myelin proteins, such as P0 and the PMP22, in the sciatic nerve of rats (Melcangi et al., 2000; Magnaghi et al., 2001), they reduce myelin abnormalities and fibers loss in aged sciatic nerve (Azcoitia et al., 2003), and promote re-myelination after a lesion (Melcangi et al., 2000).

In particular, ALLO is one of the most important neuroactive steroids involved in these actions, likely through autocrine mechanisms (Figure 7). ALLO controls the expression of different GABA-B R subunits, via a GABA-A mediated mechanism (Magnaghi et al., 2006b; Magnaghi, 2007). GABA-B subunits expression may be differently influenced, by ALLO either via a GABA-A-mediated mechanism, or by its precursors P and/or DHP after 5α-R-3α-HSD conversion into ALLO (Faroni and Magnaghi, 2011). Moreover, acting through an autocrine loop, ALLO increased the levels of GAD67 in SCs, thus stimulating GABA synthesis and providing the natural ligand for GABA-A R (Magnaghi et al., 2010). This hypothesis was corroborated by the observation that SCs possess functionally active glutamate uptake system, able to provide glutamate as a precursor for the GABA synthesis (Perego et al., 2012). SCs, in fact, possess the excitatory amino acid transporter 1 (EAAC1) in the plasma membrane and in intracellular vesicular compartments of the endocytic recycling pathway.

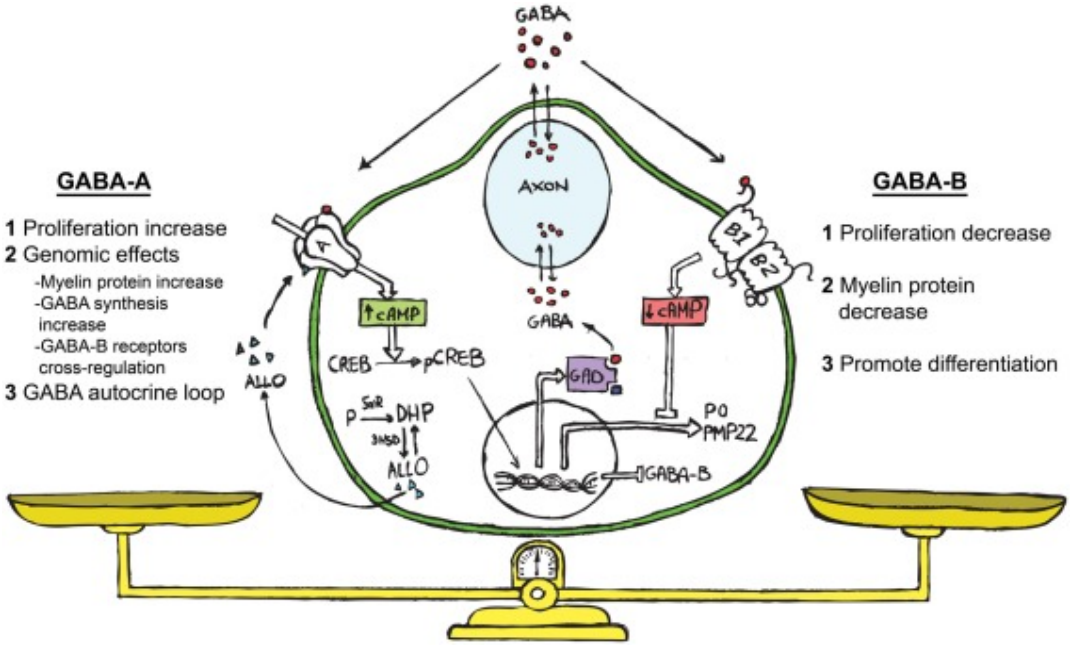

Figure 7 Schematic representation showing ALLO, GABA and its receptors acting in a bidirectional cross-talk between neurons and SC. *GABA, comes from neurons or produced directly by SC affect the paracrine cross-talk between these cells. Extracellular GABA acts on GABA-B Rs on the SCs surface, decreasing their proliferation, leading to a decrease in cAMP levels and a reduction in myelin protein expression, prompt the SCs to start the differentiation. ALLO, allosterically activates the GABA-A R on the SC surface. This modulate the expression and the responsiveness of the GABA-B R, and in turn its desensitization. Meanwhile, ALLO stimulates the SC proliferation inducing other genomic effects such as the increase of myelin proteins and the increase of GAD enzymes levels. This trigger an autocrine mechanism involving enhanced cAMP levels and PKA pathway. The balance of GABA-A or GABA-B Rs on SCs, by ALLO and GABA, starts an autocrine loop relevant for the control of SC proliferation and differentiation. (Faroni and Magnaghi, 2011).*

The SRC/FAK pathway in the PNS

Proto-oncogene tyrosine-protein kinase SRC is a non-receptor tyrosine kinase protein encoded by the *SRC* gene in humans. The SRC protein is a tyrosine-protein kinase whose activity can be inhibited by phosphorylation of its terminal. An elevated level of SRC tyrosine kinase is suggested to be linked to cancer progression by promoting other signals. SRC and SRC-family protein-tyrosine kinases are regulatory proteins that play key roles in cell differentiation, motility, proliferation, and survival.

From the N- to C-terminus, SRC contains an N-terminal 14-carbon myristoyl group, an SH4 domain, a unique segment, an SH3 domain, an SH2 domain, a protein-tyrosine kinase domain, and a C-terminal regulatory tail (Roskoski, 2005) (Figure 8).

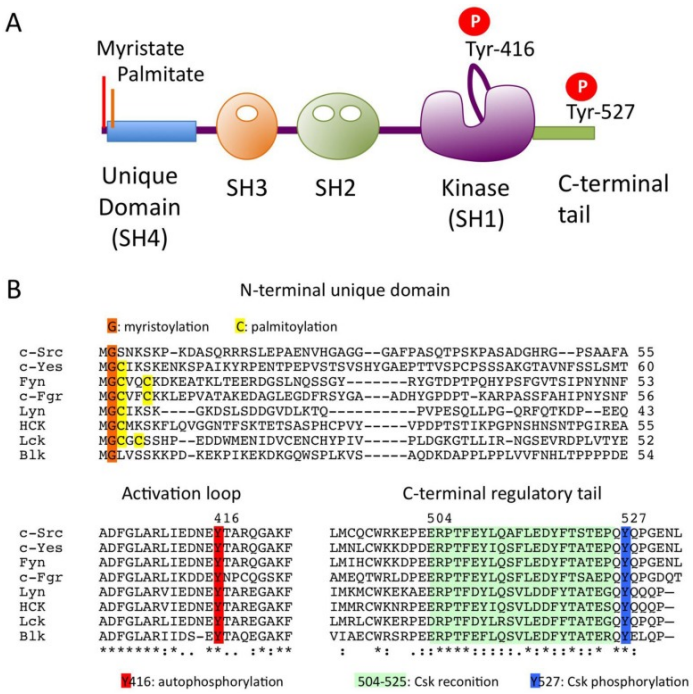

Figure 8 The SRC family kinases (SFKs). *(A) domain organization of SFKs; (B) Amino acid alignments of N-terminal unique domain, activation loop and C-terminal and regulatory tail in SFKs. (Okada, 2012).*

SRC is expressed ubiquitously in vertebrate cells. However, brain, osteoclasts, and platelets express higher levels of this protein than most other cells (Brown and Cooper, 1996). In fibroblasts, SRC is bound to endosomes, perinuclear membranes, secretory vesicles, and the cytoplasmic side of the plasma membrane, where it can interact with different growth factors and integrin receptors (Brown and Cooper, 1996; Thomas and Brugge, 1997). The expression of high levels of SRC in platelets (anucleate cells) and in neurons (which are post mitotic) indicates that SRC participates in processes other than cell division (Roskoski, 2005).

Mutations in this gene could be involved in the malignant progression of colon cancer. The activation of the SRC pathway has been observed in tumors from colon, liver, lung, breast and the pancreas. A common mechanism is that there are genetic mutations that result in the increased activity or in the overexpression of the SRC (Irby and Yeatman, 2002).

The SRC tyrosine kinase plays an important role in modulating signaling from growth factors receptor, integrin and steroid receptors (Fu and Simoncini, 2008). In fact, in c-SRC deficient mice, the loss of the SRC tyrosine kinase correlates with some defects on ductal development as well as in uterine and ovarian development (Kim et al., 2005). Moreover, Src is highly enriched in the developing axons of the CNS and in the PNS (Sorge et al., 1984; Fults et al., 1985), indeed SRC is an important signal transducer for axonal outgrowth. Regarding the PNS, SRC is a crucial component of different signal transduction pathways implicated in a wide range of cellular processes, including cell growth, migration and differentiation (Zhao et al., 2003). In the PNS, the Src activity is also increased during nerve regeneration (Le Beau et al., 1991; Zhao et al., 2003), whereas it enhances axon-SCs contact for nerve regrowth. Indeed, SRC is also expressed in the SCs distal from a nerve injury, decreasing with restoration of axon-

SCs cross-talk (Zhao et al., 2003). However, the molecular mechanism at the bases of the Src functions in SCs has not been fully understood.

FAK is another non-receptor protein tyrosine kinase, controlling cell motility and the turnover of focal adhesion sites (Flamini et al., 2011; Sanchez et al., 2011). FAK is relevant for SCs, being involved in regulating their proliferation, survival and differentiation (Grove et al., 2007; Grove and Brophy, 2014). When FAK is not present, developing SCs proliferate poorly, sort axons inefficiently and do not myelinate peripheral nerves. However, FAK is unnecessary for adult SCs, neither for myelin maintenance nor for re-myelination after sciatic nerve lesion (Grove and Brophy, 2014). FAK is required *in vivo* for the process of radial sorting (Grove et al., 2007). FAK phosphorylation at Tyr397 is an early event, serving to expose a docking site for Src (Schaller et al., 1994; Xing et al., 1994). Then, SRC phosphorylates some sites in FAK, promoting optimal FAK activation (Calalb et al., 1995). Therefore, the mutual phosphorylation between SRC and FAK might be a mechanism of potentiation of SCs cellular processes (Figure 9).

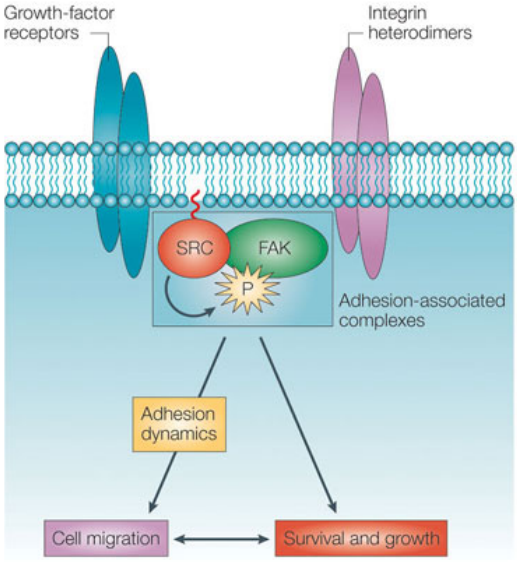

Copyright © 2005 Nature Publishing Group
Nature Reviews | Cancer

Figure 9 FAK as a signal integrator. *FAK acts to integrate signals from extracellular cues, such and growth-factor receptors and integrins, and from the upstream Src-family kinases, to control and coordinate adhesion dynamics/cell migration with survival signaling. FAK binds to integrin and Src to growth factor receptors and they bind to each other. (McLean et al., 2005)*

The Hippo pathway in the PNS

General concepts

Hippo is an intracellular signaling pathway playing a crucial role in cell proliferation, apoptosis, differentiation and development (Bae et al., 2017). Hippo acts inducing the phosphorylation of downstream factors. For instance, the phosphorylation cascades of Hippo core components [e.g. Hippo (HPO) , salvador (SAV), warts (WTS), and MOB as tumor suppressor (MATS) in Drosophila and serine/threonine kinase (MST1/2), Salvador family WW domain containing protein 1 (SAV1), large tumor suppressor (LATS1/2), and MOB kinase activator (MOB1a/b) in mammals] inhibit the activation of some transcriptional co-activators such as Yorkie (YKI), YAP, and TAZ. These co-activators function as transcription factors along with TEA domain transcription factor (TEAD) in the nucleus, increasing the expression of target genes, as connective tissue growth factor (CTGF), cysteine rich protein 61 (CYR61), AXL receptor tyrosine kinase (AXL), and Survivin. Therefore, YAP and TAZ are the major effectors of the Hippo signaling cascade. Indeed, the phosphorylation of YAP and TAZ and activation of LATS kinase are regulated by multiple mechanisms (Bae et al., 2017).

The Hippo pathway was initially identified in *Drosophila Melanogaster*, albeit, in the recent year, most of the studies focused on its function and regulation in mammalian cells. In mammals, the core of the Hippo pathway is a kinase cascade in which the mammalian MST1/2 phosphorylate and activate LATS1/2. From a physiological point of view, the output of this cascade is to restrict the activities of YAP and TAZ. The activation of YAP and TAZ leads to their translocation into the nucleus, where they bind the TEAD transcription factor family, inducing the expression of genes involved

in cell proliferation, survival, and migration (Meng et al., 2016). TEAD1-4 is a sequence-specific transcription factors that mediate the main transcriptional output of the Hippo pathway in mammalian cells (Zhao et al., 2008). Moreover, TEAD1-4 is able to bind vestigial like family member 4 (VGLL4) in the nucleus, functioning as a transcriptional repressors; this produces the dissociation of VGLL4 from TEAD1-4 and the activation of TEAD-mediated gene transcription, promoting tissue growth and inhibition of apoptosis (Koontz et al., 2013).

More in detail (Figure 10), the mechanism of the Hippo kinase cascade can be initiated by TAO kinases (TAOK1/2/3), which phosphorylate MST1/2, thereby leading to its activation (Boggiano et al., 2011; Poon et al., 2011). There are also evidence that MST1/2 can auto-phosphorylate (Praskova et al., 2004). Activation of this loop of phosphorylations is improved by MST1/2 dimerization (Glantschnig et al., 2002), but is also possible that MST1/2 activation can be promoted without requiring upstream kinases. Consequently, active MST1/2 phosphorylate SAV1 and MOB1A/B (Callus et al., 2006; Praskova et al., 2008), two scaffold proteins that assist MST1/2 in the recruitment and phosphorylation of LATS1/2 (Hergovich et al., 2006; Yin et al., 2013). Contemporary to MST1/2, two groups of mitogen-activated protein kinase (MAP4Ks), MAP4K1/2/3/5 and MAP4K4/6/7, can also directly phosphorylate LATS1/2 at their hydrophobic motifs and result in LATS1/2 activation (Meng et al., 2015). Deletion of MST1/2 and MAP4Ks is required to abolish YAP phosphorylation in response to LATS-activating signals, such as contact inhibition, energy stress, serum deprivation, and F-actin disassembly (Meng et al., 2015). Moreover, phosphorylation of YAP and TAZ leads to their binding in 14-3-3, causing YAP/TAZ cytoplasmic sequestration (Zhao et al., 2007). Furthermore, LATS-induced phosphorylation triggers subsequent phosphorylation of

YAP/TAZ by casein kinase 1δ/ε and recruitment of the E3 Ubiquitin ligase SCF complex subunit SKP1/ASK1 family protein (SCF E3 ubiquitin ligase), leading to eventual YAP/TAZ ubiquitination and degradation (Liu et al., 2010; Zhao et al., 2010a). Furthermore, YAP protein can also be degraded by autophagy (Liang et al., 2014).

In this scenario, another important key player of the complex cascade downstream Hippo, is Neurofibromin 2 (*NF*2)/Merlin. This oncosuppressor protein directly interacts with LATS1/2 and facilitates their phosphorylation by the MST1/2-SAV1 complex (Yin et al., 2013). Subsequently, LATS1/2 auto-phosphorylates (Chan et al., 2005) and in turn inactivate YAP and TAZ (Zhao et al., 2007). Activated *NF*2 may play important roles in SCs development (detailed below).

Mouse models with deletion of MST1/2, SAV1, MOB1A/B, Nf2, or LATS1/2 or YAP overexpression exhibit upregulation of TEAD, increased expansion of progenitor cells and tissue overgrowth (Chen and Harris, 2016), supporting their functional roles in the Hippo signaling pathway.

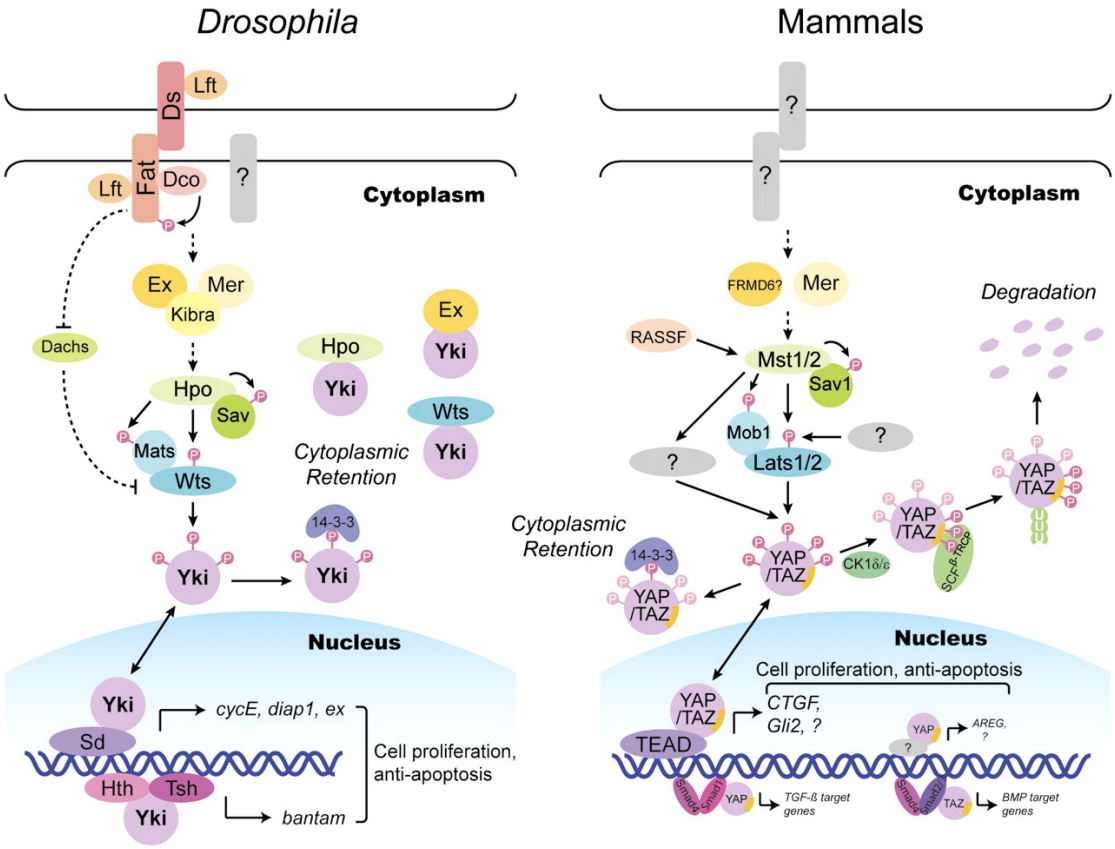

Figure 10 Models of the Hippo pathway in Drosophila and mammals. *In mammals, functional role of Fat and Ex homologs are not clear. nevertheless, Merlin may still activate the Hippo* pathway (Yokoyama et al., 2008). *Ras associated family member (RASSF), a subgroup of Ras effector proteins, may also activate Mst1/2 (Oh et al. 2006). Relationships between Hpo, Sav, Wts, and Mats are conserved in mammalian Mst1/2, Sav1 (Sav homolog), Lats1/2 (Wts homolog), and Mob (Mats homolog). Lats1/2 phosphorylates YAP on five conserved HXRXXS motifs (four on TAZ) (Zhao et al., 2007). Dependent on cell type and context, there may exist another YAP kinase in response to Mst1/2 and another Lats1/2 kinase (Zhou et al., 2009). S127 (S89 in TAZ) phosphorylation-dependent 14–3–3 binding and cytoplasmic retention are conserved in YAP/TAZ (Zhao et al., 2007). YAP is also inhibited by S381 phosphorylation, which primes serine-threonine kinase CK1d/e phosphorylation of S384, and S387 finally leads to mediated ubiquitination and degradation (Zhao et al., 2010a). Sd homologs, major YAP target transcription factors. They mediate expression of connective tissue growth factor (CTGF), GLI-Kruppel family member (Gli2), and many other target genes (Zhao et al., 2008). Amphiregulin (AREG) is induced by YAP through an unidentified transcription factor (Zhang et al., 2009). YAP and TAZ also bind Smad1 and Smad2/3 to activate expression of TGF-β and BMP target genes, respectively, to maintain stem cell pluripotency (Gao et al., 2009).*

Hippo pathway in SCs

In the PNS, it was shown that YAP and TAZ activate the mTORC1 pathway to promote myelination (Kim et al., 2005), and interact with TEAD1 to control *Pmp*22 gene expression (Lopez-Anido et al., 2016). Moreover, in the cytosol of SCs, YAP and TAZ are phosphorylated and inhibited by LATS1/2 kinases. YAP and TAZ are fundamental for immature SCs development and myelin gene regulation. These transcriptional regulators are required for SC proliferation and axonal sorting. SCs require YAP and TAZ to enter S-phase and, without them, fail to generate SCs axonal sorting (Grove et al., 2017). Moreover, they are implicated in the differentiation process, regulating the transcription of *Krox*-20 (Grove et al., 2017), which is a key modulator of the myelination in SCs (Topilko et al., 1994). The capacity of YAP and TAZ to initiate and maintain SC myelination may depend by different pathways, such as the positive regulation of zinc-finger E-box binding homeobox 2 (ZEB2) transcription factor, that promotes SC differentiation by inhibiting some differentiation repressors (Quintes et al., 2016).

Furthermore, it is important to underlie that YAP and TAZ are downstream of other regulators of myelination, including NRG-1 type III, integrin α6β, adhesion g protein coupled receptor G6 (GPR126) and wingless (WNT) (Quintes et al., 2016; Grove et al., 2017).

***NF2* gene**

NF2 gene encodes the 4.1 ezrin, radixin, moesin domain (FERM domain) protein Merlin, regulated by the intracellular adhesion and the attachment to the extracellular matrix (Rouleau et al., 1993; Okada et al., 2005). *NF2* gene maps to the long arm of chromosome 22 and encodes two Merlin isoforms (Figure 11A). The long, Merlin

isoform 1 (Merlin-1 or Merlin), has an extended carboxy-terminal tail that is encoded by exon 17. Merlin isoform 2 (Merlin-2), indeed, contains the alternatively spliced exon 16 which ends in a stop codon, encoding 11 residues following amino acid 579 (Bianchi et al., 1994). Notably, Merlin-2 does not possess carboxy-terminal residues, required for intramolecular binding between the amino-terminal FERM domain and the carboxy-terminal tail, probably determining the constitutively open conformation (Sherman et al., 1997; Gonzalez-Agosti et al., 1999). Several recent studies have found that Merlin-2 has a function in cell proliferation, working downstream mitogenic signaling in the same entity as Merlin-1 (Lallemand et al., 2009; Sher et al., 2012; Cooper and Giancotti, 2014)

General concepts

Merlin is an oncosuppressor protein with an high sequence homology to the ERM family of cytoskeletal linker proteins. In fact, in the cell membrane, Merlin suppresses mitogenic signaling and mediates contact inhibition and tumor suppression (McClatchey and Fehon, 2009). Merlin has 64% sequence similarity with family members of the conserved FERM domain at the N terminus. The FERM domain is followed by an α-helical domain and a C-terminal. In contrast to the other ERM proteins, merlin lacks the actin-binding site located in the C-terminal domain, it has a unique actin binding motif in the N-terminal domain (Xu and Gutmann, 1998). FERM proteins link the actin cytoskeleton to plasma membrane receptors (Trofatter et al., 1993). The dephosphorylated active form of Merlin suppresses RAC-PAK signalling (Shaw et al., 2001; Kaempchen et al., 2003; Okada et al., 2005). Moreover, dephosphorylated merlin restrains activation of mTORC1, independently of AKT (James et al., 2009; López-Lago et al., 2009) inhibits PI3K-AKT and FAK-SRC signalling (Rong et al., 2004; Poulikakos et al., 2006) and negatively regulates the

EGFR-RAS-ERK pathway (Jin et al., 2006; Ammoun et al., 2008). Moreover, Merlin activates the Hippo tumor suppressor signaling pathway, abolishing the transcriptional coactivators YAP/TAZ. This evidenced a conserved role for Merlin in the control of organ size, stem cell behavior, and cell proliferation (Zhao et al., 2007; Zhang et al., 2010).

Recent studies shed light also on the conformational changes that regulate Merlin intramolecular associations and downstream signaling. Merlin indeed, has a bimodal function (Figure 11B). Post-translational modifications lead to the conversion of Merlin into the inactive state, with growth inhibitory properties. Dephosphorylated and open state Merlin, indeed, is active in the contact inhibition of growth and tumor suppression (Sher et al., 2012; Cooper and Giancotti, 2014).

Merlin regulates the tight junction protein angiomotin, thus inhibiting RAC signalling (Yi et al., 2011). Nuclear localization of Merlin inhibits the $CRL4^{DCAF1}$E3 ubiquitin ligase then suppressing oncogenic expression (Li et al., 2010).

Merlin, like ERM protein, is also active as scaffold protein at the plasma membrane, where it is phosphorylated at Ser518, promoting receptor mediated events associated with cell proliferation and survival. Ser518 is substrate of p-21 activated kinase (PAK) and PKA, inactivating *Nf2* tumor suppressor activity (Shaw et al., 2001; Alfthan et al., 2004). Phosphorylated Merlin adopts an open and active configuration at the plasma membrane. Conversely, dephosphorylation at S518, mediates the transition to a closed conformation, inactivating its scaffold function and contemporarily activating its tumor suppressor function. The closed head-to-tail conformation of the active tumor-suppressor was believed to be incapable of interaction with the of growth factor receptors (Curto et al., 2007; Yogesha et al., 2011).

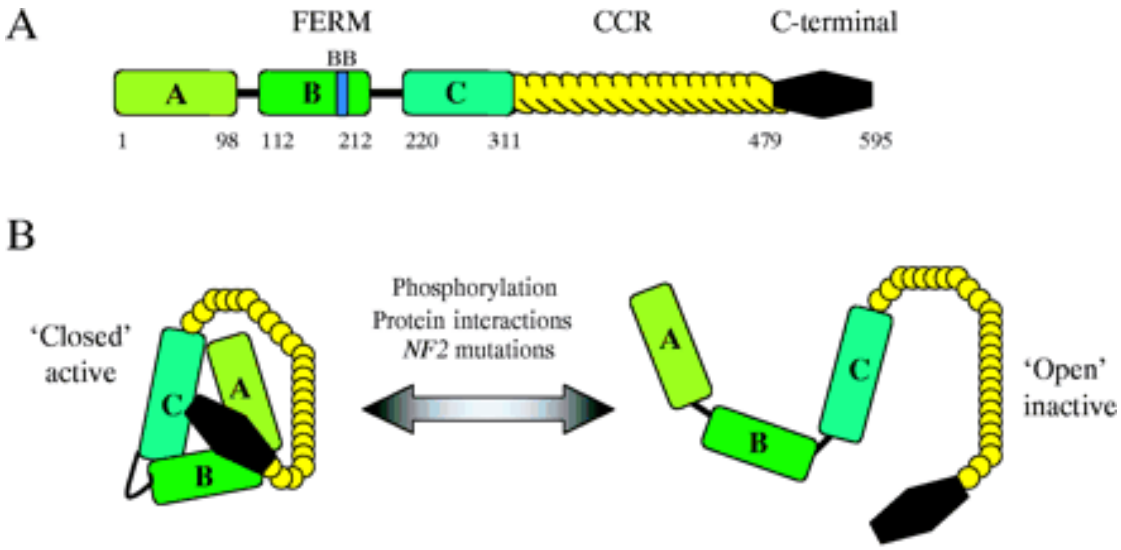

Figure 11 Merlin structure. *(A) Merlin contains three conserved protein-protein interaction domains: a FERM domain in its N-terminus and a C-terminal domain (CTD) separated by a coiled-coil (α-helical) region (CCR). Crystallography showed that the merlin FERM domain contains three subdomains, which exhibits a cloverleaf architecture. Merlin FERM has a unique `Blue Box' (BB, residues 177-183) compared with other ERM proteins. (B) Merlin can adopt two conformations: a `closed' active and `open' inactive form. Merlin can switch from these two conformations as a result of phosphorylation, lipid binding, protein interactions or NF2 mutations. (Sun et al., 2002)*

NF2 gene role in SCs

Merlin is present also in the PNS. Given that merlin is part of the ERM complex, it was expected to be located in the node of Ranvier. However, Merlin has not been detected in SCs microvilli, but was found at the level of paranodes in sciatic nerves. Paranodin, also known as contactin associated protein (Caspr), is a neuronal protein that is highly expressed in paranodal axoglial junctions. Merlin binds to paranodin through its FERM domain and, at least in CNS, it forms a complex with β1 integrin and paranodin (Denisenko-Nehrbass et al., 2003). Some factors link, directly or indirectly, Merlin to the cytoskeleton, even in the PNS. Indeed, merlin interacts with different proteins including spectrin (Scoles et al., 1998), the solute carrier family 9, sodium/hydrogen exchanger, member 3 regulator 1 (NHERF) (Murthy et al., 1998; Gonzalez-Agosti et al., 1999), the schwannomin interacting protein 1 (SCHIP1) (Goutebroze et al., 2000), the hepatocyte growth factor-regulated tyrosine kinase substrate (HRS) (Scoles et al., 2000), syntenin, CD44 (Grönholm et al., 1999; Morrison et al., 2001), β1 integrin (Obremski et al., 1998), F-actin (James et al., 2001) and paxillin (Fernandez-Valle et al., 2002).

Importantly, Merlin is a key factor for the pathogenesis of neurofibromatosis type 2 (NF2). Schwannomas are SC-derived benign tumors that occur sporadically and/or in patients with NF2 (MacCollin et al., 2003). Sporadic schwannomas and NF2 tumors show a loss of Merlin, but not of ERM proteins (Stemmer-Rachamimov et al., 1997). However, is still unclear how the loss of Merlin may impact on tumor pathogenesis, whereas a tumor suppressor function of Merlin, has been hypothezise. Studies on *Nf2 knock out* mouse models show that these animals developed schwannoma and meningiomas, which are the hallmarks of the human disease (McClatchey et al., 1998;

Giovannini et al., 1999). Moreover, conditional loss of merlin in SCs lead to hyperplasia and tumor development in mice (Giovannini et al., 2000; Kalamarides et al., 2002). Merlin-deficient schwannoma cells show cytoskeletal reorganization when compared with normal human SCs, indicating an important and evident defect of the actin cytoskeleton (Pelton et al., 1998; Bashour et al., 2002). Cytoskeletal changes were recovered after acute expression of Merlin in these cells, showing a direct role for Merlin in actin reorganization (Bashour et al., 2002).

Neurofibromatosis and Schwannomatosis

Neurofibromatosis is an heterogeneous group of hereditary syndromes that generate tumors of the CNS and PNS. The most common form is neurofibromatosis type 1 (NF1 96%), followed by NF2, (3%), and a lesser common form of schwannomatosis. Neurofibromatosis incidence is almost the same among genders and different ethnic groups. (Kresak and Walsh, 2016).

NF2 has an inherited autosomal dominant pattern with an incidence of 1 in 25,000, prevalence of 1 in 60,000, and a penetrance of approximately 0.95 (Laulajainen et al., 2008). The disease is caused by a mutation in the *NF2* gene. More than a half of the cases, are caused by sporadic gene mutations in patient with no family history of the disease (Kresak and Walsh, 2016), or a loss of *NF2* gene mutation with an high frequency of somatic mosaicism (Petrilli and Fernández-Valle, 2016). Notably, *NF2* mutations are present in several malignant cancers including mesotheliomas, colorectal, hepatic, breast, prostate, clear cell renal cell carcinoma and melanomas.

Recent publications highlights the importance of SCs-axon interactions in preventing schwannoma formation and the contribution of axonal expression of Merlin isoform 2 (Schulz et al., 2013, 2014a; b). NF2-associated schwannomas exhibit *NF2* inactivation

which manifests in a failed production of Merlin protein (Sainz et al., 1994). Indeed, Merlin protein expression has found to be highly reduced or completely absent in 11 of 14 sporadic schwannomas, 16 of 19 sporadic meningiomas and 3 of 8 sporadic ependymomas (Gutmann et al., 1997). Mutational *NF2* inactivation and loss of heterozygosity (LOH) is the cause of the most NF2-associated schwannomas and sporadic schwannomas. Transcriptional inactivation causes 15.3% of NF2-associated schwannomas and 19.3% of sporadic schwannomas (Gonzalez-Gomez et al., 2003). Moreover, one study reported that methylation of three CpG sites, in the *NF2* promoter elements was found in ~60% of vestibular schwannomas and correlated with the decreased promoter activity and mRNA expression (Kino et al., 2001). On the other hand, another study of 35 sporadic vestibular schwannomas reported that in 65% of tumors the *NF2* promoter was unmethylated and in the remaining 35% the results were inconclusive (Koutsimpelas et al., 2012). At the same time, 50-60% of sporadic meningiomas contain *NF2* somatic mutations and epigenetic inactivation (Lomas et al., 2005; Riemenschneider et al., 2006). Another study, considered 88 sporadic meningiomas, 49% exhibited allelic loss of chromosome 22, 24% had *NF2* somatic mutations and 26% had aberrant *NF2* promoter methylation, whereas in 17% of meningiomas, epigenetic *NF2* inactivation was the only cause of *NF2* deficiency. Similarly, less then 10% of sporadic ependymomas have *NF2* promoter methylation. In some schwannomas and meningiomas without genetic or epigenetic *NF2* inactivation, merlin inactivation was caused by μ-calpain, constitutive activation that mediated merlin proteolytic cleavage/degradation (Kimura et al., 1998). Finally, a recent study of meningiomas in 73 patients found a high incidence of telomerase reverse transcriptase (*TERT*) promotes mutations in there meningiomas undergoing malignant

transformation. However, *TERT* mutations were found in benign tumors. This suggests that *TERT*, independently of *NF2*, is a biomarker of malignant transformation of meningioma (Goutagny et al., 2014).

Considering that *Nf2* heterozygous mice are prone to develop cancers, primarily osteosarcomas, fibrosarcomas and hepatocellular carcinomas, it was assumed that NF2 patients commonly develop other malignant cancers (McClatchey et al., 1998). The incidence of *NF2* mutations in common human cancers is low. The transformation of schwannomas into malignant peripheral nerve tumors or development of other common cancers is very rare. Despite the fact that *NF2* mutations have been detected in multiple human tumor types, mutational analysis of 315 human carcinoma samples found a low prevalence of *NF2* mutations, in fact they were found in just 2.2% of hepatocellular, acute myelogenous leukemia and squamous cell lung carcinomas (Bianchi et al., 1994; Yoo et al., 2012).

In conclusion, despite Merlin is ubiquitary expressed in normal tissues, loss of merlin in humans mostly leads to SC-derived tumors, suggesting that a specific molecular contest and the microenvironment are strongly required for this oncogenic transformation.

The role of microRNAs in myelination

General concepts

MicroRNAs (miRNAs) are small non-coding RNA molecules containing about 22 nucleotides, which can be found in plants, animals and some viruses. They are encoded by eukaryotic nuclear DNA in plants and animals and by viral DNA in viruses. MiRNAs function in transcriptional and post-transcriptional regulation of gene expression (Chen and Rajewsky, 2007). MiRNA function via base-pairing with complementary sequences within mRNA molecules. This determine the silencing of mRNAs, which cannot be translated by ribosomes. Animal miRNAs recognize their target mRNAs by small sequence of 6-8 nucleotides (the seed region) at the 5' end of the miRNA (Lewis et al., 2003, 2005). Importantly, miRNAs may target a large and different amount of mRNA as well as mRNA may be targeted by multiple miRNAs.

The human genome may encode over 1000 miRNAs (Bentwich et al., 2005) which target about the 60% of mammalian genes. Mammalian cells use miRNA for acute and rapid regulation of gene expression, thus inducing transcriptional (Morris et al., 2004), or post-transcriptional gene silencing (Ambros, 2004; Bartel, 2004) as well as epigenetic modifications (Castanotto et al., 2005). MiRNAs target multiple mRNAs leading to post-translational repression or also to mRNA degradation (Hannon et al., 2006). The enzyme RNase III *Dicer*, processes miRNAs into segment about 22 nucleotide longer, this long mature RNA duplexes (Kim et al., 2009) are loaded into the RNA-induced silencing complex (RISC complex), which contains Argonaute (AGO) proteins (Tabara et al., 1999; Martinez et al., 2002) (Figure 12).

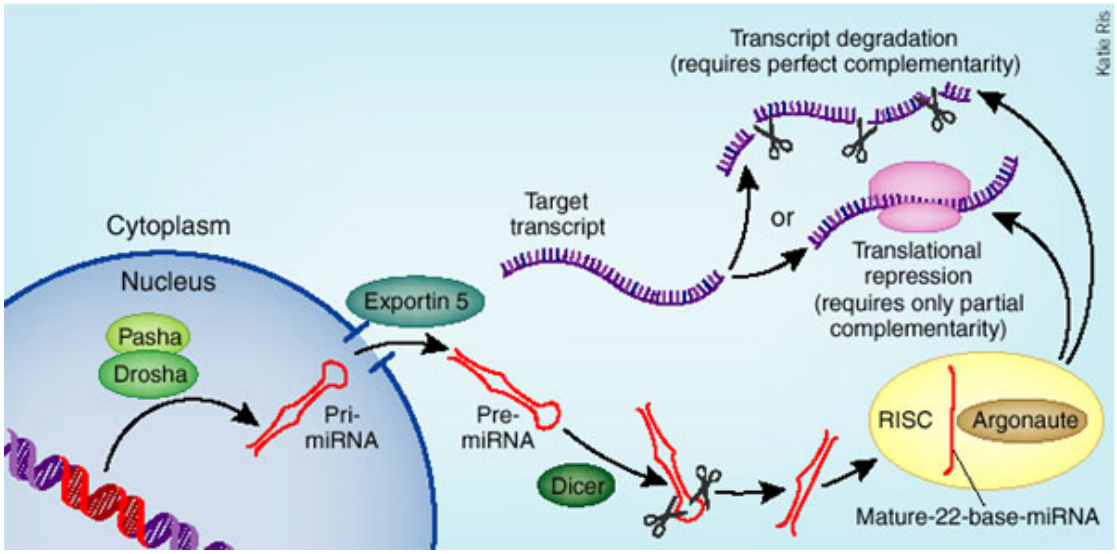

Figure 12 Synthesis and mechanism of miRNAs. *After synthesis of the primary RNA transcript (pri-miRNA), the molecule is processed by the endonucleases Pasha and Drosha to yield the pre-miRNA. Secondly, pre-miRNA is export to the cytoplasm and the mature miRNA is generated by a cleavage step mediated by Dicer. The mature miRNA is then loaded onto the RNA-induced silencing complex (RISC). This complex can affect the degradation or translational repression of mRNAs complementary sequences to the miRNA. (Melman et al., 2014).*

In general, miRNAs affect the overall protein expression state of the cell, leading to a global effect on cellular health and differentiation state. Recently, several papers have identified fundamental roles for miRNAs in controlling the development, differentiation, and health of myelinating cells of the mammalian nervous system (Dugas and Notterpek, 2011).

To study the role of miRNAs in biological processes, a typical approach is the *knock down* of *Dicer1* (Bartel, 2004), but the animal fail to survive around embryonic day 7.5 (E7.5), preventing further longitudinal studies (Bernstein et al., 2003). Therefore, to study the requirement of mature miRNAs in postnatal processes, Cre-mediated recombination is functional to obtain the disruption of DICER1, specifically in cells of interest.

MiRNAs in the nervous system

Mature miRNA production is necessary, not only for the generation of compact CNS myelin during development but, also to maintain healthy and functional myelin sheaths in adult nerves (Dugas and Notterpek, 2011) in the mammalian CNS, miRNAs are important in all stages of OL generation and myelination.

MiRNAs are able to influences OL biology, and CNS myelination, through the activation of different mechanism: the suppression of OL-precursors cell (OPCs) expressed genes, the promotion of OPCs expansion, the suppression of inappropriate non-OL gene expression in OPCs and OLs and the suppression of genes transiently required during myelin sheath formation (Dugas and Notterpek, 2011). In uncommitted neural precursors the *knock out* of *Dicer1* (by driving Cre expression from the Nestin promoter) leads to a reduction in OL lineage, both mature OLs and immature OPCs (Kawase-Koga et al., 2009). On the contrary, the disruption of DICER1 function in specific OPCs and OLs (by expressing Cre from either the *Olig1* or *Olig2* promoter) does note reduce OPC number *in vivo* (Dugas et al., 2010a; Zhao et al., 2010b). However, OPCs in which *Dicer1* is silenced do not differentiate normally, as OL differentiation and myelin formation are significantly altered in Olig1-Cre, Olig2-Cre, and 2',3'-cyclic nucleotide 3' phosphodiesterase (CNP)-Cre *Dicer1*$^{fl/fl}$ mice. OPCs purified from these animals fail to differentiate normally *in vitro* (Dugas and Notterpek, 2011). Furthermore, the specific disruption of DICER1 in fully mature OLs, by driving tamoxifen-inducible Cre expression from a myelin proteolipid protein (PLP) promoter, leads to the degradation of CNS myelin (Shin et al., 2009).

In accordance with a previous work from Lau and colleagues in 2008, that characterized miRNA expression in OLs, in 2010, two groups independently, identified miR-338 and

miR-219, that are highly induced in differentiating OLs (Dugas et al., 2010b; Zhao et al., 2010b). The expression of miR-219 is evident in mature OLs, in brain and spinal cord, while miR-338 is less expressed in the brain, as strong expression of miR-338 is only detected in the spinal cord (Dugas et al., 2010b; Zhao et al., 2010b). In addition, other two miRNA were identified as inducer of OL maturation and differentiation, miR-23a and miR-23b, (Lin and Fu; Lau et al., 2008), which reduce the expression of a gene inhibiting normal OL maturation. Albeit miR-219 promotes all stages of OL differentiation, miR-138, specifically promotes the early stages (indicated by expression of myelin proteins CNP and MBP) of OL differentiation and simultaneously suppressed the later stages identified by the myelin oligodendrocyte glycoprotein (MOG) (Dugas et al., 2010b).

On the contrary, another class of miRNAs seem to block OL differentiation. In fact, members of the miR-17-92 cluster were expressed at high levels in both OPCs and OLs, whereas were necessary to enhance OPC proliferation *in vivo* and *in vitro* (Budde et al., 2010). In particular, Budde and colleagues found that a member of this cluster, miR-19b, increases OPC proliferation *in vitro*. In general, all these findings demonstrated that different miRNAs can assume several and opposite roles in the process of OL differentiation.

MiRNAs in the PNS

Similarly to OLs in the CNS, SC differentiation and peripheral nerve myelination depends on communication between axons and glial cells. The switch in phenotype from a proliferating to a differentiated SCs involves transcriptional and translational gene regulatory mechanisms, including gene repression via miRNAs.

Several studies demonstrated that miRNAs are fundamental candidate for the regulation of peripheral nerve myelination. While some miRNAs are induced during differentiation (miR-219, -338, -138), several miRNAs present high levels in pre-myelinating SCs but then decrease during myelination (Svaren, 2014). In SCs, at least some of these miRNAs rebound after peripheral nerve injury (Viader et al., 2011b; Adilakshmi et al., 2012). In mouse models where *Dicer* was specifically ablated in SCs (using P0-Cre), the SCs underwent the normal radial sorting process, although delayed (Bremer et al., 2010b; Pereira et al., 2010; Yun et al., 2010). Nevertheless, SCs lacking *Dicer* produce no myelin and instead continue to proliferate. The *knock out* animals show a decrease in myelin gene expression and lower levels of the EGR2/KROX20 transcription factor, important factors implicated in the progression of myelination. This animals showed an induction of immature (or non-myelinating) SCs markers, such as P75/NGFR, SRY-Box2 (SOX2), NOTCH1, and C-JUN in the absence of DICER. Some studies studies show that, the use of *Dhh*-Cre failed to show any proliferation changes at P4 (Pereira et al., 2010), but in a separate study with the same Cre-driver, the increase in proliferation was seen at P22, when there are only few dividing cells in control nerve (Bremer et al., 2010a). Using the *P0* – Cre driver, *Dicer* ablation induces an increase in proliferation, that was observed before the P7, with further increase at P14 (Yun et al., 2010). Moreover, POU domain, class 3, transcription factor 1 (OCT6/POU3F1) and POU domain, class 3, transcription factor 2 (BRN2/POU3F2), pro-myelinating SCs markers, show a reduction in mRNAs levels at P4 (Bremer et al., 2010a), in accordance to the light reduction of OCT6/POU3F1 protein at P5 show in the study of Pereira and colleagues. Furthermore, many SCs arrest their cycle at a pro-myelinating stage after P20. Accordingly, immunohistochemistry performed in the *P0*-Cre study revealed an

increased number of OCT6/POU3F1 positive SCs at P22 (Yun et al., 2010). In the absence of DICER, another important parameters that is studied is the NRG/AKT pathways (Nave and Salzer, 2006) in early postnatal time points (Bremer et al., 2010a; Pereira et al., 2010). In mouse models, with a peripheral nerve-specific deletion of Dicer enzyme, SCs "arrest" the production of myelin and instead continue to proliferate and express markers of immature SCs such as SOX2 and C-JUN (Bremer et al., 2010a; Pereira et al., 2010; Yun et al., 2010). Conversely, the study of Pereira and colleagues demonstrated a persistent development of myelin profiles despite the lack of DICER, which was enhanced in dorsal roots compared to ventral roots and sciatic nerve (Pereira et al., 2010), suggesting that DICER is not required for myelin initiation. Interestingly, by using an inducible *Plp*-Cre to *knock down Dicer* in mature mice, it was shown that the loss of DICER had a small effect on myelin maintenance and on the early stages of nerve injury. Also the recovery of myelination after nerve crush injury was imperfect (Viader et al., 2011a). These data indicates that DICER is not required for the demyelination after nerve injury, but rather for re-myelination process. Studies of *Dicer knock out* mice indicated that miRNA expression is required non only for the control of differentiation status of the cell, but also for the cell cycle exit, thus for the regulation of proliferation (He et al.; Dugas and Notterpek, 2011).

Microarray analysis identified different groups of miRNAs that are developmentally regulated during maturation of SCs (Bremer et al., 2010a; Pereira et al., 2010; Yun et al., 2010; Gokey et al., 2012). In particular, analysis of miRNAs in SCs showed that miR-138 is induced during myelination. This was confirmed by the 3' UTR luciferase assays, showing that miR-138 could reduce the expression of SOX2, C-JUN and cyclin D1 (Yun et al., 2010), key factors that are downregulated during peripheral nerve

myelination. PMP22 is a candidate for post-transcriptional regulation by miRNAs, because its product is a protein whose levels are critical for normal SC function. In fact, over- and under-expression of PMP22 have been associated with hereditary demyelinating neuropathies in humans (Chance, 2004). Interestingly, by using an inducible *Plp*-Cre to *knock down DICER* in mature mice, it was shown that the loss of *Dicer* had a small effect on myelin maintenance and on the early stages of nerve injury. Also the recovery of myelination after nerve crush injury was imperfect (Viader et al., 2011a). These data indicates that *DICER* is not required for the demyelination after nerve injury, but rather for re-myelination process.

Recently, several studies applied the microarray analysis to the study of miRNA profiling in peripheral nerve after a nerve lesion (Viader et al., 2011a; Adilakshmi et al., 2012; Yu et al., 2012). It was shown an injury-induced decline in miR-338 and miR-138 in nerve. Moreover, the half of miRNAs expressed in SCs resulted regulated by the injury.

Recent findings from two different studies show that, in proximal nerve following rat sciatic nerve transection, there is an increase expression of miR-sc8, which induces the inhibition of cell proliferation and migration of SCs. Viceversa, the silencing of miR-sc8 show the enhance of cell proliferation and migration. The EGF-R was identified as the target gene of miR-sc8, thus exerting negative regulation of EGF-R by translational suppression (Gu et al., 2015). An increased and decreased expression of miR-sc3 promoted and reduced the proliferation and migration of primary SCs, respectively.

Indeed, some specific miRNAs pathways mediate cell cycle exit, such as the miR-34a that targets cyclin D1 and *Notch1* (Bremer et al., 2010a; Viader et al., 2011a). Notch1

antagonize the myelination process and promote proliferation, moreover, its expression is downregulated when SCs terminally differentiate (Woodhoo et al., 2009).

Peripheral nervous system disorders

PNS disorders are diseases of the peripheral nerves which includes diseases of the nerve roots, ganglia, plexi, autonomic nerves, sensory nerves and motor nerves (described in the PubMed database, MeSH, Ref n° 68010523). Among these the peripheral hereditary motor and sensory neuropathies represent the main subgroups.

Peripheral neuropathies (PN)

PN is a term generally referring to a damage or disease affecting nerves, which may impair motor and sensory function depending on the type of nerve affected. PN is a very heterogeneous class of disease of different origin. Indeed, common causes are systemic diseases (such as diabetes), medications (like chemotherapy, metronidazole and fluoroquinolone), antibiotics (ciprofloxacin, levaquin etc.), vitamin deficiency (vitamin B12), traumatic injury (including ischemia or radiation therapy) excessive alcohol consumption, immune system disease, coeliac disease or viral infection. PN can be idiopathic or hereditary (Hughes, 2002; Torpy et al., 2008). Other most common forms of PN are hereditary PN (HPN), including motor and sensory neuropathies (HMSN), motor neuropathies (HMN) and sensory neuropathies (HSN). The most frequent is the Charcot-Marie-Tooth (CMT) disease, which may be considered a group of heterogeneous disorders, classified on the basis of their clinical, neurophysiological, genetic and pathological features. CMT is divided into two main subtypes, CMT1 and CMT2 distinguished on the basis of electrophysiological and biopsy classification (Dyck P and Lambert EH, 1968; Harding and Thomas, 1980a). The CMT1A is the most common form and its molecular cause is ascribed to the duplication of the chromosome 17, containing the *PMP22* gene, although more than 75 genes responsible for the onset of the pathology have been identified (Table 1). These disorders are inherited as an

autosomal dominant trait, although autosomal recessive and X-linked forms may exist (Harding and Thomas, 1980b) (Table 1). However, the autosomal recessive inheritance may account for more than 30 to 50% of all forms (Dubourg et al., 2006).

Type	*Gene*	*Onset*	*Phenotype*
Autosomal dominant CMT1 (AD-CMT1)			
CMT1A	*PMP22* (duplication)	All ages	Classic form. Hypertrophy of nerves
HNPP	*PMP22* (deletion)	2 to 64 years	Recurrent entrapment neuropathies. Multifocal neuropathies
CMT1B	*MPZ*	1st–2nd decade	Clinically more severe than CMT1A
CMT1C	*LITAF*	Childhood	Abnormal gait. Occasional nerve hypertrophy. Rarely deafness
CMT1D	*EGR2*	1st decade	DSS/CHN. Possible cranial nerve involvement. Scoliosis
CMT1E	*PMP22*	Childhood	Associated with deafness
CMT1F	*NEFL*	1–13 years	CMT1 with early onset. Severe disease
CMT 'plus'	*FBLN5*	4th–5th decade	Skin hyperelasticity. Age-related macular degeneration
Autosomal dominant CMT2 (AD-CMT2)			
CMT2A	*MFN2*	6 months to 50 years	Prominent distal weakness. Late proximal weakness. Optic atrophy. CNS involvement
CMT2B	*RAB7*	2nd decade	Severe sensory loss. Foot ulcers. Arthropathy and amputations
CMT2C	*TRPV4*	Birth to 60 years	Younger more severe. Motor predominance. Vocal cord, diaphragm, respiratory involvement/dHMN
CMT2D	*GARS*	16 to 30 years	Distal upper limb predominance dHMN
CMT2E	*NEFL*	1st–5th decade	Hearing loss. Hyperkeratosis
CMT2F	*HSPB1*	Adult	Classic/dHMN
CMT2G	12q12-q13.2	2nd decade	Classic
CMT2I	*MPZ*	Late	Classic
CMT2J	*MPZ*	Late	Deafness and pupillary abnormalities
CMT2K	*GDAP1*	Variable	vocal paralysis and pyramidal features
CMT2L	*HSPB8*	15 to 33 years	Classic/dHMN
CMT2M	*DNM2*	1st–2nd decade	Tremor
CMT2N	*AARS*	15 to 50 years	Classic
CMT2O	*DYNC1H1*	Early childhood	Sometimes learning difficulties
CMT2P	*LRSAM1*	27 to 40 years	Mild. Sometimes asymmetry
CMT2Q	*DHTKD1*	13 to 25 years	Classic CMT
HMSN-P	*TFG*	17 to 55 years	Proximal involvement. Tremor. Diabetes mellitus
CMT2	*HARS*	Late onset	Sensory predominant
CMT2	*MARS*	Late onset	Motor-sensory
CMT2	*MT-ATP6*	1st–2nd decade	Motor predominant. Pyramidal signs
Dominant and recessive X linked CMT			
CMTX1	*GJB1*	1st–2nd decade	Classic. Occasional deafness
CMTX4	*AIFM1*	Early childhood	Mental retardation. Deafness
CMTX5	*PRPS1*	Childhood	Mild–moderate neuropathy Deafness. Late optic atrophy
CMTX6	*PDK3*	Childhood	Classic CMT
Dominant intermediate CMT			
DI-CMTA	10q24.1-q25.1	7 to 72 years	Classic CMT
DI-CMTB (CMT2M)	*DNM2*	1st-2nd decade	Classic CMT with neutropenia and early onset cataract
DI-CMTC	*YARS*	7–59 years	Classic CMT
DI-CMTD	*MPZ*	30–50 years	Sensory loss and weakness. Deafness/pupil disorders
DI-CMTE	*INF2*	5 to 28 years	Glomerulosclerosis and proteinuria
DI-CMTF	*GNB4*	5 to 45 years	Classic CMT
Autosomal recessive CMT1 AR-CMT1 (CMT4)			
AR-CMT1A	*GDAP1*	<2 years	Severe and progressive. Vocal cord and diaphragm paralysis in some cases
AR-CMT1B1	*MTMR2*	3 years	Severe CMT1. Facial/bulbar weakness. Scoliosis
AR-CMT1B2	*MTMR13 (SBF2)*	4–13 years	Severe CMT1. Glaucoma. Kyphoscoliosis
AR-CMT1B3	*MTMR5 (SBF1)*	5–11 years	Pes planus. Scoliosis
AR-CMT1C	*SH3TC2*	Early onset 1st–2nd decade	Severe to moderate CMT1 Scoliosis. Deafness
AR-CMT1D	*NDRG1*	<10 years	Severe CMT1. Deafness. Tongue atrophy
AR-CMT1E	*EGR2*	Birth	Congenital hypotonia. Respiratory failure. Arthrogryposis
AR-CMT1F	*PRX*	Birth to first decade	CMT1. Prominent sensory involvement
AR-CMT1G (HMSN-Russe)	*HK1*	8–16 years	Severe to moderate CMT1
AR-CMT1H	*FGD4*	<2 years	Delayed milestones. Scoliosis. Severe course
AR-CMT1J	*FIG4*	Congenital, childhood or adult	Severe disorder Similarities to motor neuron disease
AR-CMT1	*SURF1*	Childhood	Severe. Associated to cerebellar ataxia, brain MRI abnormalities and lactic acidosis
Autosomal recessive CMT2 AR-CMT2 (CMT2)			
AR-CMT2A (CMT2B1)	*LMNA*	2nd decade	Severe course. Distal and proximal weakness
AR-CMT2B (CMT2B2)	*MED25*	28 to 42 years	Classic CMT2
AR-CMT2C (CMT2B5)	*NEFL*	1st decade	Severe form
AR-CMT2F/dHMN	*HSPB1*	Variable	Sometimes proximal leg weakness
AR-CMT2H	*GDAP1*	1st decade	Pyramidal involvement. Vocal cord involvement
Autosomal recessive CMT2 AR-CMT2 (CMT2)			
AR-CMT2K (rarely AD)	*GDAP1*	Early-onset form	Severe form. Vocal cord paralysis. Skeletal deformities. Milder dominant form
AR-CMT2P	*LRSAM1*	3rd–4th decade	Cramps. Erectile dysfunction
(HMSN VI)	*MFN2*	Early onset	Optic atrophy
ARAN-NM	*HINT1*	1st decade	Neuromyotonia
GAN	*GAN*	Childhood	Severe axonal neuropathy with early onset CNS involvement. Milder form CMT-like

Table 1 Classification of HMSN or CMT diseases. *Adapted from: Tazir et al, 2014 – J Neurol Sci.*

CMT is slowly progressive and usually have an onset in the second decade of life, depending on genetic abnormalities. The classical phenotype includes limping, moderate distal sensory deficit, and distal lower amyotrophy giving an aspect of "jambs de coq". Most of patients do not complain significant sensory troubles, although 20-30% of CMT1 patients manifest pain, often musculoskeletal and rarely neuropathic. Other characteristics are decreased or absent deep tendon reflexes, balance impairment (because of proprioceptive loss) and skeletal deformities. The pes cavus and hammertoes, complete the typical CMT phenotype.

The electrophysiological study is the first approach to distinguish myelinopathies from neuronopathies or axonopathies. The severity of the neuropathy can be evaluated also by a CMT neuropathy score, a nine-time clinical examination that measures sensory symptoms, motor symptoms, arm and leg strength and nerve conduction velocities.

The therapeutic approach is similar to other chronic neuromuscular disorder and is based on physical therapy and associated rehabilitative measures. Moderate exercise and stretching to avoid osteo-articular complications are generally tolerated. Patients with limb and vertebral deformities often need corrective orthopedic surgeries.

Unfortunately, pharmacological approaches are not sufficient and the prognosis is often poor, since most of the drugs tested are not reliable. For instance, ascorbic acid, that was promising in phase I studies (Passage et al., 2004), did not improve the clinical outcomes in humans. Other drugs are used with an empirical approach. Recently, a phase II clinical trial involving patients with CMT1A treated for one year with PXT3003, a low dose combination of the three already approved drugs, baclofen, naltrexone and D-sorbitol, showed promising results. The drugs are safely and tolerable. However, the analysis of the outcomes is still in progress (Attarian et al., 2014).

Neurofibromatosis

NF1, NF2 and schwannomatosis are a spectrum of tumor syndromes caused by a mutation in different tumor suppressor genes (Blakeley and Plotkin, 2016). Mutation of these genes induce dysregulation of pathways responsible for cell division and correct proliferation, resulting in vulnerability and additional genetic alterations that evolve in cancer formation. Nevertheless, in patients with NF1, NF2 or schwannomatosis, the tumor are histologically benign (with a low incidence of malignancy), involving the CNS and the PNS. These tumors lead to the loss of nervous system function and in rare cases mortality.

NF1 is a rare pathology, with an incidence of 1 in 2500-3000 individuals, however is the main autosomal dominant disorder of the NS and one of the most common gene-inherited conditions (Vogel et al., 1999). NF1 disease can impact every system, but the skin, CNS and PNS are commonly affected. Specifically, the skin lesions include cafè au lait spots, as well as coetaneous and subcutaneous neurofibromas. Plexiform neurofibroma (pNF), is a multicellular tumor representing the most common tumor in NF1. It is composed of variety of cell types, including neuronal axons, SCs, fibroblasts, mast cells, macrophages, perineurial cells and extracellular matrix (Laycock-van Spyk et al., 2011).

NF2 has an estimated incidence of 1 in 25000-33000 births (Wiszniewski). Like NF1, is associated with multiple tumors of the CNS and PNS. The characteristic tumors in the NF2 pathology are schwannomas, occurring in intracranial or extracranial peripheral nerves and meningiomas. The diagnostic criteria include the bilateral schwannomas of the superior vestibular branch of the eight cranial nerve known as vestibular schwannoma, (VS, or acoustic neuroma) (Kresak and Walsh, 2016). Namely,

VS is the main cause of morbidity in patients affected by NF2 disease. VSs can induce bilateral sensorineural hearing loss, tinnitus, balance difficulty and deafness, facial nerve weakness and possible brainstem compression (Agrup et al., 2007). In adulthood, a more generalized symptomatic severe polyneuropathy occurs in about 3–5% of patients, often associated with an "onion bulb" appearance on nerve biopsy (Evans et al., 1992), progressing to severe muscle wasting and even death. However, around 40% of patients show evidence of polyneuropathy (Sperfeld et al., 2002) and ophthalmic features, leading often to visual acuity reduction.

Nevertheless, 41% of patients have no bilateral VSs at the onset of the pathology, for this reason, a body of diagnostic criteria has been created for NF2. These characteristics include the widely recognized “Manchester criteria” as well as additional NIH criteria shown in table below (Table 2).

Main criteria	***Additional criteria***
Bilateral vestibular schwannomas or	Unilateral vestibular schwannoma plus any two of the following: meningioma, glioma, schwannoma, or juvenile posterior lenticular opacities or
First-degree relative with neurofibromatosis type 2 plus 1-unilateral vestibular schwannomas or 2-any two of the following: meningioma, glioma, schwannoma, or juvenile posterior lenticular opacities	At least two meningiomas plus 1-unilateral vestibular schwannoma or 2-any two of: glioma, neurofibroma, schwannoma, and cataract

Table 2 Clinical diagnostic criteria for NF2. (Kresak and Walsh, 2016)

The NIH criteria include patients with no family history who have multiple schwannomas and/or meningiomas, not yet developed. Patients who have asymmetric involvement are probably mosaic (Evans et al., 1999). At very young ages, less then 18 years old, individuals presenting with an apparently isolated meningioma or vestibular schwannoma (Figure 13) (Plotkin et al., 2011) have respectively 20% and 10% likelihood of developing NF2. However, after 20 years of age this rate drops dramatically and the diagnosis becomes very difficult after 30 years of age (Plotkin et

al., 2011). The diagnostic method is: clinical and family history, cutaneous and ophtalmic examination, craniospinal magnetic resonance imaging (MRI), molecular analysis.

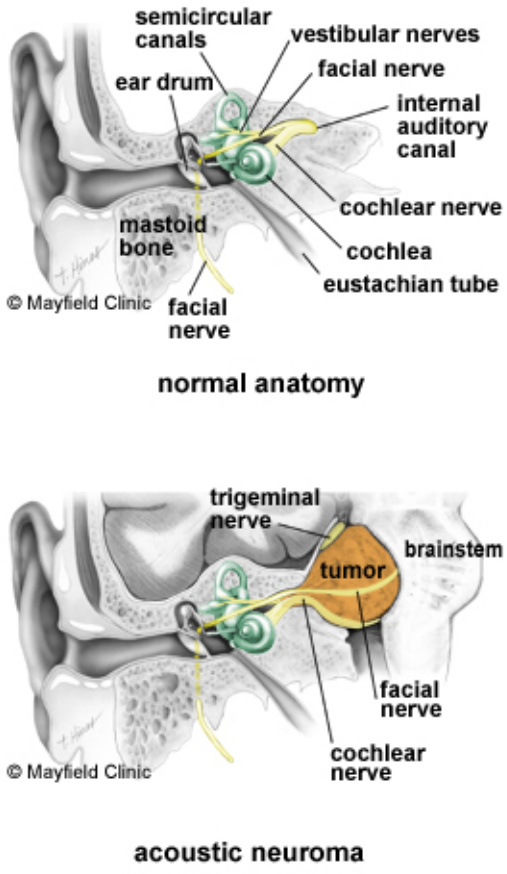

Figure 13 An acoustic neuroma expands out of the internal auditory canal, displacing the cochlear, facial, and trigeminal nerves located in the cerebellopontine angle. Eventually, the tumor compresses the brainstem. *https://www.mayfieldclinic.com/PE-Acoustic.htm*

Assessment of the frequency of NF2 in the population is possible whit clinical diagnostic criteria based on mutations in the *NF2* gene (Evans et al., 1992; Rouleau et al., 1993; Trofatter et al., 1993). However, this is difficult because there are an high number of mosaicism (Evans et al., 1998).

Standard mutation techniques detected 35-66% of pathogenic mutations (MacCollin et al., 2003; Baser et al., 2004). Detection rates are much higher for no-mosaic NF2, mosaics require testing of two tumors or sensitive Next Generation sequencing. The majority of these mutations were truncating mutations, leading to the formation of smaller and non-functional protein. Missense mutations of *NF2* gene, large deletions (which result in no protein product) cause mild phenotypes; studies conducted on different families confirmed these findings (Baser et al., 2004). The C > T transitions leading to a nonsense mutation are the most common mutations in the *NF2* gene (Ahronowitz et al., 2007). Phenotype is more variable in patients with alternative splicing mutations that manifest a mild disease (Baser et al., 2004, 2005). In particular, the mild cases bear a mosaicism, in which only a proportion of cells contain the mutated *NF2* gene, and this proportion depends on how early in development the mutation occurs. In fact, recent evidence suggests that up to 20-30% of NF2 cases without a family history are mosaic, that bear the mutation in a small population of lymphocytes, undetectable from blood samples (Kluwe et al., 2003; Evans et al., 2007). The mosaicism present mutation which can be detected by analyzing tumor material from an affected individual. If an identical mutation is found in two tumors from that individual, their offspring can be tested for the presence of the mutation. However, if an offspring has inherited the mutation, they will have a typical phenotype and usually be more severely affected than their parent, since the offspring will carry the mutation in all of their cells (Evans et al., 2007).

The management of NF2 is the surgical removal of symptomatic cranial and spinal tumors, although the surgical approach is generally complicate. It is important to balance the use of microsurgery and radiation treatment, that can be the therapeutic

option in patients who exibit aggressive tumors, poor surgical risks, or refuse surgery. This therapeutic choice may be carried on even if the tumor is larger than the size criterion for treatment (Rowe et al., 2002).

The facial weakness, after microsurgery, compromise the health of the eye, resulting in a loss of the protective blink reflex, and tear production. Moreover, if the trigeminal nerve is involved, the eye becomes exceptionally vulnerable to corneal ulceration and blindness. Beside microsurgery and the radiation therapy, the majority of NF2 patients become completely deaf, especially because the tumors in these patients are more difficult to treat than those in patients with sporadic unilateral VS. Teams experienced in the positioning of brainstem implants can offer partial auditory rehabilitation to those who are deaf, although results are minor compared to cochlear implants. Although the cochlear nerve may be left intact after surgery, its blood supply may be altered. Nonetheless, few patients can be rehabilitated successfully with a cochlear implant (Rowe et al., 2002).

Mechanical cues

Mechanobiology is a particular field of sciences that study the effect of physical forces, like stretching and compression on living systems (Halder and Bhattacharyya, 2012). Cells are able to translate a physical stimulus into biochemical signals, by activating mechanotransduction systems. By this mechanism cells control different processes such as cell behavior, growth, differentiation and also tumor progression (Dupont et al., 2011). For instance, during the embryonic development, the physical features of the extracellular matrix and mechanical forces are integral to morphogenetic processes, defining tissue organization and architecture (Mammoto and Ingber, 2010; Dupont et al., 2011). The physical stimuli that are of interest in mechanobiology include mechanical challenges and radiation exposition.

The study of mechanical stimuli that guide the development of myelinating glial cells was only recently addressed (Jagielska et al., 2012; Lourenço and Grãos, 2016). In the last year, studies on electromagnetic field (EMF) indicated that the environment may affect SCs development (Lacy-Hulbert et al., 1998). Although the nature of the forces that affect the SCs differentiation in vivo remains non fully understood, as well as their potential involvement in pathogenic alterations and tumorigenesis, SCs were shown to be mechanosensitive (Poitelon et al., 2017).

Among different intracellular mechanisms, YAP and TAZ are generally activated by mechanical stimuli, thus regulating SC proliferation and the transcription of genes encoding for basal lamina receptors (Poitelon et al., 2016).

EMF stimulation

Stimulation with EMF at low frequency (20 Hz) has been used for long time in therapy, for regenerative medicine, particularly for the promotion of nerve regeneration (Gürler et al., 2014). Brief electrical stimulation is effective in accelerating axon outgrowth across injury sites (Al-Majed et al., 2000b; Brushart et al., 2002). The electrical stimulation is also able to increase neurotrophic factors expression and, in turn, growth-associated genes (Al-Majed et al., 2000a).

Moreover, magnetotherapy uses magnetic devices includes magnetic bracelets, insoles, wrist and knee bands, back and neck braces, and even pillows and mattresses (Finegold and Flamm, 2006).

A brief post-surgical stimulation with electrical input is a cooperating therapy for nerve regeneration (Chan et al., 2016). Its potential for clinical translation has been demonstrated in two recent studies on patients with compressive neuropathy and digital nerve laceration, but the mechanism of action is still not completely elucidated. Moreover, more clinical data are required before electrical stimulation will become a mainstream therapy, especially for the assessment of possible risk. All these therapies were performed at low frequency, such as 20 Hz.

Indeed, EMF are also emitted by several common electrical devices, for example, mobile phones, emitting EMF at an intensity of 50 Hz. Epidemiologic studies (Funk and Monsees, 2006; Gürler et al., 2014) evidenced the risk of EMF exposure for the onset of neurodegenerative diseases and for different type of tumors (Carpenter, 2013), such as schwannomas. Several data obtained from clinical studies corroborated such as pathogenic correlation (Hardell et al., 2006; INTERPHONE Study Group, 2011). However, the topic is very current, given the large diffusion of

electrical devices potentially emitting EMFs, and is important to underlie that the work frequencies is a key point for the therapy.

Aims

PNS diseases are a class of heterogeneous pathologies for which there are poor and unreliable therapies. Probably, this may be in consequence of their heterogeneic mechanisms and likely unknown etiology. Nowadays, the treatments are often symptomatic and there are no specific drugs that can lead to the full nerve recovery. The identification of specific and novel therapeutic approaches is a medical need. Although is difficult, given the complicated mechanism at the bases of the pathologies. In this light, the identification of the molecular mechanisms regulating the SCs development, maturation and regeneration is fundamental for the comprehension of possible therapeutic approaches.

Several different pathways are involved in the control of SCs origin, development and maturation processes, and in this scenario the main aim of this thesis was to shed light on three different but correlated signaling: the SRC/FAK singaling, the Hippo pathway and the GABAergic signaling.

Therefore, the studies reported and discussed in this thesis can be subdivided in three experimental aims:

1. the study of SRC/FAK pathway and their interaction with neuroactive steroid ALLO, known to have a role in the myelination process, via the GABA-A R;
2. the study of the physical stimulation by EMF of the SCs, deepening the study of Hippo signaling and YAP/TAZ pathway as key regulator of SCs.
3. the study of the GABAergic system, through the identification of the mRNA expression profile in conditional *knock out* mice for the GABA-B1 R, that specifically lack GABA-B1 R in SCs.

The 1st aim has been investigated in chapter 1 and will discuss how ALLO can affect different SC features, such as motility, migration and myelination, via the activation of SRC/FAK pathway. ALLO is important for SCs myelination process as well as SRC/FAK are important for cell proliferation. Therefore, the aim of this chapter is to highlight the impact of this novel mechanism on the maturation and myelination of SCs.

Merlin is involved in the control of SCs cytoskeleton organization and proliferation. Mutations in *NF2* gene leads to the onset of the Neurofibromatosis. EMF stimulation can impact on different SCs features such as cytoskeleton rearrangements, proliferation and migration properties, via NF2 regulation and the Hippo pathway. The 2nd aim has been investigated in chapter 2 and will discuss how the exposure of EMF, as a kind of mechano-stimulation, may impact on the oncogenic transformation of SCs. The aim is to identify possible pathogenic contributory causes of Merlin changes. Moreover, the involvement of the novel pathways Hippo and YAP/TAZ will be also considered.

GABA-B1 is important for SCs myelination. This has been shown by means of conditional GABA-B1 *knock out* mice, where the transcriptomic profile shows a consistent amount of up- or downregulated genes and miRNAs. MiRNAs induce post-translational modification probably involved in the myelination process. The 3rd aim has been investigated in chapter 3 and will discuss the expression profile and miRNAs in GABA-B1 conditional *knock out* mice, with specific deletion of GABA-B1 R in SCs. The aim is to identify novel possible targets, including miRNAs, that may be downstream GABA-B1 Rs in SCs.

Materials and Methods

Animals

For the experiments discuss in Chapter 3, GABA-B1$^{fl/fl}$ (Haller et al., 2004) mice were crossed with *P0*-Cre deleter mice (Feltri et al., 1999) to obtain mice. Which were then back-crossed with GABA-B1$^{fl/fl}$ mice. The resulting *P0*-Cre/GABA-B1$^{fl/fl}$ mice, with specific deletion of GABA-B1 in Schwann cells, were chosen as experimental group (*P0*-Cre/GABA-B1$^{fl/fl}$), and were compared with GABA-B1$^{fl/fl}$ mice, chosen as control. Experiments were conducted on 3-month-old male mice. All experiments were done according to institutional guidelines and in compliance with the policy on the use of animals approved by the European Communities Council Directive (2010/63/UE) and the Italian law on the use of animals for scientific studies (D.Lgs 26/2014).

Rat Schwann cells primary cultures

For the experiments discuss in 1st and 2nd chapters, rat SCs culture were obtained by the method of Brockes (Brockes et al., 1979) with minor modifications (Magnaghi et al., 2007). Sciatic nerves from 3-day old rats were digested with 1% collagenase and 0,25% trypsin (Sigma-Aldrich, Italy), then filtered through a 30 μm nylon membrane and centrifuged 10 min at 280 g. Pellets were suspended in DMEM (Dulbecco modified eagle medium - Euroclone, Italy) plus 10 % FBS (fetal bovine serum - Life Technologies Italia, Italy) and were plated on 35 mm Petri dishes. After 24 h, the medium was supplemented with 10 μM arabinoside C (Sigma-Aldrich, Italy) then after 48 h the cultures were treated with a stream of cold DMEM-FBS 10%. The remaining cell were plated in DMEM-FBS 10% plus 10 μM forskolin (Sigma-Aldrich, Italy) and 200 μg/mL BPE (bovine pituitary extract - Invitrogen, Italy). Cells became confluent in 10 days. Immunopanning for final purification was carried out incubating the cells

30 min with mouse anti rat Thy 1.1 antibody (Serotec, Italy) followed by 500 μL of baby rabbit complement (Cedarlane, Canada). Cell suspension was seeded on 60 mm petri dishes ($9x10^4$ cells/Petri) and maintained in DMEM, 10 % FBS, 2 μM forskolin, 200 μg/mL BPE. At the third *in vitro* passage, SCs were treated for 48 h with 4 μM forskolin, then used for experiments.

EMF

For the experiments discuss in the 2nd chapter rat SCs were plated and treated with EMF at 50 Hertz (Hz) and 0.1 Tesla (T) for 10 min at 37 °C, then were used at different time points, according the specific experimental assays. SCs used as control were plated in same culture conditions, without EMF exposure.

Pharmacological treatments

For the experiments discuss in the 1st chapter rat SCs were treated for the indicated time with 10^{-6} M ALLO; a micromolar concentration was chosen to exclude any possible involvement of GABA-mediated endogenous activity. To test SCs growth, migration and chemotaxis SCs were treated with ALLO alone or ALLO plus 10^{-5} M PP2 (4-amino-5-(4-chlorophenyl)-7-(dimethylethyl)-pyrazolil-[3,4-*d*]pyrimidine) and analysed at 2, 6, 24 or 48 h, lasting until 6 DIV in the long-term SCs assay. Concentration of GABAergic agonist/anatagonist were chosen based on previous experience (Magnaghi et al., 2007; Perego et al., 2012). To analyse the role of actin dynamics, the SCs were incubated for 1 h with cytochalasin D2 x 10^{-6} before a 30 min ALLO incubation. All drugs were from Sigma. Controls cultures were treated with vehicle (ethanol).

Immunofluorescence (IFL) and confocal scanner laser microscopy

For the experiments discuss in the 1st chapter, rat SCs were seeded on slides in 12-multiwell plates ($15x10^3$ cells/well), treated for 24 h with 10^{-6} M ALLO or 10^{-6} M ALLO plus 10^{-5} M PP2, then fixed in 4 % paraformaldehyde and processed for immunostaining. SCs purity (more than 98 %) was tested with a specific antibody against glycoprotein P0 (Magnaghi et al., 2007). Phalloidin-FITC staining of f-actin (1:250 – Sigma Aldrich, Italy) was used to reveal SCs cytoskeleton. Slides were incubated overnight at 4 °C in PBS (phosphate buffer saline- Euroclone, Italy), 0,25 % BSA (Bovine serum albumin – Sigma Aldrich), 0,1 % Triton X-100 and the specific primary antibody. The following day, slides were washed and mounted using Vectashield™ (Vector Laboratories. Burlingame, CA, USA). Nuclei stained with DAPI (40,6-diamidino-2-phenylindole).

For the experiments discuss in the 2nd part of the results section, anti-NF2 antibody (1:500, Santa Cruz Biotecnology Inc, USA) and anti S100 protein (1:200, Sigma, Italy). The following day, the slides were washed two times and incubated 2 h at room temperature with Alexa-488 (green) or Alexa-594 (red) specific secondary antibody (1:800, Gibco-Life Technologies, Italy). After washing, slides were mounted using Vectashield™ (Vector Laboratories. Burlingame, CA, USA) and nuclei stained with DAPI.

Controls for the specificity of antibodies included a lack of primary antibodies. Confocal microscopy was carried out using a Zeiss LSM 510 System (Oberkochen, Germany).

Proliferation assay

For the experiments discuss in the 1st and 2nd chapters, proliferation assay on SCs was performed using an automated cell counter (Luna; Logos Biosystems Inc, USA); 10.000

cells were plated into 35 mm petri dishes and collected after 6, 24, 48 and 72 h, with trypsin 0,05 %-EDTA (Ethylendiaminetetraacetic acid) 0,02 % in PBS (Euroclone, Italy). The cells suspended in DMEM were then counted with the vital stain Trypan blue (Logos Biosystems Inc, USA), which stains only death cells.

Migration and chemotaxis assays

For the experiments discuss in the 1st chapter a wound healing assay was performed making a scratch on the bottom of the petri containing SCs, then the medium was changed with fresh medium plus mytomicin 50 ng/mL (Sigma- Aldrich, Italy) to counteract cell proliferation and the cells exposed to EMF or 10^{-6} M ALLO and 10^{-6} M ALLO plus 10^{-5} M PP2, respectively. Cells were then photographed with a scanning microscope (Axiovert 200, Zeiss) at different time points: 2, 6, 24, 48 h and for the EMF experiments also at 72 h after the scratch (*t=0*). Pictures were acquire using MetaVue software and the distances between cell fronts were measured with Image-ProPlus 6.0 (MediaCybernetics, USA), considering at least nine measurements from the top to the bottom.

For EMF experiments, treated in the 2nd chapter, migration was also tested by the Boyden chamber assay (chemotaxis) using a 48-well Boyden's chamber, according to the manufacturer's instructions (Neuroprobe, USA). Cells were exposed to EMF, also in the presence of cyclodextrin 5 mM (as well as the migration assay). In all, 28 μL of control medium (DMEM) or DMEM/FBS 1 % was placed in the lower compartment of the chamber, as chemoattractants. The open-bottom wells of the upper compartment were filled with cells (10^5 cells/well), collected by trypsin and suspended in DMEM plus 0,1 % BSA (Sigma- Aldrich, Italy). Cells migrate through a pre-coated membrane with gelatin (0,2 mg/mL in PBS, 5 days at 4 °C). After migration (overnight, 37 °C), cells adherent to the underside of the membrane were fixed by methanol and stained

according to the Diff-Quik kit (Biomap, Italy). For quantitative analysis, cells were observed and counted using a x40 objective on an optical microscope. Three random objective fields were counted for each well and the mean number of migration cells was calculated.

RNA extraction and qRT-PCR analysis

For the experiments discuss in the 2nd chapter RNA samples were extracted using Trizol (Gibco-Life Technologies, Italy) according to the manufacturer's protocol, then quantified with NanoDrop2000 (ThermoScientific, USA). Pure RNA was obtained after DNAse treatment with a specific kit (Sigma-Aldrich, USA). The retro-transcription reaction was carried with RT Iscript Supermix 5x (Bio-Rad, Italy) on 1 μg of purified RNA and the product was used to make qRT-PCR assay. Primers were designed by QuantPrime software (AG Bioinformatics Max Planck, Postdam, Germany). The following primers were used: *Nf2*: FW5'-ACGATGGCCAATGAAGCTCTGATG-3', RW5'-TGGCCTTGATTCGCTGCATCTC-3'; *P0*: FW5'-CCTGCTCTTCTCTTCTTTG-3', RW5'-CACAGCACCATAGACTTC-3'; *Pmp22*: FW5'-TCCTGTTCCTTCACATCG-3', RW5'-TGCCAGAGATCAGTCCTG-3'; α-tubulin: FW5'-TCGCGCTGTAAGAAGCAACACC-3', RW5'-GGAGATACACTCACGCATGGTTGC-3'; β2-microglobulin: FW5'-TGCTTGCAGAGTTAAACACGTCAC-3', RW5'-TTACATGTCTCGGTCCCAGGTG-3'.

The qRT-PCR was performed by measuring the incorporation of SYBR Green dye (Bio-Rad, Italy) on CFX 96 Real Time System-C1000 thermal cycler (Bio-rad, Italy). Data analysis was performed using the CFX Manager 2.0 software (Bio-rad, Italy), based on $^{\Delta\Delta}$Ct method for the relative quantification. The threshold cycle number (Ct) values of both the calibrator and the samples of interest were normalized to the Ct of the endogenous housekeeping genes. As calibrator, we used the RNA obtained from control sample.

Protein extraction and western blot analysis

Protein samples were extracted from rat SCs in lysis buffer (PBS, 1 % Nonidet P-40 and 1 mM EDTA; all from Sigma-Aldrich) containing a cocktail of protease inhibitors (Sigma-Aldrich, Italy). Samples were heated 20 min at 55 °C to denaturate secondary structure, then 15 ug was loaded onto a SDS-PAGE gel (Criterion TGX, Bio-Rad) and run at 200 V for 40 min in running buffer. Gels were electroblotted to Hybond nitrocellulose membrane (GE Healthcare, Italy). Membranes were blocked with 5 % not-fat dry milk (Bio-Rad, Italy) in PBS (Euroclone, Italy) before the incubation with the primary antibody diluted in the blocking solution. Primary antibodies used were rabbit anti-P0 (1:300, Sigma-Genosys, USA), rabbit anti-Pmp22 (1:300, Abcam, UK), mouse anti-NF2 (1:100, Santa Cruz Biotechnology, USA) and monoclonal anti-alpha-Tubulin as reference (1:500, Sigma-Aldrich, Italy). To detect ERK2 and AKT levels, 10 ug proteins were loaded and the antibodies used were the following: anti-phospho-AKT Ser473 (1:1000, Cell Signaling Technology, USA), anti-AKT (1:1000, Cell Signaling Technology, USA), anti-phospho-ERK2 Tyr185/187 (1:1000, Cell Signaling Technology, USA), anti-ERK2 (1:5000 Santa Cruz Biotechnology, USA), anti-β-Actin (1:10.000, Sigam-Aldrich, Italy). In this case, results were standardized using β-Actin as a reference. Membranes were incubated with appropriated HRP-conjugated secondary antibodies (Millipore, USA). Immunocomplexes were revealed by enhanced chemiluminescence (ECL; GE Healthcare, Italy), visualized using the Chemidoc MP Imaging System (Bio-Rad, Italy) and analyzed by the Image Lab software (Bio-Rad, Italy).

Expression profile of Hippo pathway

Rat Hippo signaling pathway RT2 Profiler PCR array (SuperArray Bioscience, USA) was used to profile the expression of 84 genes related to Hippo signaling. Total RNA was extracted from rat SCs, 2h after treatment, as described above. Single-stranded cDNA was synthesized from 2 μg of total RNA by using the SuperArray reaction ready first-strand cDNA synthesis kit. The cDNAs were mixed with SuperArray RT2 Real time SYBR green/ROX PCR master mix and real-time PCR performed in accordance with the manufacturer's instructions. Thermal cycling and fluorescence detection were performed using an ABI Prism 7700 Sequence Detection System (Applied Biosystems, Italy), then the expression of Hippo signaling regulated transcripts was compared between groups.

Genotyping

Animals genotype was determined by PCR analysis on genomic DNA, extracted from tails, sciatic nerves and liver using microLYSIS®–Plus (Microzone Limited, Haywards Heath, UK), following manufacturer's protocol. Used primers are reported in the table below (Table 3). PCR reaction with CRE-1 and CRE-2 primers on mice tails extracts allowed to determine which mice expressed the CRE recombinase; reactions with P5 and P6 on mice tails extracts allowed to determine which mice presented inserted sequences in the GABA-B1 gene. Lastly, *post-mortem* reactions with P7 and P8 on sciatic nerve and liver extracts allowed to verify the GABA-B1 exon VII and VIII specific deletion in SCs (Faroni et al., 2014a). PCR was performed in a standard reaction mix under the following conditions (30 cycles): 94°C for 30 s; 56°C for 1 min; 72°C for 1 min. A final extension step at 72°C for 10 min was performed. The amplified products were analyzed on 1.5% agarose gels.

Gene	*(5'-3')*
CRE1	5'-CCACCACCTCTCCATTGCAC-3'
CRE2	5'-GCTGGCCCAAATGTTCGTGG-3'
P5	5'-TGGGGTGTGTCCTACATGCAGCGGACGG-3'
P6	5'-GCTCTTCACCTTTCAACCCAGCCTCAGGCAGGC-3'
P7	5'-ATCTCTTCCTTGGCCTGGGTCTTTGCTTCGCTCG-3'
P8	5'-GGGTTATTTGAATATGATCGGAATTCCTCGACT-3'

Table 3 Primers used for genotype analysis on genomic DNA

Mouse SCs and DRG neurons primary cultures

SCs cultures were obtained from sciatic nerves of 3-month-old mice. Nerve was digested with 0,0625% (w/v) collagenase Type IV (Worthington Biochemical, Lakewood, NJ), dispase (0,5 mg/mL; Life Technologies Italia, Italy) and Trypsin (2,5 mg/mL; Worthington Biochemical, Lakewood, NJ), then mechanically dissociated with a pipette, filtered through a 100 μM filter (BD Biosciences, San Jose, CA) and centrifuged 5 min at 900 rpm. Pellets were re-suspended in culture medium composed by DMEM (Euroclone, Italy), 10% FBS (Life Technologies Italia, Italy), 2 % insulin growth factor-1 (IGF-1) and 2 μM forskolin. The cell suspension was then seeded on 60 mm petri dishes and grown in presence of 2 μM forskolin at 37°C, 5% CO_2, and 95% humidity. Forskolin was increased 48 hours before the experiments to 4 μM final concentration.

DRG neurons cultures were obtained from the spinal cord of 3-month-old mice. The DRGs were dissociated incubating in Ham's F12 medium (Life Technologies Italia, Italy) containing 0,125% (w/v) collagenase Type IV (Worthington Biochemical, Lakewood, NJ), then treated with 0,25% (w/v) Trypsin (Worthington Biochemical, Lakewood, NJ). The dissociated DRG neurons were filtered through a 100 μM membrane (BD Biosciences) and centrifuged 5 min at 500 rpm. Cells were then resuspended in Ham's F12 and purified on a gradient of 15% (w/v) BSA (Sigma-Aldrich, Italy). Dissociated neurons were resuspended in modified BSM (Bottenstein and Sato) medium (F12 medium plus 100 μM putrescine, 30 nM sodium selenite, 20 nM progesterone, 1 mg/mL BSA, 0,1 mg/mL transferrin, and 10 pM insulin, all Sigma-Aldrich) and 50 ng/mL nerve growth factor (NGF - Millipore, Italy). Cell suspension of DRG neurons was seeded on a 35 mm petri dish coated with poli-L-lysin and laminin (Sigma-Aldrich) then maintained at 37 °C, 5% CO_2, and 95% humidity.

Transcriptome microarray analysis

Total RNA was extracted from mouse SCs and DRG neurons with DirectZol kit (Euroclone, Italy). RNA quantity was determined by the NanoDrop ND-2000 (Thermo Scientific, Italy). The RNA integrity was determined by the RNA 28S/18S ratio using the Agilent 2100 Bioanalyzer (Agilent Technologies, Santa Clara, CA). Then samples were labeled and hybridized to the Affymetrix GeneChip Mouse Gene 2.0.ST Arrays (Santa Clara, CA) following the manufacturer's instructions. Experiments were due at the facility of Fondazione Istituto FIRC di Oncologia Molecolare (IFOM, Italy). Scanned microarray images were analyzed using the Affymetrix Gene Expression Console with the robust multiarray average normalization algorithm.

Microarray Data Analysis

Affymetrix data analysis was done in the R statistical environment using “oligo” and “limma” packages. Heat maps and scatter plots were generated using the statistical tools provided by the R and Bioconductor projects. Database mining analysis was performed by downloading the Gene Expression Omnibus (GEO) microarray data set from the National Institutes of Health NCBI GEO database and examining the expression levels of genes of interest and housekeeping genes as reported.

Data analysis and statistics

Data were statistically evaluated by GraphPad Prism 4.00 (San Diego, USA). Statistical significance between groups was determined by means of an unpaired Student’s *t*-test, one-way ANOVA with Tukey’s post-test, or by two-way ANOVA using Bonferroni’s *post-hoc* test. *P*-values < 0.05 were considered as significant.

Results and discussion

CHAPTER 1

SRC and phospho-FAK kinases are activated by ALLO promoting SC motility, morphology and myelination

SC maturation and development require the complementary activation of different intracellular signaling pathways. The SRC/FAK are important for SCs for the control of adhesion, motility and migration capability. ALLO, synthetized by SC, acts in an autocrine way on SC proliferation and motility, necessary for normal nerve development, maturation and regeneration.

In this chapter, we performed experiments in order to pursue the aim 1 of this thesis regarding the hypothesis that the mechanism underlying the ALLO actions on SCs involve the signaling intermediates SRC and FAK.

ALLO regulates SC morphology and motility

Data previously collected in our and others laboratories demonstrated that ALLO increases SC proliferation, particularly via GABA-A mediated mechanisms (Faroni et al., 2012; Perego et al., 2012). First, the cells were exposed to ALLO 10^{-6} M for 24 h and it was found that *in vitro* treatment with ALLO 10^{-6} M induced SCs morphological rearrangements, giving to these cells the capability to assume the typical spindle-shaped morphology (Figure 14a). This effect was counteracted by the co-treatment with the selective inhibitor of SRC kinase, PP2 10^{-5} M, [PP2 10^{-5} M concentration was chosen on the base of previous experiments (Zheng et al., 2012). Indeed, SCs co-treated with ALLO and PP2 for 24 h showed changes in morphology, resembling flattened cells (Figure 14a). This data suggested the involvement of SRC signaling cascade in the control of the ALLO-induced changes in SCs morphology. A direct involvement of Src

was further corroborated by phalloidin IFL. ALLO proved able to enhance the typical spindle-shaped morphology of SCs, as shown by stress fibers immunostaining (Figure 14b, central panels and Figure15). Furthermore, ALLO induces formation of radial lamellipodia in SCs (Figure 13b, central panels and Figure 14). The simultaneous PP2 co- treatment changed the SCs morphology towards an enlarged and flattened phenotype, in which the lamellipodia were significantly reduced (Figure 14b, lower panels and Figure 15), still suggesting a strong involvement of SRC in the ALLO-regulated SCs adhesion.

Furthermore, to test the long-term effects of ALLO and PP2 (i.e. Src involvement) on morphology and adhesion, the SCs cultures were treated and analyzed at 6 DIV. Exposure to ALLO 10^{-6} M still promoted the growth and the characteristic spindle-shaped morphology (Figure 14c), whereas the SCs culture exposed contemporary to ALLO and PP2 10^{-5} M appeared suffering and decreased in number (Figure 14c).

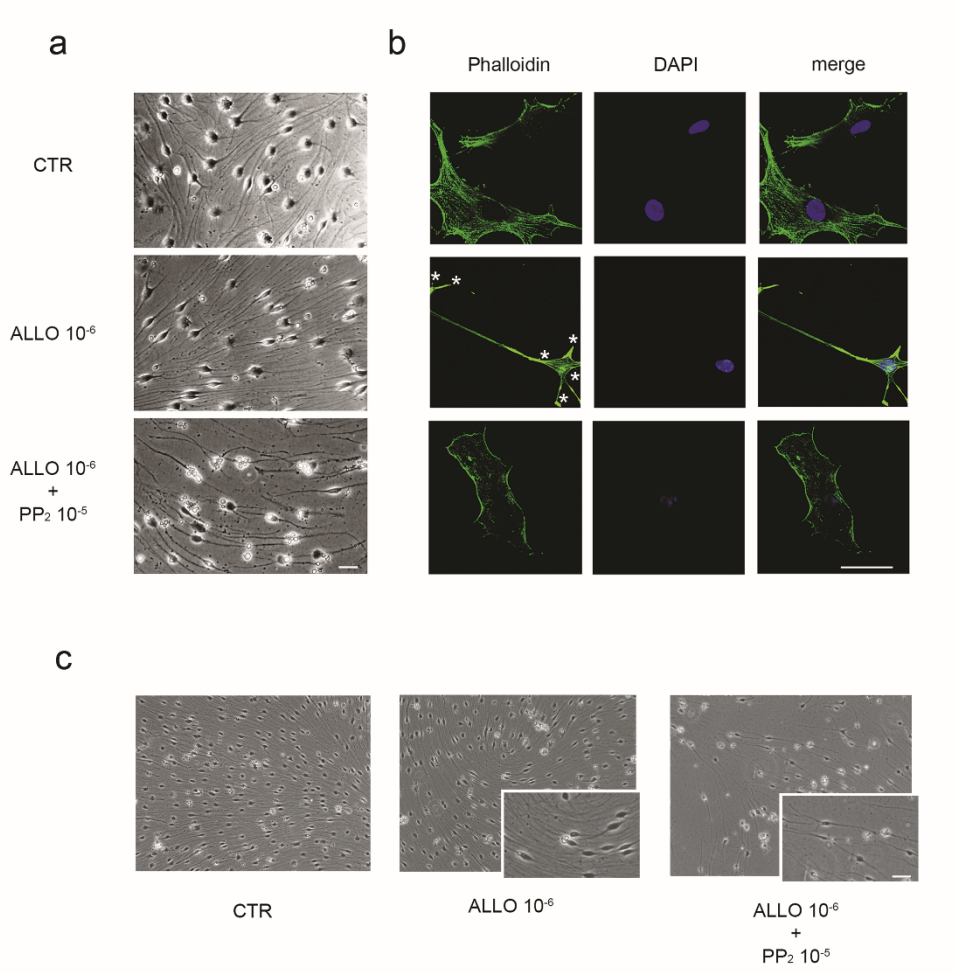

Figure 14 ALLO regulates SCs morphology. *(a) Light microscopy images of SCs treated for 24 h with ALLO 10^{-6} M and ALLO plus the Src inhibitor PP2 10^{-5} M. ALLO treatment induced the typical SCs spindle-shaped morphology that changed versus flattened cells following PP2 exposure. CTR, control cultures exposed to vehicle. Bar 10 µm. (b) ALLO treatment induced SCs morphological rearrangements in actin cytoskeleton, as assessed by immunopositivity for f-actin (phalloidin-FICT, in green). After 24 h, ALLO 10^{-6} M enhanced the stress fibers and radial lamellipodia formation in SCs (white asterisks in central panels), whereas the simultaneous PP2 10^{-5} M co-treatment changed the SCs, enlarging shape and reducing lamellipodia (lower panels). Dapi (in blue). Bar 10 µm. (c) ALLO and PP2 also exerted long- term effects (at 6 DIV) on SCs morphology and adhesion. Exposure to ALLO 10^{-6} M, indeed, promoted the characteristic spindle-shaped morphology (Figure 14c central panel; see also cell details at higher magnification). Conversely, SCs simultaneously exposed to ALLO 10-6 M plus PP2 10-5 M degenerated and decreased in number (Figure 14c right panel; see cell details at higher magnification). CTR, control cultures exposed to vehicle. Bar 10 µm.*

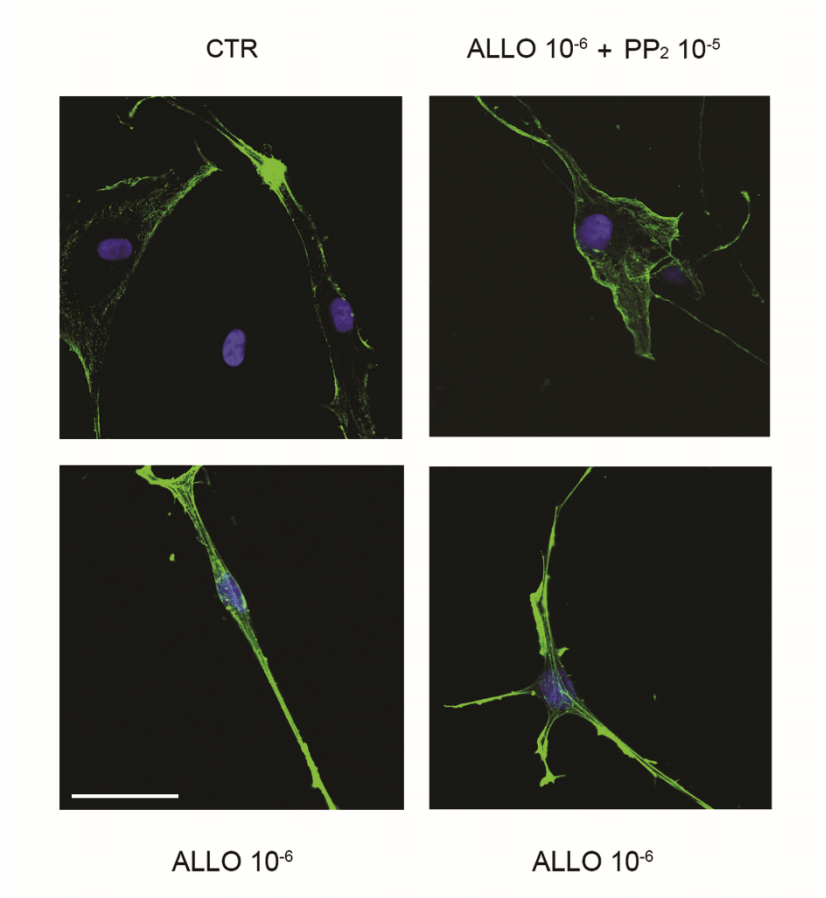

Figure 15 *After 24 h, ALLO 10^{-6} M treatment induced SCs morphological rearrangements in actin cytoskeleton, as assessed by immunopositivity in green for f-actin (phalloidin-FICT, upper right panel). ALLO 10^{-6} M plus 4-amino-5-(4-chlorophenyl)-7-(dimethylethyl)-pyrazolil-[3,4-d]pyrimidine (PP2) 10^{-5} M co-treatment enlarged SCs shape and reduced lamellipodia (lower left and right panels). CTR, control culture (upper left panel). Dapi in blue. Bar 10 µm.*

Then, it was interesting to analyse whether ALLO may control SC migration. To assess this hypothesis, we designed a wound-healing assay on a SCs monolayer treated with ALLO 10^{-6} M was performed. A great number of SCs were able to repopulate the wounded region within 24 h (Figure 16b), achieving a complete closure of the two sides at later time, 48 h (Figure 17). ALLO 10^{-6} M exposure induced a stimulation of SCs migration (Figure 16b) compard to controls (Figure 16a), that was significantly increased ($p < 0.001$; $F = 30.72$) at 2, 6 and 24 h after treatment (Figure 16d). This effect was significantly blocked ($p < 0.001$; $F = 30.72$) by the simultaneous co-treatment with

PP2 10^{-5} M (Figure 16c), vs controls (Figure 16a), confirming that ALLO stimulation might be via Src activation. Furthermore, a 24 h ALLO treatment induced a significant increase ($p < 0.001$; $F = 30.72$) in SC response to chemotactic agents. The Boyden's chamber assay, indeed, indicated that the ALLO- exposed SCs were responsive to a chemotactic agent, such as FBS. The number of migrating cells was significantly augmented ($p < 0.05$; $F = 78.36$) after 24 h treatment with ALLO 10^{-6} M. These findings suggested that ALLO makes SCs more responsive to the chemoattractants (Figure 16e). The simultaneous co-treatment of SCs for 24 h with ALLO 10^{-6} M plus PP2 10^{-5} M significantly reduced ($p < 0.01$; $F = 78.36$) the response to FCS, still evidencing that SRC is involved in the ALLO's induced chemoattractant responsivity of SCs.

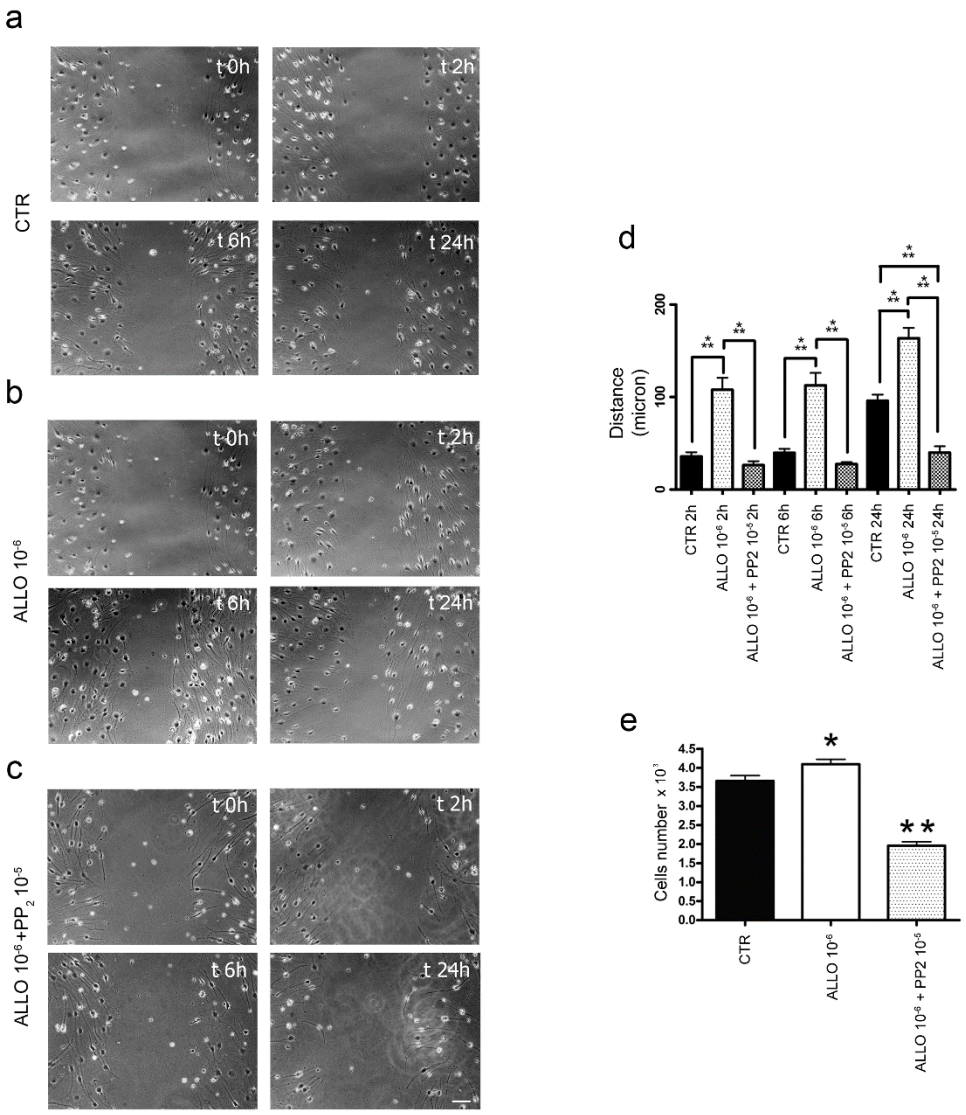

Figure 16 ALLO regulates SCs' motility and chemoattractant responsivity. *(a) Microscopic images of control (CTR) SCs cultures showing a scratch on the bottom of the well (t 0 h). Medium was replaced and cell proliferation was blocked with 50 ng/mL mitomycin. SCs were photographed at 2 (t 2 h), 6 (t 6 h) and 24 h (t 24 h) after the scratch. (b) Microscopic images of SCs undergoing a scratch on the bottom of the well (t 0 h). Medium was replaced and cell proliferation was blocked by adding 50 ng/mL mitomycin. SCs were treated with ALLO 10-6 M and analysed at t 2 h, t 6 h and t 24 h. (c) Microscopic images of SCs undergoing a scratch on the bottom of the well (t 0 h). Medium was replaced and cell proliferation was blocked by adding 50 ng/mL mito- mycin. Then SCs were treated with ALLO 10^{-6} M plus PP2 10^{-5} M and analysed at t2h, t6h and t24h .Bar10 µm. (d)Histograms of cell distance (µm) of SCs treated, respectively, with ALLO 10^{-6} M (light dotted columns) or ALLO 10^{-6} plus PP2 10^{-5} M (grey dotted columns) versus controls (CTR, black columns). Treatments with ALLO produced a significant increase in cell migration (***$p < 0.001$) at 2, 6 and 24 h, completely restored by the treatment with PP2 10^{-5} M (***$p < 0.001$). The distance (µm) was calculated as difference between measurements of empty space at time 0 and other time points (2, 6 and 24 h). Data are expressed as the mean ±SEM (N = 3) of 3 independent experiments. Two-way ANOVA*

*using Tukey's multiple comparison post hoc test was used for statistical analysis. F = 30.72 (e) SCs exposure to ALLO significantly increases the responsiveness to the chemotactic agent FCS 1%. Migrating cell number (per well) of SCs treated, respectively, with ALLO 10-6M (white column, *p < 0.05) or ALLO 10-6 M plus PP2 10^{-5} M (grey dot column, **p < 0.01) was calculated after 18 h versus controls (CTR, black column). Data are expressed as the mean ±SEM (N = 3) of 3 independent experiments. One-way ANOVA using Tukey's multiple comparison post hoc test was used for statistical analysis. F = 78.36.*

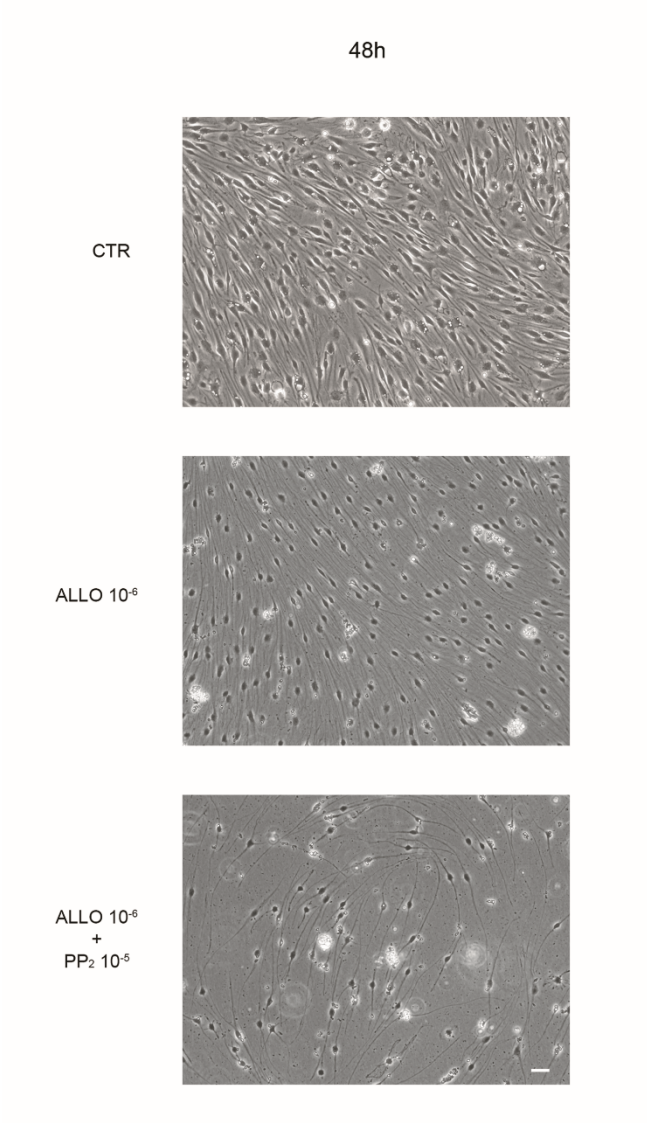

Figure 17 Microscopic images at 48 h (48 h) of SCs undergoing the scratch assay. *SCs in culture achieved the complete closure of the two sides at 48 h, independently of treatment: vehicle (control, CTR), ALLO 10^{-6} M alone or in combination with PP2 10^{-5} M. Bar 10 µm.*

ALLO actions in SCs involve the modulation of SRC and p-FAK pathways

Given the importance of SRC and FAK protein kinases it was interesting to investigate wether these features, may be involved in the cytoskeleton reorganization and migration changes of SC after ALLO treatment.

First, ALLO treatment increased the expression of total SRC and p-SRC, respectively, after 30 and 60 min. Data were normalized for actin (50 kDa) housekeeping protein (Figure 18a), which levels from different experiments were within 10% of each other. Quantitative evaluation at 30 min showed a significant decrease in p-SRC/ SRC ratio ($p < 0.05$; $F = 6.61$), likely because of an increase in total SRC (Figure 18b). Then, at 60 min, a significant increase in p- SRC/SRC ratio ($p < 0.05$, $F = 16.69$) was observed; this was because of an increase in p-SRC (Figure 18c). Altogether, data confirmed a decrease in p-SRC/SRC ratio at 30 min, then an increase at 60 min, suggesting that ALLO lightly stimulates SRC synthesis, in turn inducing its phosphorylation (Figure 18b).

FAK as a signaling protein downstream SRC activation. Therefore, it was investigated the effect of ALLO on FAK expression. FAK showed a protein profile in line with SRC. Indeed, the levels of total p-FAK were increased after 30 and 60 min post ALLO treatment (Figure 18a). The quantitative evaluation at 30 and 60 min after actin normalization) showed a significant increase in p- FAK/FAK ratio ($p < 0.05$; $F = 6.71$, 30 min; $F = 18.01$, 60 min), mainly because of an increase in p-FAK at both time points considered (Figure 18d and e). These results agree with the hypothesis that FAK phosphorylation is likely downstream SRC activation.

ALLO modulation of SRC and p-FAK pathways partially involves GABA-A dependent mechanism

To speculate on the receptor mediating the ALLO-dependent activation of SRC and FAK, the attention was focused first on SRC at 30 min, that is proved to be the early time-point showing significant modifications. Moreover, trying to mimic ALLO effects via GABA-A R, the SCs were treated with muscimol 10^{-3} M alone (selective GABA-A agonist) or ALLO 10^{-6} M plus bicuculline 10^{-4} M (selective GABA-A antag- onist) respectively. Muscimol treatment decreased the p-SRC levels (Figure 19a). The quantitative analysis, after actin normalization, confirmed the significant ($p < 0.05$; $F = 8.92$) decrease in p-SRC with muscimol, in turn producing a significant decrease in the p-SRC/SRC ratio ($p < 0.05$; $F = 8.92$) (Figure 19b). In agreement with data above (see Fig. 19b), the treatment with ALLO significantly decreased the p-SRC/SRC ratio ($p < 0.05$; $F = 8.92$), supporting the GABA-A mediated inactivation of this pathway (Figure 19b). Furthermore, co-treatment with ALLO plus bicuculline counteracted the ALLO's effects on SRC and p-SRC respectively (Figure 19a). Quantitative evaluation (after actin normalization) showed that the p-SRC/SRC ratio after bicuculline treatment was like controls (Figure 19b). This data further suggested that ALLO acts via a GABA-A activation.

Secondly, the quantitative analysis, after actin normalization, showed that ALLO significantly ($p < 0.05$; $F = 14.85$) increased the p-FAK and p-FAK/FAK levels (Figure 19d). Muscimol 10^{-3} M alone did not produce any significant change, suggesting that GABA-A mediated mechanisms should not be involved in this control. The simultaneous treatment with ALLO plus bicuculline 10^{-4} M, however, potentiates significantly ($p < 0.05$; $F = 14.85$) the ALLO-induced rising of p-FAK and p-FAK/FAK

ratio (Figure 19d), suggesting that ALLO may be re-addressed towards different signaling pathways, likely via PR or the putative membrane progesterone receptor (mPR).

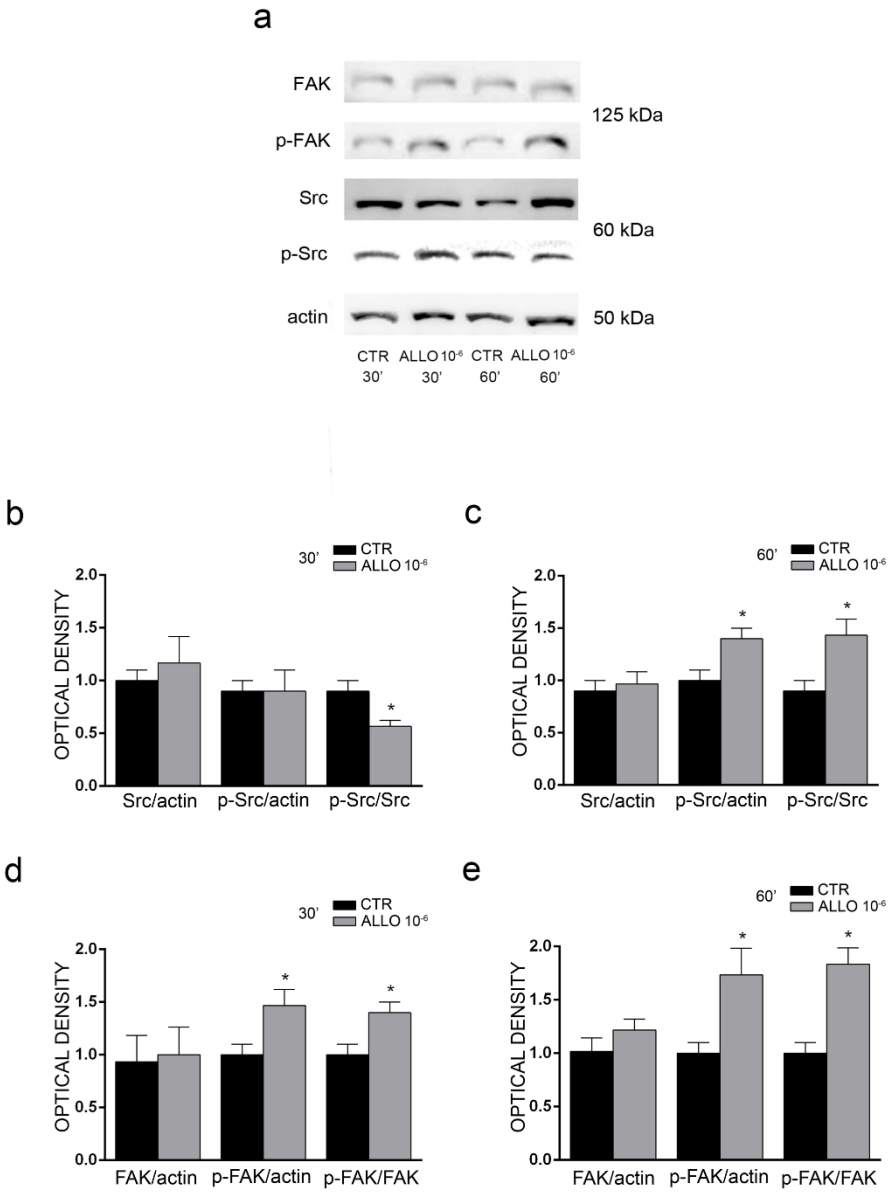

Figure 18 ALLO administration to SCs results in Src and phospho-FAK (p-FAK) activation. *(a) Images are representative of western blot analysis for the total and phosphorylated forms of FAK (125 kDa), and Src (60 kDa), at 30 and 60 min after treatment with ALLO 10^{-6} M. Actin was used as housekeeping. CTR, controls. Quantitative histograms of the ratio Src/actin, p-Src-actin and p-Src/ Src at 30 min (b) or 60 min (c) after treatment with ALLO 10^{-6} M (grey columns) versus control (CTR, black columns). Quantitative histograms of the ratio FAK/actin, p-FAK/actin and p-FAK/FAK at 30 min (d) or 60 min (e) after treatment with ALLO 10-6 M (grey columns) versus control (CTR, black columns). Data are expressed as the mean ±SEM (N = 6) of 3 independent experiments. One-way ANOVA followed by Tukey's multiple comparison post hoc test (*p < 0.05 vs. controls, CTR) was used for statistical analysis. F=6.61(b);F=16.69(c);F=6.71(d);F=18.01(e).*

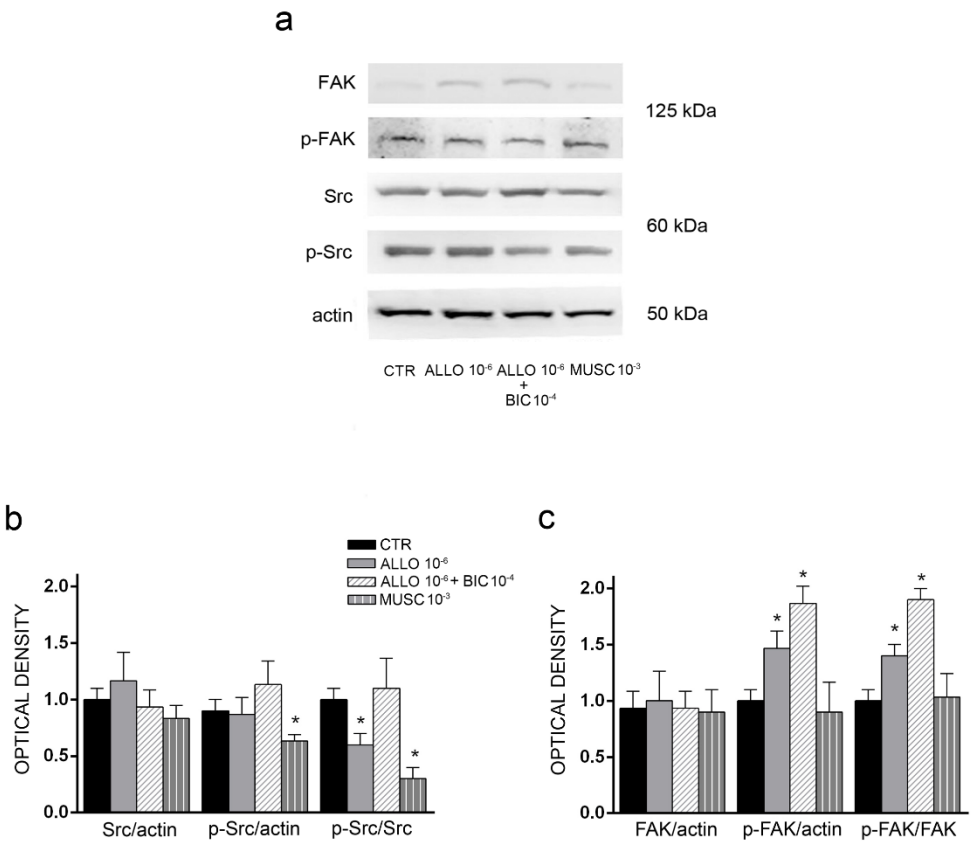

Figure 19 ALLO modulation in SCs partially involves GABA-A-dependent mechanisms. *(a) Images are representative of western blot analysis for the total and phosphorylated form of FAK (125 kDa), and Src (60 kDa) after 30 min treatment with: ALLO 10^{-6} M; ALLO 10-6 M + bicuculline 10^{-4} M; muscimol 10^{-3} M. Actin was used as housekeeping. CTR, controls. (b) Quantitative histograms of the ratio Src/actin, p-Src/actin and p-Src/Src at 30 min after treatment with ALLO 10^{-6} M alone (grey columns), ALLO 10^{-6} M + bicuculline 10^{-4} M (diagonal line columns) or muscimol 10^{-3} M alone (vertical line columns) versus control (CTR, black columns). (c) Quantitative histograms of the ratio FAK/actin, p-FAK/actin and p-FAK/ FAK at 30 min after treatment with ALLO 10^{-6} M alone (grey columns), ALLO 10^{-6} M + bicuculline 10^{-4} M (diagonal line columns) or muscimol 10^{-3} M alone (vertical line columns) versus control (CTR, black columns). Data are expressed as the mean ±SEM (N = 6) of 3 independent experiments. One-way ANOVA followed by Tukey's multiple comparison post hoc test (*$p < 0.05$ vs. controls, CTR) was used for statistical analysis. F = 8.92 (b); F = 14.85 (c).*

ALLO modulation of SRC and p-FAK pathways depends by actin remodeling

The qualitative analysis of western immunoblots showed that, a potent inhibitor of actin polymerization and cytoskeleton remodeling, cytochalasin D, induced an apparent ALLO potentiation of SRC protein levels (Figure 20a). In principle, this effect indicated that changes in actin cytoskeleton might strengthen ALLO's action in SCs. However, the quantitative evaluation of p-SRC/SRC ratio showed no statistical significant changes following a 30-min ALLO treatment in the presence of cytochalasin D 2 x 10^{-6} M (Figure 20b). Treatment with ALLO alone, indeed significantly decreased the pSRC/SRC ratio ($p < 0.05$; $F = 3.97$).

Regarding FAK, a similar qualitative trend was observed (Figure 20a); Cytochalasin D treatment induced an increase in p-FAK levels (Figure 20a). Quantification of p-FAK and p-FAK/FAK ratio still confirmed the significant stimulation induced by ALLO ($p < 0.05$; $F = 3.86$), whereas no change in p-FAK/FAK ratio following cytochalasin D treatment was observed (Figure 20b).

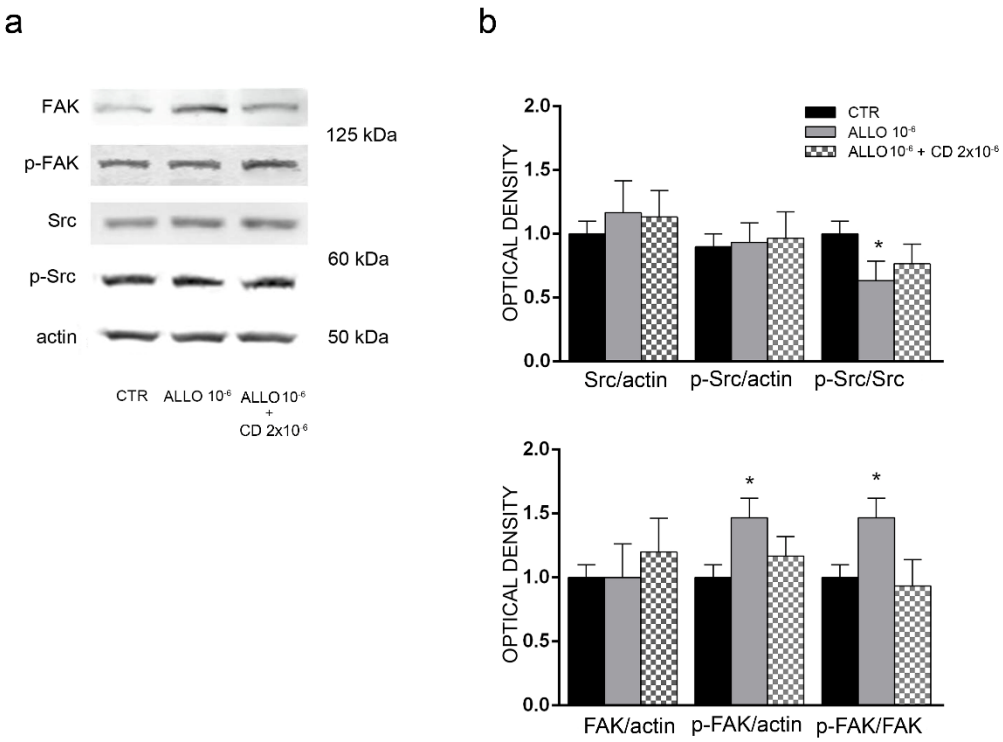

Figure 20 ALLO modulation in SCs depends by actin remodelling. *(a) Images are representative of western blot analysis for the total and phosphorylated forms of FAK (125 kDa), and Src (60 kDa), following a 30 min treatment with ALLO 10^{-6} M or ALLO 10^{-6} + cytochalasin D (CD) 2 x 10^{-6} M. Actin was used as house- keeping. CTR, controls. Quantitative histograms of the ratio Src/actin, p-Src/actin, p-Src/Src (b) and FAK/actin, p-FAK/actin and p-FAK/ FAK (c) at 30 min after treatment with ALLO 10^{-6} M (grey columns) or ALLO plus cytochalasin D 2 x 10^{-6} M (CD, squared columns) versus control (CTR, black columns). Data are expressed as the mean ±SEM (N = 6) of 3 independent experiments. One-way ANOVA followed by Tukey's multiple comparison post hoc test (*p < 0.05 vs. controls, CTR) was used for statistical analysis. F = 3.97 (b); F = 3.86 (c).*

Discussion

In accordance with previous observations (Perego et al., 2012), this work provides evidence that ALLO controls SCs motility and morphological changes, supporting proliferation. ALLO is also able to induce myelination, and these processes involve the activation of SRC and p-FAK signaling. Moreover, ALLO modulation of SRC and p-FAK pathways involves GABA-A dependent mechanisms and relies on actin rearrangements.

It is known that ALLO, synthesized and/or metabolized in SCs, have an important role in the control of myelination, nociception and nerve regeneration (Magnaghi et al., 2006c, 2010; Faroni and Magnaghi, 2011; Patte-Mensah et al., 2014). ALLO exerts a stimulatory action on the PMP22 levels in vitro (Magnaghi et al., 2006a; Melcangi and Panzica, 2009; Perego et al., 2012), inducing the in vivo myelination in injured adult and aged rats (Melcangi et al., 1999; Azcoitia et al., 2003). ALLO participates in the regulation of myelination program by controlling the expression of important transcription factors, such as KROX-20 and SRY-Box10 (SOX10) (Magnaghi et al., 2007). In SCs, ALLO takes part in orchestrating these processes by activating integrated mechanisms that, in turn, involve the GABA synthesis, as well as the GABA-A and GABA-B receptors modulation (Faroni and Magnaghi, 2011; Procacci et al., 2012). Namely, through a PKA-dependent autocrine loop ALLO stimulates the GABA synthesis (Magnaghi et al., 2010), while through a GABA-A-activated PKC-dependent action, ALLO regulates the EAAC1 activity, providing glutamate as GABA precursor in SCs (Perego et al., 2012). However, other protein kinases, such as PKC-epsilon, seem to be involved in ALLO's effects on SCs. Recently, it was suggested that PKC-epsilon may be regulated in DRG neurons by conditioned medium obtained from SCs treated

with 10^{-6} M ALLO (Puia et al., 2015) whether ALLO may alter PKC-epsilon directly in SCs is now under evaluation.

ALLO acts mainly through the GABA-A receptor in a concentration-dependent manner (Majewska et al., 1986; Rupprecht and Holsboer, 1999; Lambert et al., 2003). In the low nano-molar range ALLO's action is allosteric, enhancing the action of the natural ligand GABA, while in the micro-molar range, ALLO directly gates the GABA-A receptor channel (Callachan et al., 1987; Puia et al., 1990). However, the intrinsic cellular mechanisms regulating most of the ALLO-mediated processes are unknown. Therefore, this work speculated on the ALLO's mechanisms that might affect the cellular and biological processes regulating SCs.

Data in the literature evidenced the participation of SRC in the control of cell migration and differentiation (Zhao et al., 2003). In agreement with thus capacity of SRC, it was interestingly to investigate whether ALLO controls SCs morphology and motility via a SRC signaling. These findings corroborate the importance of SRC in the onset of peripheral myelination (Hossain et al., 2010).

As previously reported, EAAC1 delivery on the SCs membrane is stimulated by ALLO and prevented by actin de-polymerization, suggesting that also EAAC1 participates in the control of the rapid ALLO-mediated effects on SC morphology and proliferation (Perego et al., 2012). These phenomena are likely exerted because ALLO can promote the selective EAAC1 binding to proteins tethering the transporter to the actin cytoskeleton. In SCs, ALLO accumulated actin at the leading edge and in the filopodia, whose number was significantly increased (Perego et al., 2012). In addition, here we proved that, beside EAAC1 involvement, the ALLO's effects on actin rearrangements may involve SRC/p-FAK. It is important to underline that in the experimental model,

ALLO's effects on actin remodeling did not entail any alteration in the actin protein levels, which remain within 10% variation among samples analyzed.

Other progestagens were shown to be implicated in the control of actin polymerization and branching as well as in FAK complex formation. These effects seemed to be mediated via the classic PR. Interestingly, these phenomena may be relevant for neuronal plasticity and dendritic spine turnover (Sanchez et al., 2013). Nevertheless, the SRC/FAK signaling cascade might be implicated in the glial cells functions, albeit it was never completely studied in these cells, neither in the CNS nor in the PNS. Only FAK was shown to be required for proliferation, spreading and differentiation of SCs (Grove et al., 2007; Grove and Brophy, 2014). However, FAK does not seem to be required myelin maintenance of adult SCs, nor for re-myelination after nerve injury (Grove and Brophy, 2014). This suggests a role for FAK primarily in SCs development. However, in several models FAK was downstream SRC and upstream moesin activation (Sanchez et al., 2013).

Taken together, these findings corroborate the hypothesis that the ALLO-mediated GABA-A control of SCs may be responsible for the delayed differentiation observed in vivo, following neuroactive steroid treatment (Melcangi et al., 2000; Azcoitia et al., 2003).

Beside the GABA-A involvement in the ALLO's mediated changes of SCs, other mechanisms involving the mPRs or the metabotropic GABA-B Rs might participate in regulating some of the SC changes observed. Indeed, these findings show that SRC seems to be controlled directly by ALLO through a GABA-A dependent mechanisms, whereas FAK might be partially regulated via this receptor. Other signaling systems involving the classic PR or the membrane mPR receptors might be also considered as possible FAK regulators. In addition, some of the effects induced by ALLO might be

due to its retro-conversion in DHP and/or P, still interacting with the classic PR or non-classic mPR, steroid receptors. However, the observation that ALLO-mediated effects on proliferation, chemotactic response and myelination are counteracted by the co-treatment with the specific SRC inhibitor PP2 seem to exclude such a hypothesis.

Finally, apart the well-known capability of ALLO in controlling PNS myelination (Melcangi et al., 1999; Azcoitia et al., 2003; Magnaghi et al., 2006a), ALLO may also regulates myelination and the internode length. Although it is difficult to determine whether such control is exclusively dependent on SRC activation, data from the literature support this relationship. Indeed, SCs from *Lck* -/- *knock out* mice (*Lck*, a lymphoid cell kinase belonging to the SRC kinase family) showed shorter and fewer internodes upon myelination, associated to delayed and altered myelination (Ness et al., 2013). Given that, a functional relationship between the internodal length and nerve conduction velocity was proved (Wu et al., 2012), it was suggested that ALLO, likely via indirect mechanisms, may have important physiological functions in regulating the nerve conduction velocity in peripheral nerves.

In conclusion, this study demonstrated the important role of the neuroactive steroid ALLO in regulating the SCs development and maturation. These effects are mediated mostly by GABA-A receptor and SRC/FAK signaling cascade, resulting in SCs actin remodeling, migration, chemoattractant responsivity and proliferation (Figure 20). The comprehension of these mechanisms may provide the basis for the control of SCs physiological processes and for the development of new therapies for the PN.

CHAPTER 2

Tumor suppressor *Nf2*/Merlin drives SCs changes following EMF exposure through Hippo-dependent mechanism

Mutations of the *NF2* gene, encoding the tumor suppressor protein merlin where shown in sporadic and vestibular schwannomas affecting SCs. Several efforts have been addressed to identify possible factors, even environmental, that regulate neurofibromas development.

In this chapter we performed experiments in order to pursue the aim 2 of this thesis investigating how the exposure of SCs to an EMF of 50 Hz, an environmental challenge able to modulate biological processes, can affect SCs features such as morphology, proliferation, migration and myelinating capability.

Exposure to EMF induces changes in SC morphology and proliferation

SCs primary cultures from 3-day-old rats were used for the experiments. These cells showed the peculiar spindle-shape morphology *in vitro*. Cell purity, more than 98%, was assessed performing immunostaining for the typical specific markers P0 and protein S100 (Figure 21a).

To test the effects of EMF on SC biological features, EMF intensity of 50 Hz, 0.1T for 10 min was applied (Figure 21b). EMF exposure induced morphologic rearrangements in actin cytoskeleton, which might be critical for SCs differentiation and myelination. SCs turn from a spindle- shaped to an enlarged phenotype, indicating a dysregulation in the differentiation program. In fact, cells exposed to the treatment resemble to the undifferentiated phenotype (Figure 21c).

The effects of EMFs on cell proliferation was evaluated in order to test whether EMF exposure may induce other SCs biological changes. Specifically, SCs count was evaluated in vitro at 6, 24, 48 and 72 h following EMF exposure (Figure 21d). The effect already present after 24 h became significantly evident at longer times, 48 and 72 h ($P < 0.05$). Furthermore, a second EMF exposure after 24 h strongly increased SCs proliferation at 48 and 72 h (Figure d), likely suggesting an additive effect of EMF on SCs proliferation. This effect was not dependent on a decrease in cell death. Indeed, EMF did not induce any sign of cell death or changes in cells viability at all time points considered, even after a double exposure (Figure 21e).

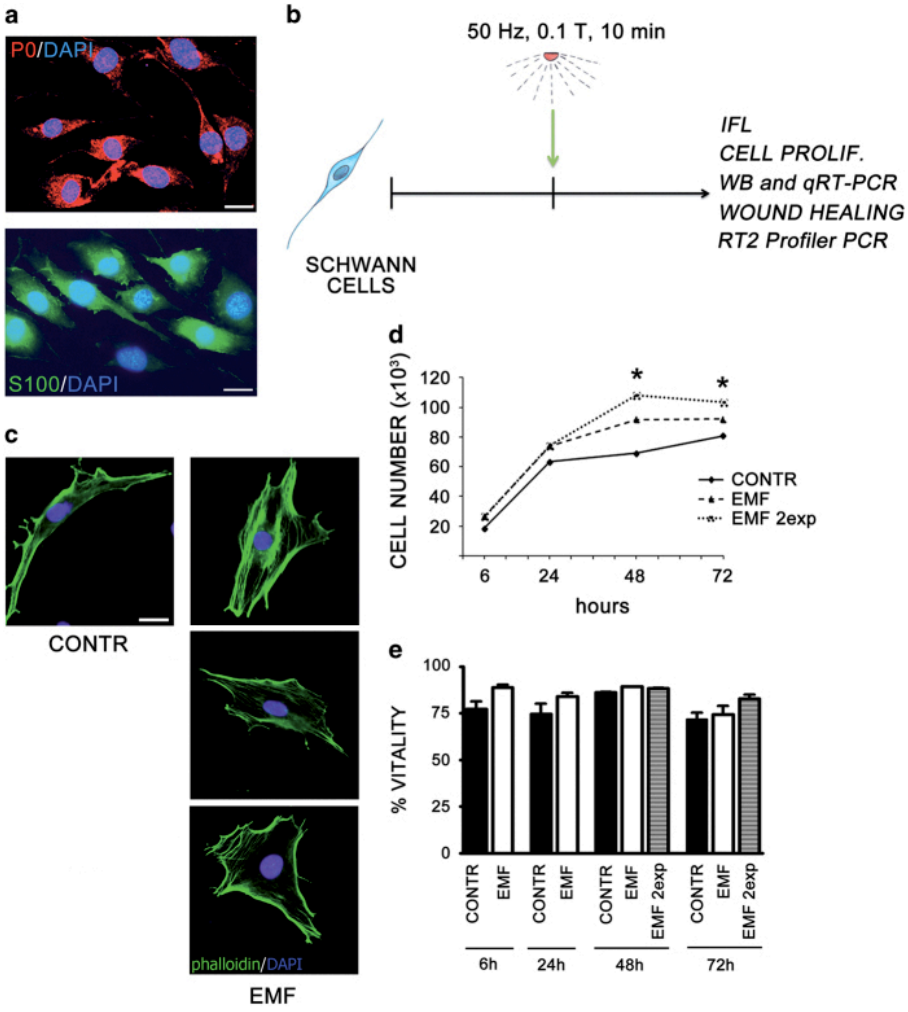

Figure 21 SCs change morphology and proliferation following EMF exposure. *(a) Merge image of SC characterized by immunopositivity for P0 and S100 markers, respectively (anti-P0-594, in red; anti-s100-488, in green), showing a cell purity more than 98%. Nuclei were stained with DAPI, in blue. Scale bar 10 µm. (b) Scheme of the experimental model used. SCs were exposed to EMF of 50 Hz, 0.1 T, for 10 min, then cells were assayed for proliferation, migration, vitality, chemoresponsivity, morphology, western blot, qRT-PCR and RT2 profiler PCR. (c) EMF exposure induces SCs morphologic rearrangements in actin cytoskeleton, as assessed by immunopositivity for f-actin (phalloidin-FICT, in green). SCs turned from a spindle-shaped, characteristic of a more differentiated phenotype, to an enlarged shape, that better represent a SC in its proliferative state, suggesting alterations in the differentiation program. Nuclei were stained with DAPI, in blue. Scale bar 10 µm. (d) SCs proliferation was assessed at 6, 24, 48 and 72 h, following a single (dashed line) or double (dot line) EMF exposure. EMFs produced a significant (*P<0.05) increase in cell proliferation. Experiments were repeated at least three times and data expressed as cell number (×103). Two-way ANOVA using Bonferroni's post hoc test was used for statistical analysis. (e) Percentage of SCs vitality was assessed at 6, 24, 48 and 72 h, following a single (white columns) or double (gray columns) EMF exposure, but no significant changes in SCs vitality were observed. Controls (CONTR, black columns). The values are means ± S.D. (N = 3).*

SCs exposed to EMFs possess greater migratory and chemotactic

After evaluating SC changes in morphology and proliferation a wound-healing assay, on a cell monolayer, and Boyden chamber assays, to measure chemotaxis, were performed. EMF exposure promoted the SC motility. Indeed, a great number of SCs were able to repopulate the wounded region within 24 h, achieving a complete closure of the two sides at later times, 48 and 72 h (Figure 22a). EMF exposure induced a significant increase ($P < 0.05$) in SC motility at 6 and 24h, corroborating the EMF effect on cell migration. The concomitant presence of mitomycin 50 ng/ml excluded any proliferative component on the gap closure. The effect was significantly counteracted ($P < 0.05$) by a pretreatment with cyclodextrin 5 mM (Figure 22c), a molecule used to produce changes in membrane cholesterol, thus indicating that a disorganization in lipid rafts and cell membrane architecture may alter the SC migratory response to the EMF. This is in accordance with the morphologic rearrangement in actin cytoskeleton seen in Figure 22c.

SCs chemotactic response was then evaluated by mean of Boyden chamber assay. EMF-exposed SCs were more responsive to a chemotactic agent, such as FBS (Figure 22d). The co-treatment with 5 mM cyclodextrin reverted the chemotactic migration to the control levels. This effect strongly suggested the hypothesis that an autocrine factor, tightly interacting with the cell membrane, may regulate the SCs development. Likely by this mechanism the SCs address their fate toward a proliferative state and in turn change their migration and chemotactic responsiveness.

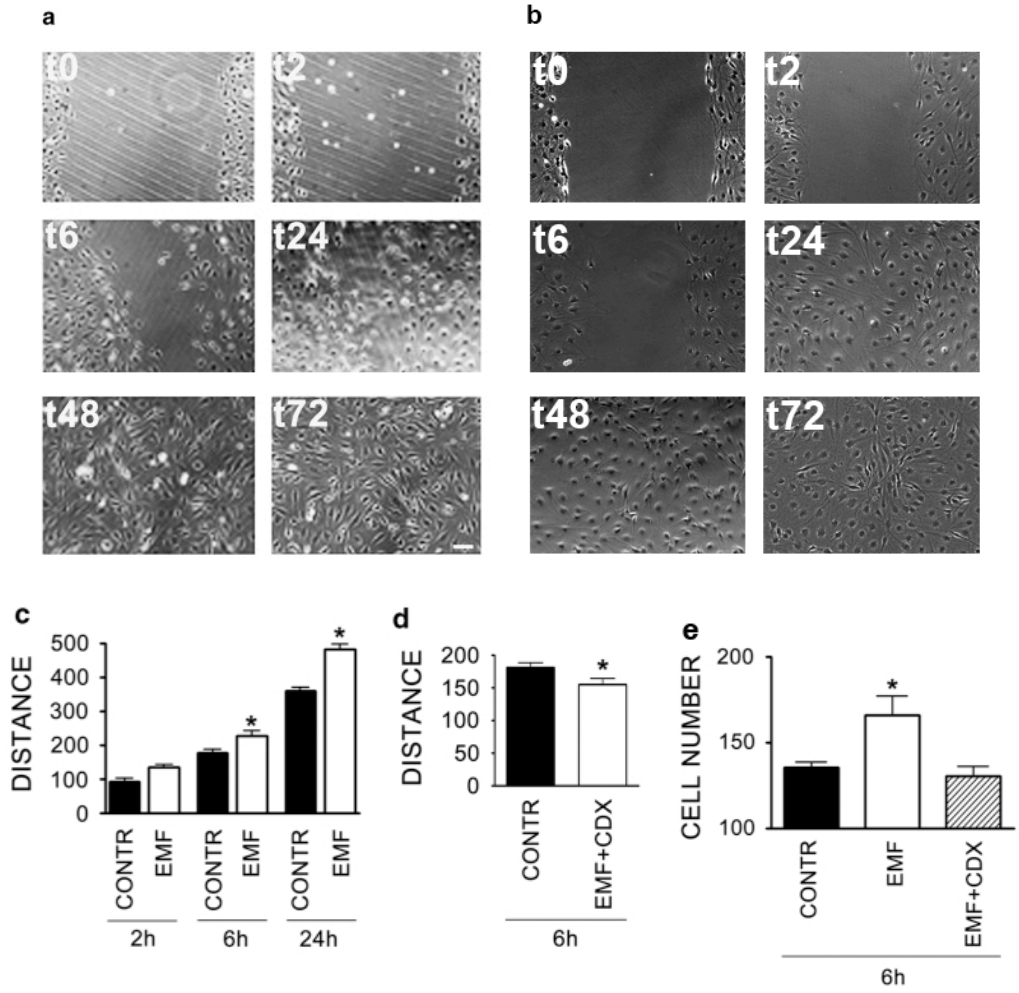

Figure 22 SCs migration and chemoresponsivity are increased following 10 min EMF exposure. *(a) Microscopic images of SCs cultures, exposed to EMF, in which a scratch has been done on the bottom of the well (t0). Medium was replaced and cell proliferation was blocked by adding 50 ng/ml mitomycin. SCs migrate after 2 (t2) and 6 (t6) h, closing the wound region within 24 h (t24). A complete closure was seen at 48 (t48) and 72 (t72) h. Scale bar 10 μm. (b) Microscopic images of control SCs cultures, in which a scratch has been done on the bottom of the well. (t0). Medium was replaced and cell proliferation was blocked by adding 50 ng/ml mitomycin. SCs migrate after 2 (t2) and 6 (t6) h, less than in the treated SCs. Control SCs do not completely close the wound region in 24 (t24) h, they complete the closure of the wounded region in 48 (t48) h, more slowly than in the treated SCs. Scale bar 10 μm. (c) Histograms of cell distance (μm) of SCs exposed to 10 min EMF (EMF, white columns) versus controls (CONTR, black columns). EMFs produced a significant (*P o 0.05) increase in cell migration at 6 and 24 h. The distance (μm) was calculated as difference between measurements of empty space at time 0 and following time points (2, 6 and 24 h). The values are means ± S.D. (N = 3). (d) Distance (μm) of SCs exposed for 6 h to 10 min EMF was significantly counterbalanced (*P o 0.05) by pre-treatment with cyclodextrin 5 mM (EMF+CDX, white column). Experiments and data were calculated versus controls (CONTR, black columns), as above. The values are means ± S.D. (N = 3). (e) A 10-min EMF exposure make the SCs significantly (*P o 0.05) responsive to the chemotactic agent FCS 1%. Migrating cell number (per well) of SCs exposed (EMF, white column) was calculated after 6 h, versus controls (CONTR, black columns). SCs co-treated with 5 mM cyclodextrin reversed the chemotactic response to the control levels (diagonal lines column). The values are means ± S.D. (N = 3). One-way ANOVA using Tukey's post-test was used for all statistical analysis.*

Expression of myelin proteins P0 and PMP22 is changed in EMF-exposed SCs

The increase in proliferation/migration observed was associated with a decrease in myelinating parameters. Overall, the gene expression of two specific myelin proteins of the PNS, the glycoprotein P0 and the PMP22, significantly dropped down (at least $P < 0.05$) in SCs exposed to EMF at 2, 6 and 24 h (Figure 23a). In accordance, also the protein levels were significantly downregulated ($P < 0.05$), whereas the effects were acute at later times, 6 and 24 h post exposure (Figure 23b). Overall, the effects seemed to be larger for PMP22.

Merlin levels are decreased in SCs exposed to EMFs

Changes in the tumor suppressor Merlin are predictive of oncogenic transformations of SCs. After 2h of EMF exposure, the qRT-PCR analysis showed a significant 25% decrease in Merlin gene expression after treatment (compared to control; $P < 0.05$); this effect was not evident at later time points (Figure 23c). In accordance, Merlin protein levels were equally downregulated in SCs, as shown by the immunoblot in Figure 3d. Quantitative data confirmed a significant 25% downregulation ($P < 0.05$) of merlin protein levels 2h after EMF exposure, while no changes were observed at later time points (Figure 23d). Decreased levels of Merlin gene has been associated with defects of SC bipolar extension, according to the enlarged SC morphologic phenotype observed (Figure 21b). However, aside the decreased in the Merlin levels also a different cellular distribution was observed (Figure 23e). In SCs exposed to EMF, Merlin appeared more localized in the cytoplasm rather than in the nucleus (controls). Such an effect corroborated the loss of Merlin suppressor function, which necessarily would occur through a nuclear localization.

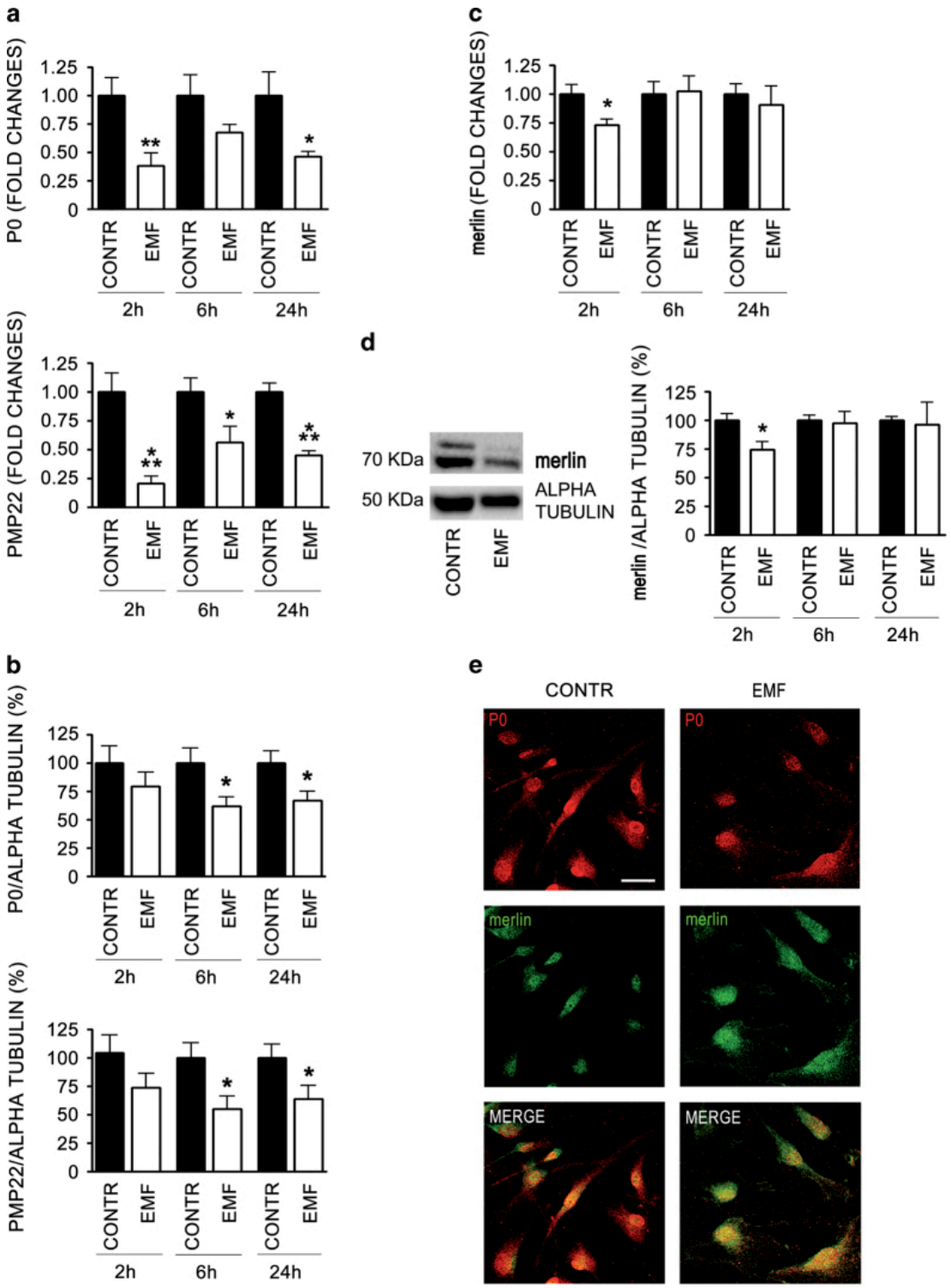
a
P0 (FOLD CHANGES)
1.25
1.00
0.75
0.50
0.25
0
CONTR
EMF
2h
6h
24h
PMP22 (FOLD CHANGES)
b
P0/ALPHA TUBULIN (%)
125
100
75
50
25
PMP22/ALPHA TUBULIN (%)
c
merlin (FOLD CHANGES)
d
70 KDa
50 KDa
merlin
ALPHA TUBULIN
merlin /ALPHA TUBULIN (%)
e
CONTR
EMF
P0
merlin
MERGE

Figure 23 Myelin proteins (P0 and PMP22) and Nf2/Merlin are decreased following 10 min EMF exposure. *(a) Relative quantification by qRT-PCR of mRNA levels, coding for proteins P0 and PMP22 respectively, showed a decreased expression at all time points considered, 2, 6 and 24 h. Data were normalized to the housekeeping genes α-tubulin and β2-microglobulin and expressed as difference (ΔΔCt) versus controls, then averaged for each experimental group. The columns control (CONTR, black) and EMF-exposed SC (EMF, white) were expressed as fold changes. The values are means ± S.D. (N = 3). *P < 0.05, **P < 0.01, ***P < 0.001. (b) Western blot analysis corroborated the decrease of P0 and PMP22 in EMF-exposed SCs (EMF, white columns), with significant effects at later times, 6 and 24 h (*P < 0.05). Data were normalized for α-tubulin, were expressed as percentage versus controls (CONTR, black columns). The values are means ± S.D. (N = 3). (c) Neurofibromin 2 (Nf2) mRNA levels were assayed by qRT-PCR, showing a significant decrease (*P<0.05) 2h after EMF exposure. Data normalized to α-tubulin and β2-microglobulin were expressed as difference (ΔΔCt) versus controls, then averaged for each experimental group. The columns control (CONTR, black) and EMF-exposed SC (EMF, white) were expressed as fold changes. The values are means ± S.D. (N = 3). (d) Accordingly, also the Nf2 protein levels were decreased 2 h following EMF exposure. Qualitative immunoblot (left panel) showing that the specific band for Nf2 (70 KDa) was downregulated in SCs. The α-tubulin (50 KDa) was used as a housekeeping protein. Quantitative data (right panel) confirmed a significant downregulation of Nf2/merlin at 2 h (*P < 0.05, white columns), while no changes were observed at 6 and 24 h. Experiments were normalized for α -tubulin, and expressed as percentage versus controls (CONTR, black columns). The values are means ± S.D. (N = 3). One-way ANOVA using Tukey's post-test was used for all statistical analysis. (e) Confocal images showed a different cellular distribution of Nf2/merlin. SCs were immunopositive for the specific markers P0 (red) and Nf2 (green). Merge images (yellow) revealed that merlin was more localized in the cytoplasm of EMF-exposed SCs, rather than in the nucleus (CONTR). Scale bar 10 μm.*

ERK and AKT signaling pathways are activated in SCs following EMF exposure

In order to identify possible pathways involved in SCs transformation and proliferation outcomes, ERK and AKT signaling were investigated. Both ERK (RAS/RAF/MEK/ERK) and AKT (PI3K/AKT) signaling pathways, which modulate biochemical pathways controlling cell growth and apoptosis, were activated. Western blot analysis confirmed that pERK significantly rose at 2 h (48,5%; $P < 0.001$), then significantly decreased at 6 h (53,3%; $P < 0.001$); tERK levels, indeed, showed a light but significant decrease at 2 h (21,9%; $P < 0.05$), then a significant increase at 6 h (83,4%; $P < 0.001$; Figure 24b). Analysis of pERK/tERK ratio confirmed that ERK signaling was activated at short time (+74,6%; 2 h), and deactivated within 6 h after EMF exposure (-78,3%; $P < 0.001$; Figure 24b).

AKT analysis showed a similar trend of activation. Quantitative immunoblots analysis confirmed pAKT significant increase at 2 h (74,9%; $P < 0.001$), without changes 6 h after EMF exposure; tAKT levels were significantly augmented only 6 h after EMF exposure (51,3%; $P < 0.001$; Figure 24c). Analysis of pAKT/tAKT ratio showed a trend of AKT activation (even not significant) at short time (2 h), and AKT significant deactivation within 6 h after EMF exposure (-36,9%; $P < 0.001$; Figure 24c).

Taken together these data corroborate an early activation of both signaling pathways, ERK and AKT, in controlling SCs proliferation, 2 h following EMF exposure. Both signaling pathways were turned off within 6 h following EMF exposure.

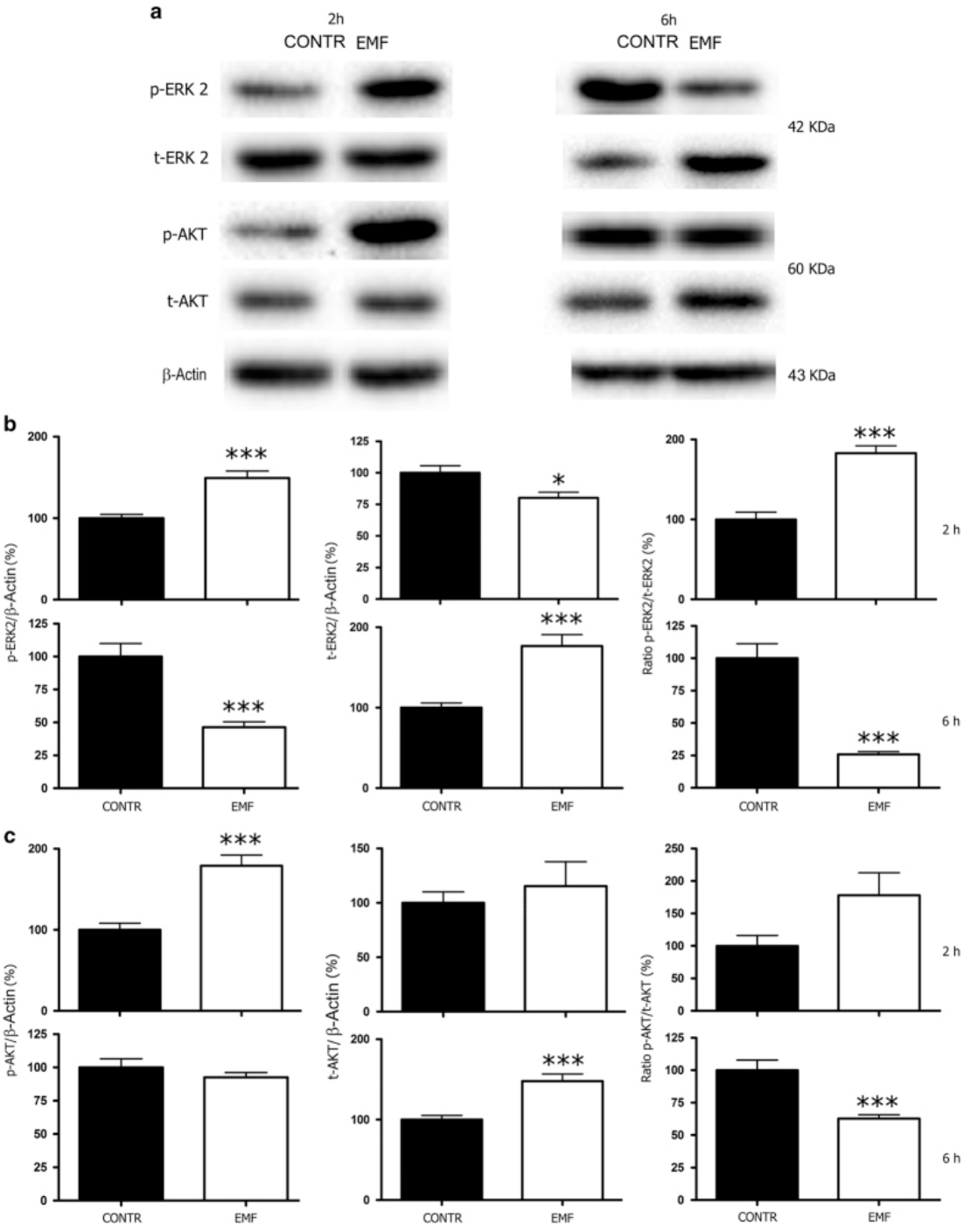
a
2h
CONTR EMF
6h
CONTR EMF
p-ERK 2
t-ERK 2
p-AKT
t-AKT
β-Actin
42 KDa
60 KDa
43 KDa
b
p-ERK2/β-Actin (%)
t-ERK2/β-Actin (%)
Ratio p-ERK2/t-ERK2 (%)
2 h
6 h
CONTR
EMF
c
p-AKT/β-Actin (%)
t-AKT/ β-Actin (%)
Ratio p-AKT/t-AKT (%)
2 h
6 h
CONTR
EMF

Figure 24 ERK and AKT signaling pathways are activated in SCs following 10 min EMF exposure. *(a) Representative immunoblots showing the variations in phosphorylated ERK 2 (pERK 2), total ERK 2 (tERK 2), both 42 KDa, phosphorylated AKT (pAKT), total AKT (tAKT), both 60 KDa, in SCs at 2 and 6 h following EMF exposure. The β-actin (43 KDa) was used as a housekeeping protein. (b) Quantitative data at 2 h showed that pERK levels significantly increased (***P<0.001), while tERK levels decreased (*P<0.05); the pERK/tERK ratio showed that ERK signaling was activated 2h following EMF exposure (***P<0.001, white columns). Indeed, pERK levels significantly decreased at 6h (***P<0.001), while tERK significantly increased at 6 h (***P < 0.001); pERK/tERK ratio indicated that this signaling pathway was deactivated within 6 h following EMF exposure (***P<0.001). Experiments were normalized for β-actin, and expressed as percentage versus controls (CONTR, black columns). The values are means ±S.D. (N=3). (c) Quantitative data at 2h showing that pAKT levels significantly increased (***P<0.001), while tAKT levels were unchanged; the pAKT/tAKT ratio showed an activation trend, even not significant. At 6 h, pAKT levels did not change but tAKT levels were significantly rised (***P < 0.001); pAKT/tAKT ratio revealed a significant deactivation within 6 h after EMF exposure (***P < 0.001, white columns). Experiments were normalized for β-actin, and expressed as percentage versus controls (CONTR, black columns). The values are means ± S.D. (N = 3). One-way ANOVA using Tukey's post-test was used for all statistical analysis.*

Dysregulation of the Hippo signaling pathway is a consequence of EMF exposure

RT2 profiler PCR array was performed in order to study the possible involvement of Hippo pathway in SCs exposed to EMF. At least 21 genes that are upstream or downstream mediators of Hippo pathway, were found to be regulated. Bioinformatic analysis, however, revealed a downregulation of some of these genes, differently involved in the whole Hippo pathway (Figure 25a). More in detail, some proteins involved in cell polarity, such as Angiomotin like-2 (AMOTL2) and Crumbs homolog (CRB) protein complex (including proteins 1, 2 and 3), showed a decrease in gene expression levels (Figure 25b). As expected, Merlin expression was decreased, in accordance with qRT-PCR and immunoblot results (Figures 23c and d). Other proteins, such as dachsous protein (DCHS, a member of transmembrane proteins belonging to the cadherin superfamily), transmembrane cadherin proteins (FAT) or proto-oncogen protein1 (WNT1), involved in cell adhesion and myelinogenesis respectively, were also found to be changed (Figure 25b).

On the basis of these results, the interest was focused on AMOTL2 and CRB (1, 2, 3), two proteins involved in cell morphologic rearrangements and polarity changes, as part of the tight-junction complex. Validation by qRT-PCR of the analysis previously performed in SC confirmed a significant downregulation (at least $P < 0.05$) of their expressions following EMF exposure (Figure 25c). We analyzed the transcriptional co-activator YAP1, which is a downstream effector of Hippo pathway related to CRB/AMOTL tight junction was analyzed. The qRT-PCR analysis confirmed a significant downregulation ($P < 0.001$) of YAP1 in SCs after EMF exposure (Figure 25d). Interestingly, YAP1 cellular localization was also changed. In control SCs, YAP1 was localized mainly in the nucleus, supporting its physiologic activity in the control of

proliferation and apoptosis. In exposed SCs, indeed, YAP nuclear localization was diminished, being YAP1 mostly present in the cytoplasm (Figure 25e). In accordance, the absence of apoptosis in EMF-exposed SCs was strengthened by the lack of characteristic apoptotic nuclei, as observed by the IFL analysis (Figure 25e).

Altogether these findings supported the involvement of Hippo pathway downstream to Merlin changes in SCs. This may be responsible of the YAP-mediated anti-apoptotic and proliferative effects observed on SCs (Figure 25f).

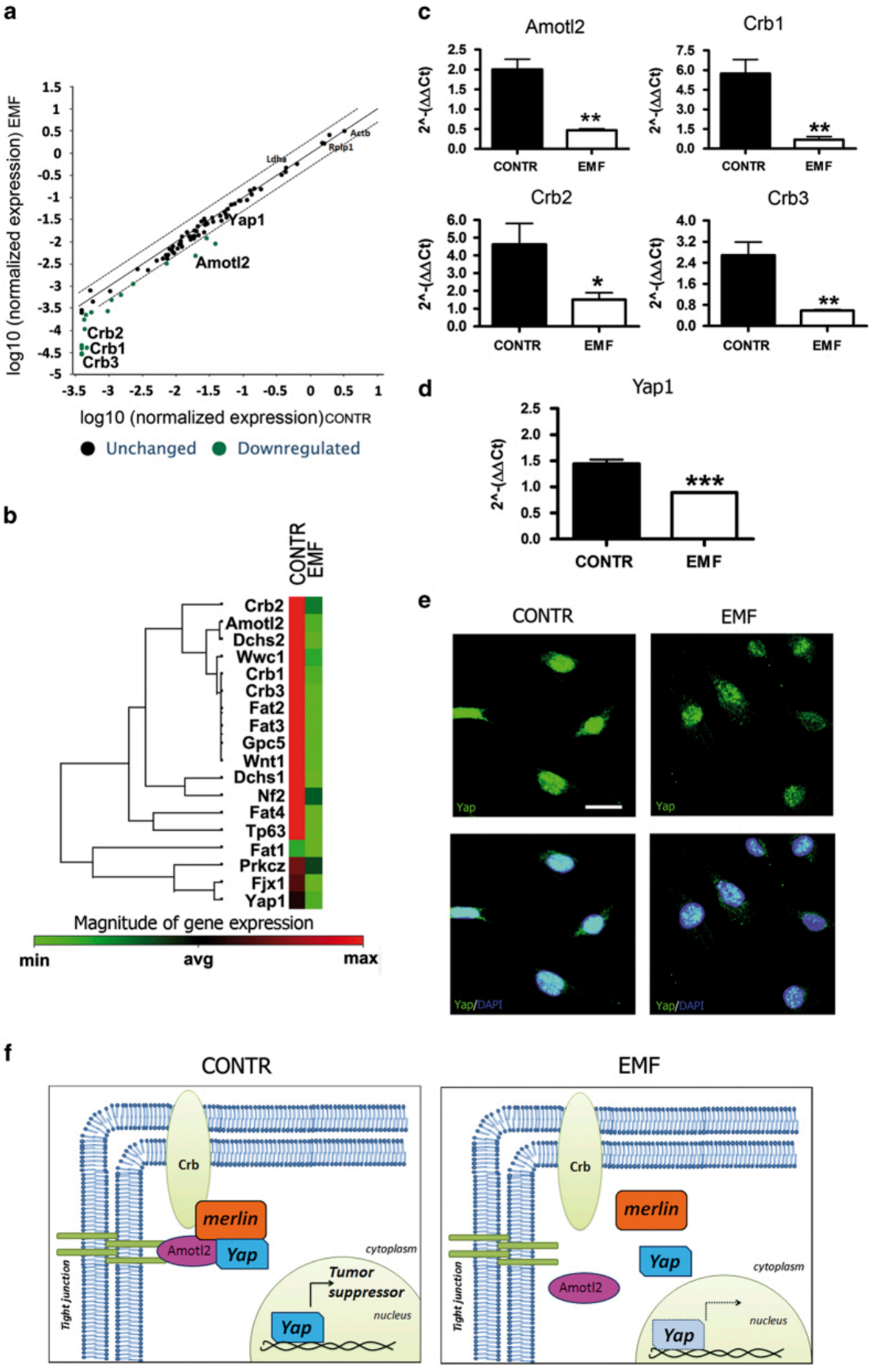
a
log10 (normalized expression) EMF
log10 (normalized expression)CONTR
Actb
Rplp1
Ldha
Yap1
Amotl2
Crb2
Crb1
Crb3
Unchanged
Downregulated
b
CONTR
EMF
Crb2
Amotl2
Dchs2
Wwc1
Crb1
Crb3
Fat2
Fat3
Gpc5
Wnt1
Dchs1
Nf2
Fat4
Tp63
Fat1
Prkcz
Fjx1
Yap1
Magnitude of gene expression
min
avg
max
c
Amotl2
Crb1
Crb2
Crb3
2^-(ΔΔCt)
CONTR
EMF
d
Yap1
e
CONTR
EMF
Yap
Yap/DAPI
f
CONTR
EMF
Crb
merlin
Amotl2
Yap
cytoplasm
Tumor suppressor
nucleus
Tight junction

Figure 25 Hippo and YAP1 are altered in SCs at 2 h following EMF exposure. *(a) Overview of the scatter plot of expression of 84 genes, related to the Hippo pathway, in which at least 21 genes were found to be changed (downregulated, green dots) in EMF-exposed SCs, versus controls (CONTR). The black line indicates fold changes (2−ΔΔCt) of 1. The dot lines indicate the desired fold change in gene expression threshold. Experiments were repeated at least three times, and normalized for β-actin (Actb), lactate dehydrogenase A (Ldha) and the 60S acidic ribosomal protein P1 (Rplp1). (b) Scheme of hierarchical clustering of normalized genes examined by RT2 profiler PCR array. Some genes coding for proteins involved in cell polarity, such as angiomotin like-2 protein (Amotl2) and Crumbs homolog proteins 1, 2 and 3 (Crb1, Crb2 and Crb3 respectively), as well as proteins involved in cell adhesion and myelinogenesis, such as dachsous proteins (Dchs), transmembrane cadherin proteins (Fat) or proto-oncogen protein1 (Wnt1), showed a decreased expression following EMF exposure (green square), versus controls (CONTR, red square). Also Yes-associated protein 1 (Yap1) was found to be downregulated. (c) Amotl2, Crb1, 2 and 3 gene expressions quantification was done by qRT-PCR, confirming a significant expression decrease following EMF exposure. Data were normalized to the housekeeping genes β-actin and Ldha, and expressed as difference (ΔΔCt) versus controls, then averaged for each experimental group. The columns control (CONTR, black) and EMF-exposed SC (EMF, white) were expressed as fold changes. The values are means ±S.D. (N=3). One-way ANOVA using Tukey's post-test was used for statistical analysis. *P<0.05, **P<0.01. (d) Also Yap1 gene expressions quantification by qRT-PCR confirmed a significant decrease (***P<0.001) following EMF exposure. Data were normalized, calculated and repeated as described above. Control (CONTR, black column) and EMF-exposed SC (EMF, white column) were expressed as fold changes (means ±S.D.; N=3). (e) Confocal images showed a different cellular distribution of Nf2/merlin. SCs were immunopositive for the specific markers P0 (red) and Nf2 (green). Merge images (yellow) revealed that merlin was mostly localized in the cytoplasm of EMF-exposed SCs, rather than in the nucleus (CONTR). Scale bar 10 μm. (f) Model of the Hippo/Yap pathway involvement. In control SCs, Yap functions as tumor suppressor, assembling with Amotl2, Crb and merlin to maintain the tight junctions. In EMF-exposed SCs, the tight-junction complex is disassembled and Yap is more localized in the cytoplasm.*

Discussion

Overall, these findings show that the tumor suppressor *Nf2*/Merlin is downregulated in SCs after the exposition to EMFs, leading to an altered morphology, proliferation, migration and SCs myelinating capability. These findings are associated with a consistent modulation of ERK/AKT and Hippo signaling pathways. In other words, SCs change their shape from spindle-shaped to an enlarged phenotype (Figure 21b), suggesting that EMFs alter their differentiation program.

It is well known that during the differentiation SCs switch from flat into a spindle-shaped phenotype, resembling the cells that start myelination process *in vivo*, which presents a reorganization of f-actin cytoskeleton and the appearance of the stress fiber bundles (Li et al., 2003). Therefore, the morphologic changes point to a SC de-differentiation process. This phenomenon matches with a specific increase in cell proliferation (Figure 21d). It has been hypothesized that an autocrine growth factor and/or the translocation/recycling of membrane receptors may be responsible for the SC proliferation changes. Interestingly, in agreement with our previous observations the transport to the plasma membrane of GABA-B1 receptor and the neuronal excitatory amino acid transporter EAAC1/EAAT3, which localize in the elongated SC tips, appears to be associated with cytoskeleton rearrangements required for the GABAergic functionality in SCs (Perego et al., 2012; Procacci et al., 2012).

The balance between proliferating and myelinating challenges in SCs may regulate their development toward the myelinating and/or the non-myelinating phenotype (Mirsky et al., 2008; Roberts and Lloyd, 2012). In this light, an increase in proliferation/migration probably correspond to a decrease in myelinating parameters. Moreover, the changes in P0 and PMP22 protein expressions levels, are in line with this hypothesis (Figures 23a

and b). Furthermore, the decrease in the proto-oncogene protein WNT1 (Figure 25b) fits with the diminished P0 and PMP22 levels (Tawk et al., 2011), corroborating the reversion in the myelinating program in the SC exposed to the EMF.

The analysis of mRNA/protein levels, as well as the phosphorylation of ERK and AKT revealed an activation of this pathways (Figure 24), raising the possibility that EMF affects SC proliferation via mechanisms involving the ERK/AKT signaling pathways. This possibility agrees with previous observations obtained in schwannomas cells, where merlin is lost while the ERK pathway is activated (Pećina-Šlaus, 2013).

Merlin is an important tumor suppressor factor, acting at the cell-to-cell tight junctions to allow the contact inhibition of growth, thus repressing proliferation (Das et al., 2015). Merlin was proved to inhibit mitogenic signaling by interacting with different target effectors at the cell membrane surface (McClatchey and Giovannini, 2005; Lallemand et al., 2009). The EMF ability to alter membrane integrity may cause tight-junctions remodeling, inducing mitogenic signals via ERK. The reduced levels of CRB and AMOTL (Figures 25b and c) suggest an impairment in tight-junction protein complex stability, entailing a dissociation of the AMOTL/Merlin complex (Figure 25f). If this holds true, merlin could relocates to the cytoplasm (Figure 25e), likely promoting ERK activation and cell proliferation, as demonstrated also by others (Morrison et al., 2007; Das et al., 2015). These findings suggest that the tight junctions are altered by EMFs, then leading to the loss of adhesion properties and to the increase in migrating capability (Figure 22). This is supported by the evidence that a disorganization in the cell membrane architecture abolishes the EMF effects on SCs migration (Figures 22c and d). Therefore, in line with the increased migrating capability in SCs, the decreased levels of Merlin may be predictive of the oncogenic transformation.

Evidence from the literature indicate that the Hippo pathway has a key role in the regulation of the tight-junction complex (Lacy-Hulbert et al., 1998). Interestingly, in this study was found an important modulation of the Hippo/YAP pathway in SCs. This contributes to the tight-junction complex and, when activated, it serves as tumor suppressor to limit cell growth. The dysregulation of the Hippo downstream effector YAP (Figure 25d), produces an increased cell proliferation and decreased differentiation (Plouffe et al., 2015), in line the results herein provided. It is also important to underline that AKT promotes YAP cytosolic localization, resulting in its loss from the nucleus (Basu et al., 2003). Interestingly, the increased AKT levels were associated with higher YAP immunopositivity in the cytoplasm (Figure 25e).

In conclusion, a series of changes (i.e., tight-junction alterations, merlin decrease, SC migration, chemo-responsivity increase, YAP downregulation and redistribution), resulting into determining a reduction of the Hippo pathway were observed. All these changes are relevant for the control of SCs fate following 50 Hz-EMF exposure. Notably, the reduction of the oncosuppressor properties in SCs, resulting in an altered differentiation program, may be pathologically relevant for the schwannoma transformation. The identification of some altered mechanisms opens new questions on the exposure of SCs to the EMFs, although the fine identification of the intracellular signaling need further investigation. It is important to underline that although the therapeutic use of low-frequency (20Hz) EMFs has been proposed to promote peripheral nerve regeneration (Sisken et al., 1989; Sherafat et al., 2012), the 50 Hz frequency is commonly used in several medical devices for magnetotheraphy (Saliev et al., 2014; Yan et al., 2015) and in other electric devices. Unfortunately, when SCs are altered by EMF exposure, the risk to develop a neurofibroma might rise. The increasing

risk of the onset of vestibular schwannomas, coming from the long-term use of wireless phones, is still debated and needs further investigations, however, data from clinical case–control studies corroborate this pathogenic correlation (Hardell et al., 2006; Cardis and Schuz, 2011) and open new medical questions that need to be elucidated.

CHAPTER 3

Transcriptomic profile of *in vitro* SCs and DRG neurons of GABA-B1 conditional *knock out* mice.

GABA-B Rs are important for SCs control of myelination and for their commitment to a non-myelinating phenotype during development. Interestingly, the *P0*-Cre/GABA-B1$^{fl/fl}$ mice presented also axon modifications, suggesting the existence of SC non-autonomous effects mediated through the neuronal compartment. Other mechanisms, occurring in the neuronal compartment, may concur to the morphological and behavioural changes observed in the peripheral nerve of mice lacking GABA-B1 specifically in SCs.

Given these assumption, the studies summarized in this chapter pursue the aim 3 of this thesis that is to characterize *in vitro* the primary SCs and DRG neurons from *P0*-Cre/GABA-B1$^{fl/fl}$, analyzing also their whole trancriptome by Affimetrix GeneChip array. Particular interest has been focused on miRNAs analysis, because, as I mentioned in the Introduction, several papers showed fundamental roles for miRNAs in the control of development, differentiation, and health of myelinating cells of the mammalian nervous system (Dugas and Notterpek, 2011).

Set up and characterization in vitro of the SCs and DRG neurons cultures from *P0*-Cre/GABA-B1$^{fl/fl}$ mice

First, SCs and DRGs neurons cultures were characterized assessing the genotype and the positivity for some biochemical and morphological parameters. SCs were labelled with the specific antibody. P0, a typical marker for SCs, or S100, able to label both cells of neural origin and SCs in their first stage of development/differentiation. Phalloidin

was used to evaluate some differences in the actin citoskeleton rearrangement. As shown in Figure 26, SCs were immunopositive for P0 and for S100, the most important and characteristic marker of SCs. There were no evident morphologic differences between cells from *P0*-Cre/GABA-B1$^{fl/fl}$ (experimental) and GABA-B1$^{fl/fl}$ (control) mice. Moreover, there were no changes in cytoskeleton organization. This evidence suggested that SCs did not change their morphology, still possessing the capability proliferate and differentiate *in vitro*.

DRG neurons were characterized, showing a good morphology *in vitro*. These cells were stained for S100, NF200 and CGRP, and no significant differences were found between the experimental and the control mice (Figure 27). To check whether the deletion of the GABA-B1 gene may affect SCs proliferation, viability and migration, several experiments were performed. The cell number was analysed under phase contrast light microscope, in presence of different concentration of the mitogen factor forskolin, generally known as cAMP inducer. This is in order to test whether the SCs from *P0*-Cre/GABA-B1$^{fl/fl}$ mice preserve basal proliferating characteristics. As shown in figure 28, the basal SCs from control mice, apparently increased when forskolin concentration was higher, changing from 2 to 10 μM. The morphology of SCs exposed to different forskolin concentrations: 2, 4, 10 and 100 μM was tested by IFL, using an antibody against P0 marker. The qualitative assessment of cell number (Figure 29) showed an increase in proliferation of SCs from conditional mice, depending on forskolin concentration. However, the quantitative proliferation assay revealed that SCs from experimental *P0*-Cre/GABA-B1$^{fl/fl}$ mice, at shorter time points (48 and 72 h), did not show any significant differences between 4 and 100 μM forskolin concentration (Figure 30).

To assess the migratory capability of SCs a wound healing assay was performed in

presence of mytomicin-C 50 ng/mL, to block cell proliferation. SCs from experimental animal, showed a significant decrease in migration capability at 48 and 72 hours after treatment (Figure 31).

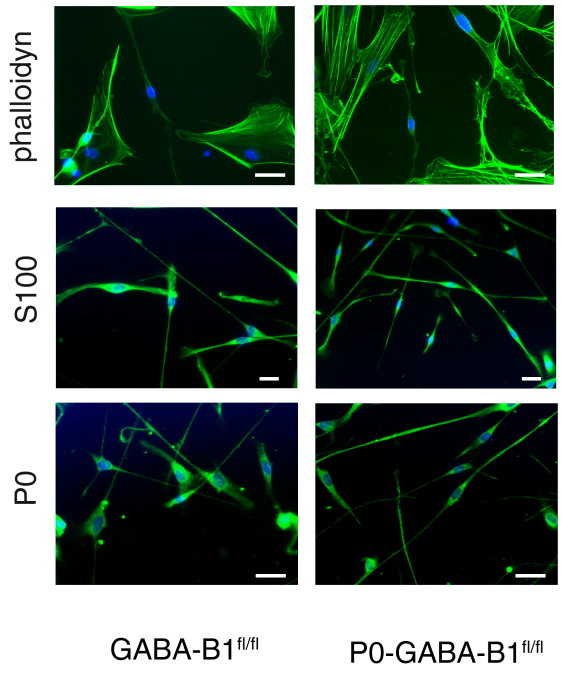

Figure 26 SCs characterization. *SCs were stained with Phalloidin they did not show any difference in the actin cytoskeleton. SCs were also immunopositive for S100 and for P0, the most important and characteristic marker of SCs. There are no evident differences between cells from P0-CRE/GABA-B1fl/fl experimental and GABA-B1fl/fl (control) mice.*

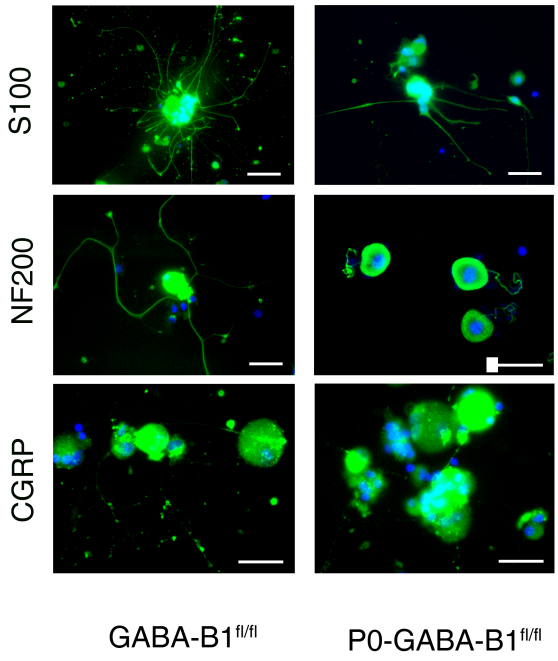

Figure 27 DRG neurons characterization. *DRG neurons were stained for S-100, for NF200 and CGRP, and also in this case, no significant differences were found between the experimental and the control mice.*

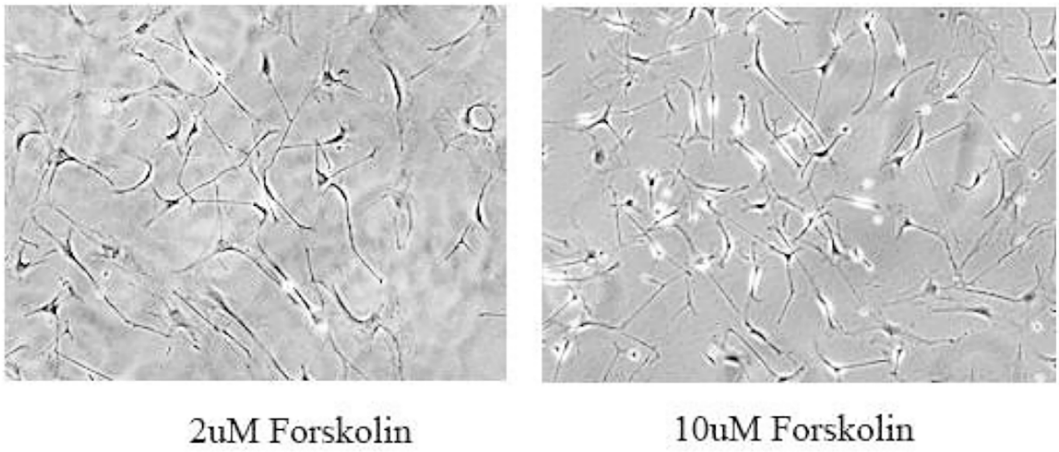

Figure 28 *Picture from phase- contrast light microscope of SCs from GABA-B1fl/fl mice treated with two different concentration of forskolin (2 and 10 μM).*

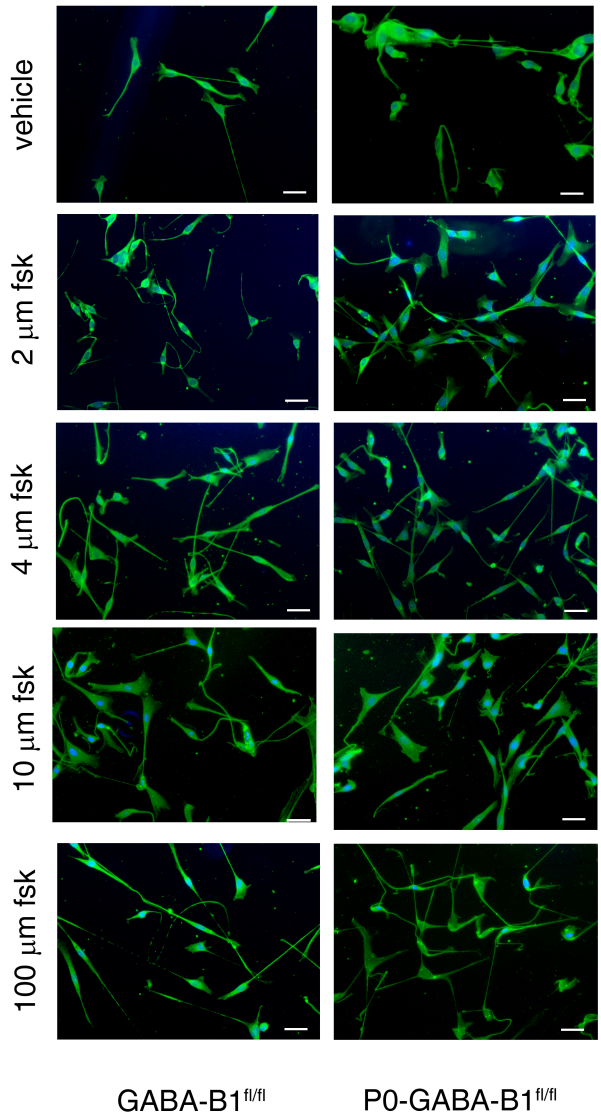

Figure 29 Exposure of SCs to different forskolin concentrations. *SCs were exposed to several forskolin concentration: 2, 4, 10 and 100 µM. Differences in cell morphology were evaluated in immunofluorescence analysis using an antibody against P0 marker.*

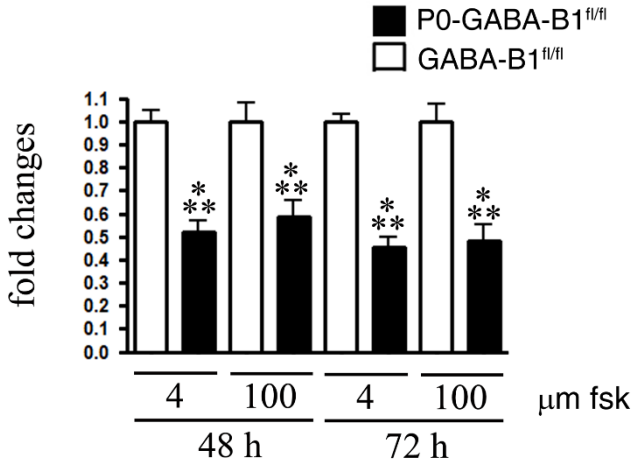

Figure 30 Proliferation assay on SCs from P0-Cre/GABA-B1 $^{fl/fl}$ and GABA-B1 $^{fl/fl}$. *SCs proliferation was assessed at 48 and 72 h, with two different fsk concentration (4 and 100 μM). In P0-Cre/GABA-B1 $^{fl/fl}$ mice SCs decrease in number, in all the condition considered (*P<0,001). Experiments were repeated at least three times and data expressed as cell number (×103). Two-way ANOVA using Bonferroni's post hoc test was used for statistical analysis.*

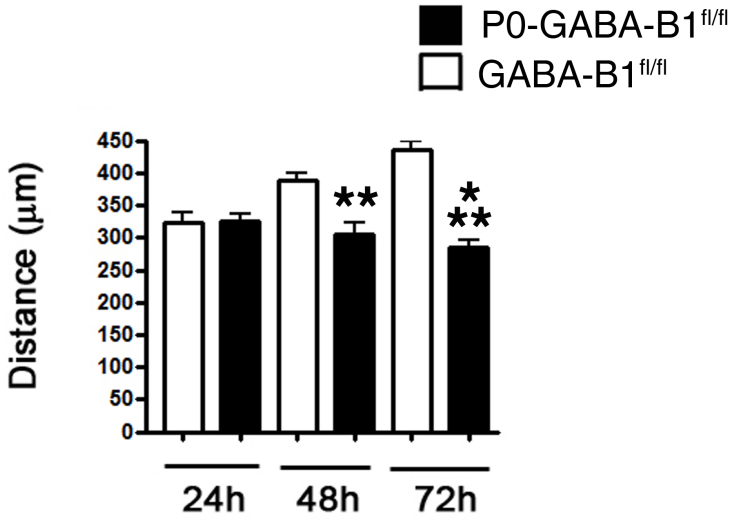

Figure 31 Migratory capability of SCs performed with a wound healing assay. *The distance between cells was measured with the Image-ProPlus software. As it shown in the graph, SCs from experimental animal, show a significant decreased in migration capability at 48 and 72 hours.*

Transcriptomic analysis on SCs from *P0*-Cre/GABA-B1$^{fl/fl}$ mice

The GABA-B1 receptor was further investigated by evaluating the transcriptomic expression profile of SCs and DRG neurons from *P0*-Cre/GABA-B1$^{fl/fl}$ mice. To this purpose, the transcriptomic profile was assessed by the Affimetrix GeneChip array technology. The results obtained from SCs and DRG neurons revealed that a considerable number of genes were modulated by the selective deletion of the GABA-B1 receptor in the SCs (Figure 32). These data supported the importance of the cross-regulation between SCs and neurons downstream the GABA-B1 activation in SCs. In particular, in SCs we observed changes in the expression of several genes coding for proteins involved in different pathway or intracellular signaling: cytokines, chemokines, proteins of the extracellular matrix, protein regulating cell proliferation, etc. About 41300 transcripts were analyzed, founding 2.66% (corresponding to 1099 genes) differently expressed genes. The first set of 276 genes, were differently expressed in *P0*-Cre/GABA-B1$^{fl/fl}$ mice, with a gene expression level that was log2 scaled. In particular, 38 downregulated and 238 upregulated genes in *P0*-Cre/GABA-B1$^{fl/fl}$ mice (Figure 32), were worth of investigation.

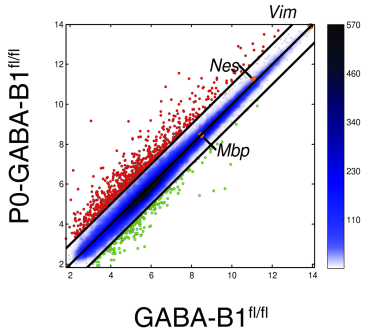

Figure 32 Pairwise scatter plot Ctr vs GABA in SCs. *The black lines are the boundaries of the 1-fold changes in gene expression levels between the paired samples. Gene up-regulated in ordinates samples compared with abscissas samples are shown in red circles; those down-regulated are shown in green. The positions of some markers are shown as orange dots. The color bar to the right indicates the scattering density, the higher is the scattering density the darker the blue. The gene expression levels are log2 scaled.*

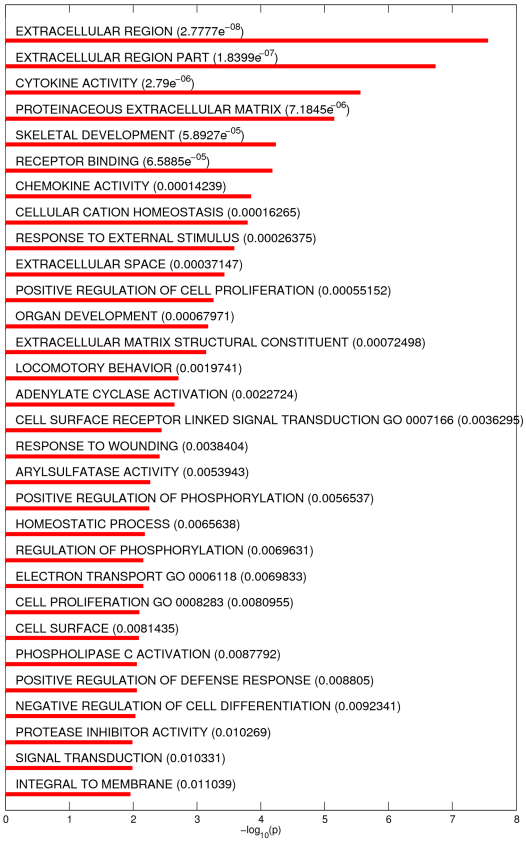

Figure 33 Plot bar of the -log10(p) of the significant enriched terms of Ctr-<-GABA-Log2(2). *The longer the bar, the higher is the statistical significance of the enrichment (in parenthesis are written the p-values). Transcriptomic expression profile of SCs cultures from P0-Cre/GABA-B1$^{fl/fl}$ (experimental) or GABA-B1$^{fl/fl}$ (control) mice by the Affimetrix GeneChip array technology (19). We analysed 41345 transcripts, founding 2.66% (corresponding to 1099 genes) differently expressed genes. Then we focused on the first set of 276 genes, which are differently expressed in P0-Cre/GABA-B1$^{fl/fl}$ mice, with a gene expression level that was log2 scaled. We found 38 downregulated and 238 upregulated genes in P0-Cre/GABA-B1$^{fl/fl}$ mice (20).*

Transcriptomic analysis on DRG neurons from *P0*-Cre/GABA-B1$^{fl/fl}$ mice

The same analysis was performed on DRG neurons revealing apparent changes in the expression of genes coding for proteins that control different intracellular signaling (Figure 34-35). In this case, the attention was focused on the first set of 59 genes, which were differently expressed in *P0*-Cre/GABA-B1$^{fl/fl}$ mice, with a gene expression level that was log2 scaled. In particular, 33 downregulated and 26 upregulated genes in *P0*-Cre/GABA-B1$^{fl/fl}$ mice. Interestingly, these genes were related to the acetylcholine transmission pathway and the ion channels nicotinic receptors. Among nicotinic receptors, the expression of 3 fundamental subunits, respectively *Chrna3*, *Chrnb3* and *Chrnb4* were considered. Statistical analysis did not show any significant change in all the subunits studied (Figure 35), evidencing no substantial changes in DRG neurons of *P0*-Cre/GABA-B1$^{fl/fl}$ mice.

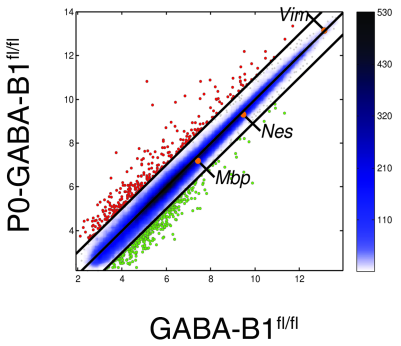

Figure 34 Pairwise scatter plot Ctr vs Exp in DRGs. *The black lines are the boundaries of the 1-fold changes in gene expression levels between the paired samples. Gene up-regulated in ordinates samples compared with abscissas samples are shown in red circles; those down-regulated are shown in green. The positions of some markers are shown as orange dots. The color bar to the right indicates the scattering density, the higher is the scattering density the darker the blue. The gene expression levels are log2 scaled.*

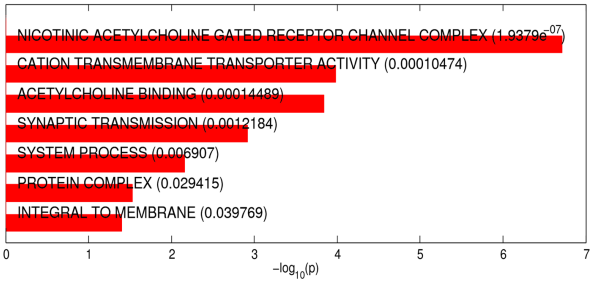

Figure 35 Plot bar of the -log10(p) of the significant enriched terms of Ctr-<-Exp-Log2(2). *The longer the bar, the higher is the statistical significance of the enrichment (in parenthesis are written the p-values) There were not statistically significantly enriched terms in this category.*

MiR-338-3p is modulated in SCs of *P0*-Cre/GABA-B1$^{fl/fl}$ mice: qRT-PCR and in silico analysis

Transcriptomic analysis showed that some miRNAs were up- or downregulated in *P0*-Cre/GABA-B1$^{fl/fl}$ mice. Namely, the analysis was focused on miR-338, which has been implicated in SC differentiation (Zhao *et al.*, 2010; Gokey *et al.*, 2012). First, miR-338 expression was confirmed in SCs cultures from both *P0*-CRE/GABA-B1$^{fl/fl}$ and GABA-B1$^{fl/fl}$ mice, finding a significant downregulation (*P<0,01) of the miR-338 3p segment (miR-338-3p), while the 5p segment did not change (Figure 36).

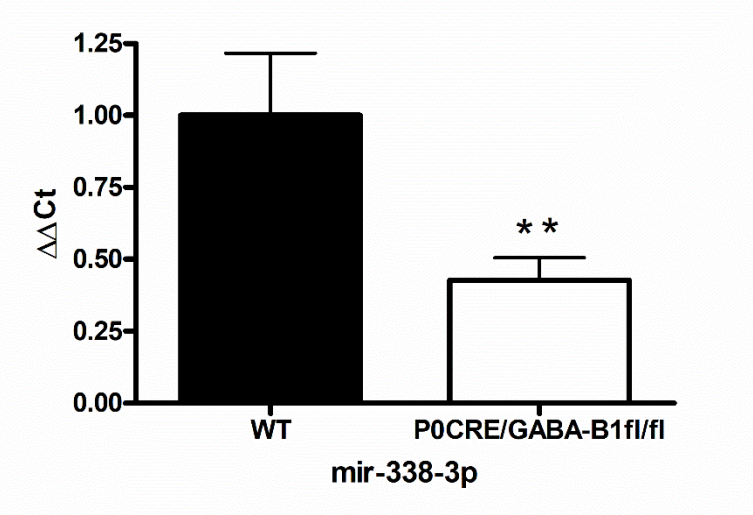

Figure 36 mRNA expression of miR-338-3p. *Relative quantification by qRT-PCR of mRNA levels, coding for mir-338-3p showed a decreased expression in P0-Cre/GABA-B1$^{fl/fl}$ mice. Data were normalized to the housekeeping genes hsa-103 and expressed as difference (ΔΔCt) versus WT. The WT column (black) and P0-Cre/GABA-B1$^{fl/fl}$ (white) were expressed as fold changes. The values are means ± S.D. (N = 3). **P < 0.01*

Then, to investigate the potential role of miR-338-3p, an *in silico* analysis was performed on the mouse MyMIR databases. A list of 729 putative target transcripts of miR-338-3p in mouse was found. Thereafter, STRING, a Gene Ontology (GO) based tools, showed that these targets were significantly clustered in 3 principal pathways: "Biological process" (BP), "Molecular function" (MF), "Cellular compartment" (CC). Biological process, suggesting that miR-338-3p takes part in their regulation. We found that the main GO biological pathways involved were: nervous system development, anatomical structure morphogenesis, signal transduction, intracellular signaling transduction, synaptic transmission and cell-cell signaling. For all of these biological processes the fold enrichment in miR-338-3p targets was calculated using the following formula:

$$\text{Fold enrichment} = \frac{m \div n}{M \div N}$$

m = genes target in a BP; n =all genes target in the list; M = all genes in a BP; N = all genes in the genoma (see Figure 37).

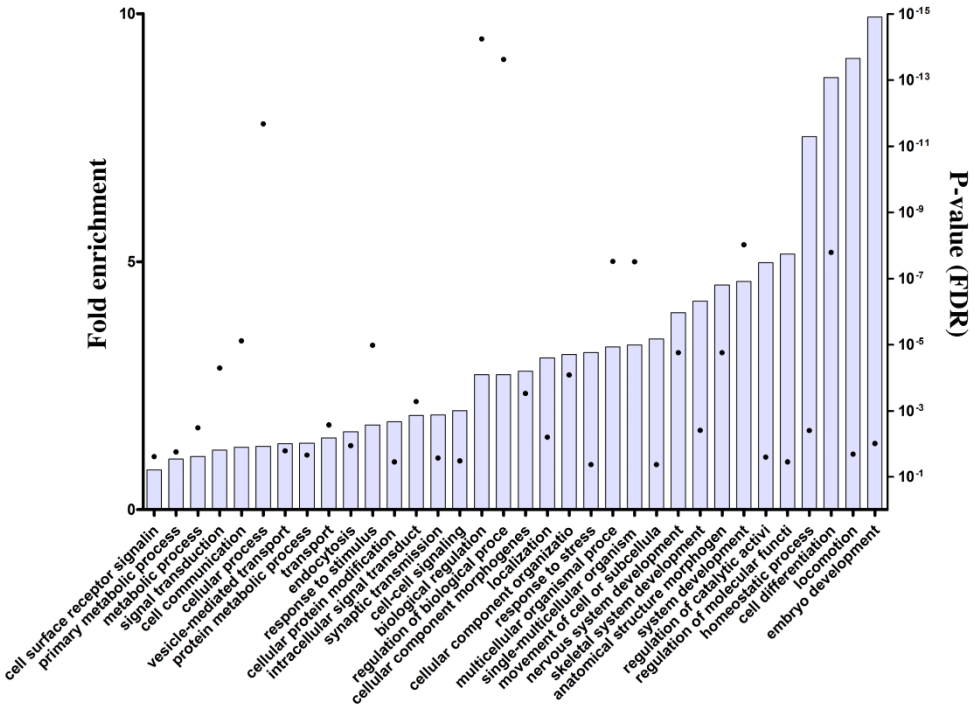

Figure 37 Gene Ontology biological processes (GO BPs) related to SC development are enriched in miR-338-3p targets. *Histograms show the significant GO BPs enriched in miR-338-3p target transcripts (Fold enrichment compared to expected value=1; see left axis). Dots represent p-value (with FDR correction) of the prediction for each GO BP (see right axis; log10 scale).*

Discussion

In the last decades the role of the neurotransmitters, such as GABA, in the control of neuron-glia cell interaction in the PNS received great attention (Fields and Burnstock, 2006; Loreti et al., 2007). With particular attention to the PNS, the study of total GABA-B1 -/- mice (total null mice) showed biochemical, anatomical and functional changes. Indeed, with morphological and molecular alterations in myelin as well as an increased number of small caliber axons and small DRG neurons was observed. These mice revealed also changes in sensory nociceptive functions (Magnaghi et al., 2008a).

Successively, the role of the GABA-B1 receptor PNS myelination was tested by the specific inactivation of the receptor only in SCs, demonstrating SC-autonomous effects. However, further studies showed signs of SC degeneration, such as tomacula, fractured myelin, and partial or complete uncompaction of myelin. In line with these results, also the percentage of fibers with irregular profile, an index of myelin dysregulation, was strongly augmented (Faroni et al., 2014a). Overall, these effects were considered SC-non-autonomous. Therefore, in order to investigate the involvement of SCs on DRG neurons in the nerve features occurring following GABA-B1inactivation, we performed the present study.

First, the SCs and DRG neurons cultures were characterized with specific antibodies. No differences between *P0*-Cre/GABA-B1$^{fl/fl}$ and GABA-B1$^{fl/fl}$ mice, were found demonstrating that the GABA-B1 receptor selective deletion in SCs has no influences on SCs morphology and on the DRG neurons morphology.

The exposure to different forskolin concentrations apparently increases SC proliferation in control mice. However, the quantitative analysis of SCs number from the *P0*-Cre/GABA-B1$^{fl/fl}$ mice showed a decrease in proliferation with no

significant differences between the different concentrations considered (Figure 30). Indeed, the migration capability, in the conditional *knock out* mice was significantly diminished (Figure 31).

Taken together, these findings evidenced the possibility that the GABA-B1 deletion in SCs induces some modification in the mRNA expression profile of the same cells, in turn able to produce changes in functional features, like proliferation and migration.

To assess these hypothesis, we did several transcriptomic analyses on SCs and DRG neurons cultures obtained from these animals, to shed light on the possible changes in mRNA expression levels of different genes that regulate the functional changes. In particular the Affymetrix GeneChip array technology changes in SCs. In these cells, we observed changes in the expression level of several genes coding for protein like cytokines, chemokines, proteins of the extracellular matrix, protein regulating cell proliferation. Interestingly, among these genes, there are different miRNA that are down or upregulated in SCs cultures from *P0*-Cre/GABA-B1$^{fl/fl}$.

The miRNAs are involved in post-transcriptional regulation of different genes in different type of cells, controlling physiological processes and determining pathological condition (Dugas and Notterpek, 2011).

It is also remarkable that some miRNAs are induced during differentiation (miR-219, -338, -138) and some other are high in pre-myelinating SCs and OL but then decrease during myelination (Svaren, 2014). Moreover, at least in SCs, some of this miRNAs rebound after peripheral nerve injury (Viader et al., 2011b; Adilakshmi et al., 2012; Yu et al., 2012).

Microarray analysis identified a series of miRNAs that are developmentally regulated during maturation of SCs (Bremer et al., 2010b; Pereira et al., 2010; Yun et al., 2010;

Gokey et al., 2012). Our results show that miRNA-338 is modulated in SCs cultures from P0-CRE/GABA-B1$^{fl/fl}$, in line with the recent literature that demonstrates the involvement of mir-338 in the OL and SCs differentiation process. These preliminary results were validated by qRT-PCR analysis so that and the future perspective is to silence mir-338 and evaluate different cell parameters, such as the expression of characteristic proteins involved in the maturation/differentiation on development of SCs.

Conclusion

In this thesis are described different lines of research pursued during my PhD program. These studies were aimed to the investigation of three distinct and interplaying pathways, that have a role in the maturation and myelination processes of SCs.

In the first part of this work, it was studied the molecular mechanism of ALLO actions in SCs, elucidating the role of the SRC/FAK pathways. ALLO modulation of the SRC and p-FAK pathways involves GABA-A R mediated mechanisms. ALLO and SRC/FAK determine SC actin remodeling, controlling SC motility and morphological changes, beside proliferation and myelination. These findings supported the comprehension of the GABA-A R role in the PNS myelination process and demonstrate that ALLO and the GABAergic system are a promising tool for the treatment of PNS disorders.

Regarding the second part, it was demonstrated that SCs exposed to EMF change their characteristic features, under the control of the Hippo pathway. The tumor suppressor *Nf2*/Merlin, upstream the Hippo pathway, is downregulated in exposed SCs, determining alterations in proliferation, migration, morphology and myelination capability. These evidences open an important discussion on the use of EMFs in regenerative medicine and emphasise the exposition to EMFs, which may represent a common but risky challenge for the nervous system. Notably, the reduction of *Nf2* oncosuppressor, following EMF exposure, results in altered cell differentiation program, that may be pathologically relevant for the schwannoma transformation.

Lastly, in the third part of this work, it was also studied the relevance of transcriptional modifications on SCs following GABA-B1 deletion. GABA-B1 R conditional *knock out* mice showed alterations in myelinating capability. The transcriptomic expression profile was assessed showing a deregulation in many genes involved in primary

biological processes of SCs. Among these, an important issue may be represented by miRNAs. Particularly, miR-338-3p, known to be involved in CNS myelination, was an interesting target for the study of the myelination process under GABA-B R control. In fact, it was found, at least *in silico*, that miR-338-3p targets many genes involved in myelination.

Altogether, our findings shed light on novel, important and promising pathways involved in SC functions and PNS myelination. Hopefully, they contribute to deepen the knowledge of the mechanisms responsible of inherited and acquired PN, in order to find new and reliable therapeutic approaches for these pathologies.

References

Adilakshmi T, Sudol I, Tapinos N. 2012. Combinatorial action of miRNAs regulates transcriptional and post-transcriptional gene silencing following in vivo PNS injury. PLoS One [Internet] 7:e39674. Available from: http://www.ncbi.nlm.nih.gov/pubmed/22792185

Agrup C, Gleeson M, Rudge P. 2007. The inner ear and the neurologist. J Neurol Neurosurg Psychiatry [Internet] 78:114–22. Available from: http://www.ncbi.nlm.nih.gov/pubmed/17229743

Ahronowitz I, Xin W, Kiely R, Sims K, MacCollin M, Nunes FP. 2007. Mutational spectrum of the NF2 gene: a meta-analysis of 12 years of research and diagnostic laboratory findings. Hum Mutat [Internet] 28:1–12. Available from: http://www.ncbi.nlm.nih.gov/pubmed/16983642

al-Dahan MI, Thalmann RH. 1996. Progesterone regulates gamma-aminobutyric acid B (GABAB) receptors in the neocortex of female rats. Brain Res [Internet] 727:40–8. Available from: http://www.ncbi.nlm.nih.gov/pubmed/8842381

Al-Majed AA, Brushart TM, Gordon T. 2000a. Electrical stimulation accelerates and increases expression of BDNF and trkB mRNA in regenerating rat femoral motoneurons. Eur J Neurosci [Internet] 12:4381–90. Available from: http://www.ncbi.nlm.nih.gov/pubmed/11122348

Al-Majed AA, Neumann CM, Brushart TM, Gordon T. 2000b. Brief electrical stimulation promotes the speed and accuracy of motor axonal regeneration. J Neurosci [Internet] 20:2602–8. Available from: http://www.ncbi.nlm.nih.gov/pubmed/10729340

Alfthan K, Heiska L, Grönholm M, Renkema GH, Carpén O. 2004. Cyclic AMP-dependent protein kinase phosphorylates merlin at serine 518 independently of p21-activated kinase and promotes merlin-ezrin heterodimerization. J Biol Chem [Internet] 279:18559–66. Available from: http://www.ncbi.nlm.nih.gov/pubmed/14981079

Allodi I, Udina E, Navarro X. 2012. Specificity of peripheral nerve regeneration: interactions at the axon level. Prog Neurobiol [Internet] 98:16–37. Available

from: http://www.ncbi.nlm.nih.gov/pubmed/22609046

Ambros V. 2004. The functions of animal microRNAs. Nature [Internet] 431:350–5. Available from: http://www.ncbi.nlm.nih.gov/pubmed/15372042

Ammoun S, Flaiz C, Ristic N, Schuldt J, Hanemann CO. 2008. Dissecting and targeting the growth factor-dependent and growth factor-independent extracellular signal-regulated kinase pathway in human schwannoma. Cancer Res [Internet] 68:5236–45. Available from: http://www.ncbi.nlm.nih.gov/pubmed/18593924

Armstrong SJ, Wiberg M, Terenghi G, Kingham PJ. 2007. ECM molecules mediate both Schwann cell proliferation and activation to enhance neurite outgrowth. Tissue Eng [Internet] 13:2863–70. Available from: http://www.ncbi.nlm.nih.gov/pubmed/17727337

Arthur-Farraj P, Wanek K, Hantke J, Davis CM, Jayakar A, Parkinson DB, Mirsky R, Jessen KR. 2011. Mouse schwann cells need both NRG1 and cyclic AMP to myelinate. Glia [Internet] 59:720–33. Available from: http://www.ncbi.nlm.nih.gov/pubmed/21322058

Arthur-Farraj PJ, Latouche M, Wilton DK, Quintes S, Chabrol E, Banerjee A, Woodhoo A, Jenkins B, Rahman M, Turmaine M, Wicher GK, Mitter R, Greensmith L, Behrens A, Raivich G, Mirsky R, Jessen KR. 2012. c-Jun reprograms Schwann cells of injured nerves to generate a repair cell essential for regeneration. Neuron [Internet] 75:633–47. Available from: http://www.ncbi.nlm.nih.gov/pubmed/22920255

Asada H, Kawamura Y, Maruyama K, Kume H, Ding RG, Kanbara N, Kuzume H, Sanbo M, Yagi T, Obata K. 1997. Cleft palate and decreased brain gamma-aminobutyric acid in mice lacking the 67-kDa isoform of glutamic acid decarboxylase. Proc Natl Acad Sci U S A [Internet] 94:6496–9. Available from: http://www.ncbi.nlm.nih.gov/pubmed/9177246

Attarian S, Vallat J-M, Magy L, Funalot B, Gonnaud P-M, Lacour A, Péréon Y, Dubourg O, Pouget J, Micallef J, Franques J, Lefebvre M-N, Ghorab K, Al-

Moussawi M, Tiffreau V, Preudhomme M, Magot A, Leclair-Visonneau L, Stojkovic T, Bossi L, Lehert P, Gilbert W, Bertrand V, Mandel J, Milet A, Hajj R, Boudiaf L, Scart-Grès C, Nabirotchkin S, Guedj M, Chumakov I, Cohen D. 2014. An exploratory randomised double-blind and placebo-controlled phase 2 study of a combination of baclofen, naltrexone and sorbitol (PXT3003) in patients with Charcot-Marie-Tooth disease type 1A. Orphanet J Rare Dis [Internet] 9:199. Available from: http://www.ncbi.nlm.nih.gov/pubmed/25519680

Azcoitia I, Leonelli E, Magnaghi V, Veiga S, Garcia-Segura LM, Melcangi RC. 2003. Progesterone and its derivatives dihydroprogesterone and tetrahydroprogesterone reduce myelin fiber morphological abnormalities and myelin fiber loss in the sciatic nerve of aged rats. Neurobiol Aging [Internet] 24:853–60. Available from: http://www.ncbi.nlm.nih.gov/pubmed/12927767

Bae JS, Kim SM, Lee H. 2017. The Hippo signaling pathway provides novel anti-cancer drug targets. Oncotarget [Internet] 8:16084–16098. Available from: http://www.ncbi.nlm.nih.gov/pubmed/28035075

Barber RP, Vaughn JE, Saito K, McLaughlin BJ, Roberts E. 1978. GABAergic terminals are presynaptic to primary afferent terminals in the substantia gelatinosa of the rat spinal cord. Brain Res [Internet] 141:35–55. Available from: http://www.ncbi.nlm.nih.gov/pubmed/624076

Barres BA, Koroshetz WJ, Swartz KJ, Chun LL, Corey DP. 1990. Ion channel expression by white matter glia: the O-2A glial progenitor cell. Neuron [Internet] 4:507–24. Available from: http://www.ncbi.nlm.nih.gov/pubmed/1691005

Bartel DP. 2004. MicroRNAs: genomics, biogenesis, mechanism, and function. Cell [Internet] 116:281–97. Available from: http://www.ncbi.nlm.nih.gov/pubmed/14744438

Baser ME, Kuramoto L, Joe H, Friedman JM, Wallace AJ, Gillespie JE, Ramsden RT, Evans DGR. 2004. Genotype-phenotype correlations for nervous system tumors in neurofibromatosis 2: a population-based study. Am J Hum Genet [Internet]

75:231–9. Available from: http://www.ncbi.nlm.nih.gov/pubmed/15190457

Baser ME, Kuramoto L, Woods R, Joe H, Friedman JM, Wallace AJ, Ramsden RT, Olschwang S, Bijlsma E, Kalamarides M, Papi L, Kato R, Carroll J, Lázaro C, Joncourt F, Parry DM, Rouleau GA, Evans DGR. 2005. The location of constitutional neurofibromatosis 2 (NF2) splice site mutations is associated with the severity of NF2. J Med Genet [Internet] 42:540–6. Available from: http://www.ncbi.nlm.nih.gov/pubmed/15994874

Bashour A-M, Meng J-J, Ip W, MacCollin M, Ratner N. 2002. The neurofibromatosis type 2 gene product, merlin, reverses the F-actin cytoskeletal defects in primary human Schwannoma cells. Mol Cell Biol [Internet] 22:1150–7. Available from: http://www.ncbi.nlm.nih.gov/pubmed/11809806

Basu S, Totty NF, Irwin MS, Sudol M, Downward J. 2003. Akt phosphorylates the Yes-associated protein, YAP, to induce interaction with 14-3-3 and attenuation of p73-mediated apoptosis. Mol Cell 11:11–23.

Baulieu EE. 1997. Neurosteroids: of the nervous system, by the nervous system, for the nervous system. Recent Prog Horm Res [Internet] 52:1–32. Available from: http://www.ncbi.nlm.nih.gov/pubmed/9238846

Le Beau JM, Tedeschi B, Walter G. 1991. Increased expression of pp60c-src protein-tyrosine kinase during peripheral nerve regeneration. J Neurosci Res [Internet] 28:299–309. Available from: http://www.ncbi.nlm.nih.gov/pubmed/1709691

Belelli D, Harrison NL, Maguire J, Macdonald RL, Walker MC, Cope DW. 2009. Extrasynaptic GABAA receptors: form, pharmacology, and function. J Neurosci [Internet] 29:12757–63. Available from: http://www.ncbi.nlm.nih.gov/pubmed/19828786

Belelli D, Lambert JJ. 2005. Neurosteroids: endogenous regulators of the GABA(A) receptor. Nat Rev Neurosci [Internet] 6:565–75. Available from: http://www.ncbi.nlm.nih.gov/pubmed/15959466

Ben-Ari Y. 2002. Excitatory actions of gaba during development: the nature of the

nurture. Nat Rev Neurosci [Internet] 3:728–39. Available from: http://www.ncbi.nlm.nih.gov/pubmed/12209121

Bentwich I, Avniel A, Karov Y, Aharonov R, Gilad S, Barad O, Barzilai A, Einat P, Einav U, Meiri E, Sharon E, Spector Y, Bentwich Z. 2005. Identification of hundreds of conserved and nonconserved human microRNAs. Nat Genet [Internet] 37:766–70. Available from: http://www.ncbi.nlm.nih.gov/pubmed/15965474

Bernstein E, Kim SY, Carmell MA, Murchison EP, Alcorn H, Li MZ, Mills AA, Elledge SJ, Anderson K V, Hannon GJ. 2003. Dicer is essential for mouse development. Nat Genet [Internet] 35:215–7. Available from: http://www.ncbi.nlm.nih.gov/pubmed/14528307

Bianchi AB, Hara T, Ramesh V, Gao J, Klein-Szanto AJ, Morin F, Menon AG, Trofatter JA, Gusella JF, Seizinger BR. 1994. Mutations in transcript isoforms of the neurofibromatosis 2 gene in multiple human tumour types. Nat Genet [Internet] 6:185–92. Available from: http://www.ncbi.nlm.nih.gov/pubmed/8162073

Blaesse P, Airaksinen MS, Rivera C, Kaila K. 2009. Cation-chloride cotransporters and neuronal function. Neuron [Internet] 61:820–38. Available from: http://www.ncbi.nlm.nih.gov/pubmed/19323993

Blakeley JO, Plotkin SR. 2016. Therapeutic advances for the tumors associated with neurofibromatosis type 1, type 2, and schwannomatosis. Neuro Oncol [Internet] 18:624–38. Available from: http://www.ncbi.nlm.nih.gov/pubmed/26851632

Boerboom A, Dion V, Chariot A, Franzen R. 2017. Molecular Mechanisms Involved in Schwann Cell Plasticity. Front Mol Neurosci [Internet] 10:38. Available from: http://www.ncbi.nlm.nih.gov/pubmed/28261057

Boggiano JC, Vanderzalm PJ, Fehon RG. 2011. Tao-1 phosphorylates Hippo/MST kinases to regulate the Hippo-Salvador-Warts tumor suppressor pathway. Dev Cell [Internet] 21:888–95. Available from: http://www.ncbi.nlm.nih.gov/pubmed/22075147

Boileau AJ, Pearce RA, Czajkowski C. 2005. Tandem subunits effectively constrain GABAA receptor stoichiometry and recapitulate receptor kinetics but are insensitive to GABAA receptor-associated protein. J Neurosci [Internet] 25:11219–30. Available from: http://www.ncbi.nlm.nih.gov/pubmed/16339017

Bowery NG, Doble A, Hill DR, Hudson AL, Shaw JS, Turnbull MJ, Warrington R. 1981. Bicuculline-insensitive GABA receptors on peripheral autonomic nerve terminals. Eur J Pharmacol [Internet] 71:53–70. Available from: http://www.ncbi.nlm.nih.gov/pubmed/6263651

Bremer J, O'Connor T, Tiberi C, Rehrauer H, Weis J, Aguzzi A. 2010a. Ablation of Dicer from murine Schwann cells increases their proliferation while blocking myelination. PLoS One [Internet] 5:e12450. Available from: http://www.ncbi.nlm.nih.gov/pubmed/20805985

Bremer J, O'Connor T, Tiberi C, Rehrauer H, Weis J, Aguzzi A. 2010b. Ablation of dicer from murine Schwann cells increases their proliferation while blocking myelination. PLoS One 5.

Brockes JP, Fields KL, Raff MC. 1979. Studies on cultured rat Schwann cells. I. Establishment of purified populations from cultures of peripheral nerve. Brain Res 165:105–118.

Bronstein JM. 2000. Function of tetraspan proteins in the myelin sheath. Curr Opin Neurobiol [Internet] 10:552–7. Available from: http://www.ncbi.nlm.nih.gov/pubmed/11084316

Brown DA, Adams PR, Higgins AJ, Marsh S. 1979. Distribution of gaba-receptors and gaba-carriers in the mammalian nervous system. J Physiol (Paris) [Internet] 75:667–71. Available from: http://www.ncbi.nlm.nih.gov/pubmed/232722

Brown DA, Marsh S. 1978. Axonal GABA-receptors in mammalian peripheral nerve trunks. Brain Res [Internet] 156:187–91. Available from: http://www.ncbi.nlm.nih.gov/pubmed/212161

Brown MT, Cooper JA. 1996. Regulation, substrates and functions of src. Biochim

Biophys Acta [Internet] 1287:121–49. Available from: http://www.ncbi.nlm.nih.gov/pubmed/8672527

Brushart TM, Aspalter M, Griffin JW, Redett R, Hameed H, Zhou C, Wright M, Vyas A, Höke A. 2013. Schwann cell phenotype is regulated by axon modality and central-peripheral location, and persists in vitro. Exp Neurol [Internet] 247:272–81. Available from: http://www.ncbi.nlm.nih.gov/pubmed/23707299

Brushart TM, Hoffman PN, Royall RM, Murinson BB, Witzel C, Gordon T. 2002. Electrical stimulation promotes motoneuron regeneration without increasing its speed or conditioning the neuron. J Neurosci [Internet] 22:6631–8. Available from: http://www.ncbi.nlm.nih.gov/pubmed/12151542

Budde H, Schmitt S, Fitzner D, Opitz L, Salinas-Riester G, Simons M. 2010. Control of oligodendroglial cell number by the miR-17-92 cluster. Development [Internet] 137:2127–32. Available from: http://www.ncbi.nlm.nih.gov/pubmed/20504959

Buddhala C, Hsu C-C, Wu J-Y. A novel mechanism for GABA synthesis and packaging into synaptic vesicles. Neurochem Int [Internet] 55:9–12. Available from: http://www.ncbi.nlm.nih.gov/pubmed/19428801

Calalb MB, Polte TR, Hanks SK. 1995. Tyrosine phosphorylation of focal adhesion kinase at sites in the catalytic domain regulates kinase activity: a role for Src family kinases. Mol Cell Biol [Internet] 15:954–63. Available from: http://www.ncbi.nlm.nih.gov/pubmed/7529876

Callachan H, Cottrell GA, Hather NY, Lambert JJ, Nooney JM, Peters JA. 1987. Modulation of the GABAA receptor by progesterone metabolites. Proc R Soc Lond B Biol Sci [Internet] 231:359–369. Available from: http://eutils.ncbi.nlm.nih.gov/entrez/eutils/elink.fcgi?dbfrom=pubmed&id=2888123&retmode=ref&cmd=prlinks%5Cnpapers2://publication/uuid/703CD033-FA10-418A-9CFE-13D3FC0D1910

Callus BA, Verhagen AM, Vaux DL. 2006. Association of mammalian sterile twenty kinases, Mst1 and Mst2, with hSalvador via C-terminal coiled-coil domains,

leads to its stabilization and phosphorylation. FEBS J [Internet] 273:4264–76. Available from: http://www.ncbi.nlm.nih.gov/pubmed/16930133

Campana WM. 2007. Schwann cells: activated peripheral glia and their role in neuropathic pain. Brain Behav Immun [Internet] 21:522–7. Available from: http://www.ncbi.nlm.nih.gov/pubmed/17321718

Cardis E, Schuz J. 2011. Acoustic neuroma risk in relation to mobile telephone use: Results of the INTERPHONE international case-control study. Cancer Epidemiol 35:453–464.

Carpenter DO. 2013. Human disease resulting from exposure to electromagnetic fields. Rev Environ Health [Internet] 28:159–72. Available from: http://www.ncbi.nlm.nih.gov/pubmed/24280284

Castanotto D, Tommasi S, Li M, Li H, Yanow S, Pfeifer GP, Rossi JJ. 2005. Short hairpin RNA-directed cytosine (CpG) methylation of the RASSF1A gene promoter in HeLa cells. Mol Ther [Internet] 12:179–83. Available from: http://www.ncbi.nlm.nih.gov/pubmed/15963934

Castelnovo LF, Bonalume V, Melfi S, Ballabio M, Colleoni D, Magnaghi V. 2017. Schwann cell development, maturation and regeneration: a focus on classic and emerging intracellular signaling pathways. Neural Regen Res [Internet] 12:1013–1023. Available from: http://www.ncbi.nlm.nih.gov/pubmed/28852375

Celotti F, Melcangi RC, Martini L. 1992. The 5 alpha-reductase in the brain: molecular aspects and relation to brain function. Front Neuroendocrinol [Internet] 13:163–215. Available from: http://www.ncbi.nlm.nih.gov/pubmed/1468601

Chan EHY, Nousiainen M, Chalamalasetty RB, Schäfer A, Nigg EA, Silljé HHW. 2005. The Ste20-like kinase Mst2 activates the human large tumor suppressor kinase Lats1. Oncogene [Internet] 24:2076–86. Available from: http://www.ncbi.nlm.nih.gov/pubmed/15688006

Chan KM, Curran MWT, Gordon T. 2016. The use of brief post-surgical low

frequency electrical stimulation to enhance nerve regeneration in clinical practice. J Physiol [Internet] 594:3553–9. Available from: http://www.ncbi.nlm.nih.gov/pubmed/26864594

Chance PF. 2004. Genetic evaluation of inherited motor/sensory neuropathy. Suppl Clin Neurophysiol [Internet] 57:228–42. Available from: http://www.ncbi.nlm.nih.gov/pubmed/16106622

Charles KJ, Calver AR, Jourdain S, Pangalos MN. 2003. Distribution of a GABAB-like receptor protein in the rat central nervous system. Brain Res [Internet] 989:135–46. Available from: http://www.ncbi.nlm.nih.gov/pubmed/14556935

Charles KJ, Evans ML, Robbins MJ, Calver AR, Leslie RA, Pangalos MN. 2001. Comparative immunohistochemical localisation of GABA(B1a), GABA(B1b) and GABA(B2) subunits in rat brain, spinal cord and dorsal root ganglion. Neuroscience [Internet] 106:447–67. Available from: http://www.ncbi.nlm.nih.gov/pubmed/11591450

Chen J, Harris RC. 2016. Interaction of the EGF Receptor and the Hippo Pathway in the Diabetic Kidney. J Am Soc Nephrol [Internet] 27:1689–700. Available from: http://www.ncbi.nlm.nih.gov/pubmed/26453611

Chen K, Rajewsky N. 2007. The evolution of gene regulation by transcription factors and microRNAs. Nat Rev Genet [Internet] 8:93–103. Available from: http://www.ncbi.nlm.nih.gov/pubmed/17230196

Chen S, Rio C, Ji R-R, Dikkes P, Coggeshall RE, Woolf CJ, Corfas G. 2003. Disruption of ErbB receptor signaling in adult non-myelinating Schwann cells causes progressive sensory loss. Nat Neurosci [Internet] 6:1186–93. Available from: http://www.ncbi.nlm.nih.gov/pubmed/14555954

Chen S, Velardez MO, Warot X, Yu Z-X, Miller SJ, Cros D, Corfas G. 2006. Neuregulin 1-erbB signaling is necessary for normal myelination and sensory function. J Neurosci [Internet] 26:3079–86. Available from: http://www.ncbi.nlm.nih.gov/pubmed/16554459

Chen Z-L, Yu W-M, Strickland S. 2007. Peripheral regeneration. Annu Rev Neurosci [Internet] 30:209–33. Available from: http://www.ncbi.nlm.nih.gov/pubmed/17341159

Chernousov MA, Yu W-M, Chen Z-L, Carey DJ, Strickland S. 2008. Regulation of Schwann cell function by the extracellular matrix. Glia [Internet] 56:1498–507. Available from: http://www.ncbi.nlm.nih.gov/pubmed/18803319

Cooper J, Giancotti FG. 2014. Molecular insights into NF2/Merlin tumor suppressor function. FEBS Lett [Internet] 588:2743–52. Available from: http://www.ncbi.nlm.nih.gov/pubmed/24726726

Curto M, Cole BK, Lallemand D, Liu C-H, McClatchey AI. 2007. Contact-dependent inhibition of EGFR signaling by Nf2/Merlin. J Cell Biol [Internet] 177:893–903. Available from: http://www.ncbi.nlm.nih.gov/pubmed/17548515

D'Antonio M, Droggiti A, Feltri ML, Roes J, Wrabetz L, Mirsky R, Jessen KR. 2006. TGFbeta type II receptor signaling controls Schwann cell death and proliferation in developing nerves. J Neurosci [Internet] 26:8417–27. Available from: http://www.ncbi.nlm.nih.gov/pubmed/16914667

Das T, Safferling K, Rausch S, Grabe N, Boehm H, Spatz JP. 2015. A molecular mechanotransduction pathway regulates collective migration of epithelial cells. Nat Cell Biol [Internet] 17:276–287. Available from: http://www.ncbi.nlm.nih.gov/pubmed/25706233

Denisenko-Nehrbass N, Goutebroze L, Galvez T, Bonnon C, Stankoff B, Ezan P, Giovannini M, Faivre-Sarrailh C, Girault J-A. 2003. Association of Caspr/paranodin with tumour suppressor schwannomin/merlin and beta1 integrin in the central nervous system. J Neurochem [Internet] 84:209–21. Available from: http://www.ncbi.nlm.nih.gov/pubmed/12558984

Dong Z, Brennan A, Liu N, Yarden Y, Lefkowitz G, Mirsky R, Jessen KR. 1995. Neu differentiation factor is a neuron-glia signal and regulates survival, proliferation, and maturation of rat Schwann cell precursors. Neuron [Internet] 15:585–96. Available from: http://www.ncbi.nlm.nih.gov/pubmed/7546738

Le Douarin NM, Teillet M a. 1973. The migration of neural crest cells to the wall of the digestive tract in avian embryo. J Embryol Exp Morphol 30:31–48.

Dubourg O, Azzedine H, Verny C, Durosier G, Birouk N, Gouider R, Salih M, Bouhouche A, Thiam A, Grid D, Mayer M, Ruberg M, Tazir M, Brice A, LeGuern E. 2006. Autosomal-recessive forms of demyelinating Charcot-Marie-Tooth disease. Neuromolecular Med [Internet] 8:75–86. Available from: http://www.ncbi.nlm.nih.gov/pubmed/16775368

Dugas JC, Cuellar TL, Scholze A, Ason B, Ibrahim A, Emery B, Zamanian JL, Foo LC, McManus MT, Barres BA. 2010a. Dicer1 and miR-219 Are required for normal oligodendrocyte differentiation and myelination. Neuron [Internet] 65:597–611. Available from: http://www.ncbi.nlm.nih.gov/pubmed/20223197

Dugas JC, Cuellar TL, Scholze A, Ason B, Ibrahim A, Emery B, Zamanian JL, Foo LC, McManus MT, Barres BA. 2010b. Dicer1 and miR-219 Are Required for Normal Oligodendrocyte Differentiation and Myelination. Neuron 65:597–611.

Dugas JC, Notterpek L. 2011. MicroRNAs in oligodendrocyte and Schwann cell differentiation. Dev Neurosci [Internet] 33:14–20. Available from: http://www.ncbi.nlm.nih.gov/pubmed/21346322

Dupont S, Morsut L, Aragona M, Enzo E, Giulitti S, Cordenonsi M, Zanconato F, Le Digabel J, Forcato M, Bicciato S, Elvassore N, Piccolo S. 2011. Role of YAP/TAZ in mechanotransduction. Nature [Internet] 474:179–83. Available from: http://www.ncbi.nlm.nih.gov/pubmed/21654799

Dyck P, Lambert EH. 1968. Lower motor and primary sensory neuron diseases with peroneal muscular atrophy: Ii. neurologic, genetic, and electrophysiologic findings in various neuronal degenerations. Arch Neurol [Internet] 18:619–625. Available from: http://dx.doi.org/10.1001/archneur.1968.00470360041003%5Cnhttp://archneur.jamanetwork.com.proxy.library.vanderbilt.edu/data/Journals/NEUR/15469/archneur_18_6_003.pdf

Einheber S, Hannocks MJ, Metz CN, Rifkin DB, Salzer JL. 1995. Transforming

growth factor-beta 1 regulates axon/Schwann cell interactions. J Cell Biol [Internet] 129:443–58. Available from: http://www.ncbi.nlm.nih.gov/pubmed/7536747

Evans DG, Birch JM, Ramsden RT. 1999. Paediatric presentation of type 2 neurofibromatosis. Arch Dis Child [Internet] 81:496–9. Available from: http://www.ncbi.nlm.nih.gov/pubmed/10569966

Evans DG, Huson SM, Donnai D, Neary W, Blair V, Newton V, Harris R. 1992. A clinical study of type 2 neurofibromatosis. Q J Med [Internet] 84:603–18. Available from: http://www.ncbi.nlm.nih.gov/pubmed/1484939

Evans DG, Wallace AJ, Wu CL, Trueman L, Ramsden RT, Strachan T. 1998. Somatic mosaicism: a common cause of classic disease in tumor-prone syndromes? Lessons from type 2 neurofibromatosis. Am J Hum Genet [Internet] 63:727–36. Available from: http://www.ncbi.nlm.nih.gov/pubmed/9718334

Evans DGR, Ramsden RT, Shenton A, Gokhale C, Bowers NL, Huson SM, Pichert G, Wallace A. 2007. Mosaicism in neurofibromatosis type 2: an update of risk based on uni/bilaterality of vestibular schwannoma at presentation and sensitive mutation analysis including multiple ligation-dependent probe amplification. J Med Genet [Internet] 44:424–8. Available from: http://www.ncbi.nlm.nih.gov/pubmed/17307835

Faroni A, Castelnovo LF, Procacci P, Caffino L, Fumagalli F, Melfi S, Gambarotta G, Bettler B, Wrabetz L, Magnaghi V. 2014a. Deletion of GABA-B receptor in Schwann cells regulates remak bundles and small nociceptive C-fibers. Glia [Internet] 62:548–65. Available from: http://www.ncbi.nlm.nih.gov/pubmed/24474699

Faroni A, Magnaghi V. 2011. The neurosteroid allopregnanolone modulates specific functions in central and peripheral glial cells. Front Endocrinol (Lausanne) [Internet] 2:103. Available from: http://www.ncbi.nlm.nih.gov/pubmed/22654838

Faroni A, Mobasseri SA, Kingham PJ, Reid AJ. 2015. Peripheral nerve regeneration:

Experimental strategies and future perspectives. Adv Drug Deliv Rev 82:160–167.

Faroni A, Smith RJP, Procacci P, Castelnovo LF, Puccianti E, Reid AJ, Magnaghi V, Verkhratsky A. 2014b. Purinergic signaling mediated by P2X7 receptors controls myelination in sciatic nerves. J Neurosci Res 92:1259–1269.

Faroni A, Terenghi G, Magnaghi V. 2012. Expression of Functional gamma-Aminobutyric Acid Type A Receptors in Schwann-Like Adult Stem Cells. J Mol Neurosci [Internet] 47:619–630. Available from: http://www.ncbi.nlm.nih.gov/pubmed/22215379

Feltri ML, D'Antonio M, Previtali S, Fasolini M, Messing A, Wrabetz L. 1999. P0-Cre transgenic mice for inactivation of adhesion molecules in Schwann cells. Ann N Y Acad Sci 883:116–123.

Feltri ML, Poitelon Y, Previtali SC. 2016. How Schwann Cells Sort Axons. Neurosci 22:252–265.

Feltri ML, Suter U, Relvas JB. 2008. The function of RhoGTPases in axon ensheathment and myelination. Glia [Internet] 56:1508–17. Available from: http://www.ncbi.nlm.nih.gov/pubmed/18803320

Fernandez-Valle C, Tang Y, Ricard J, Rodenas-Ruano A, Taylor A, Hackler E, Biggerstaff J, Iacovelli J. 2002. Paxillin binds schwannomin and regulates its density-dependent localization and effect on cell morphology. Nat Genet [Internet] 31:354–62. Available from: http://www.ncbi.nlm.nih.gov/pubmed/12118253

Fields RD, Burnstock G. 2006. Purinergic signalling in neuron{\textendash}glia interactions. Nat Rev Neurosci [Internet] 7:423–436. Available from: http://www.nature.com/doifinder/10.1038/nrn1928

Finegold L, Flamm BL. 2006. Magnet therapy. BMJ [Internet] 332:4. Available from: http://www.ncbi.nlm.nih.gov/pubmed/16399710

Flamini MI, Sanchez AM, Genazzani AR, Simoncini T. 2011. Estrogen regulates

endometrial cell cytoskeletal remodeling and motility via focal adhesion kinase. Fertil Steril [Internet] 95:722–6. Available from: http://www.ncbi.nlm.nih.gov/pubmed/20869705

Fontana X, Hristova M, Da Costa C, Patodia S, Thei L, Makwana M, Spencer-Dene B, Latouche M, Mirsky R, Jessen KR, Klein R, Raivich G, Behrens A. 2012. c-Jun in Schwann cells promotes axonal regeneration and motoneuron survival via paracrine signaling. J Cell Biol [Internet] 198:127–41. Available from: http://www.ncbi.nlm.nih.gov/pubmed/22753894

Fritschy J-M, Panzanelli P. 2014. GABAA receptors and plasticity of inhibitory neurotransmission in the central nervous system. Eur J Neurosci [Internet] 39:1845–65. Available from: http://www.ncbi.nlm.nih.gov/pubmed/24628861

Fu XD, Simoncini T. 2008. Extra-nuclear signaling of estrogen receptors. IUBMB Life 60:502–510.

Fults DW, Towle AC, Lauder JM, Maness PF. 1985. pp60c-src in the developing cerebellum. Mol Cell Biol [Internet] 5:27–32. Available from: http://www.ncbi.nlm.nih.gov/pubmed/3920510

Funk RHW, Monsees TK. 2006. Effects of electromagnetic fields on cells: physiological and therapeutical approaches and molecular mechanisms of interaction. A review. Cells Tissues Organs [Internet] 182:59–78. Available from: http://www.ncbi.nlm.nih.gov/pubmed/16804297

Gago N, El-Etr M, Sananès N, Cadepond F, Samuel D, Avellana-Adalid V, Baron-Van Evercooren A, Schumacher M. 2004. 3alpha,5alpha-Tetrahydroprogesterone (allopregnanolone) and gamma-aminobutyric acid: autocrine/paracrine interactions in the control of neonatal PSA-NCAM+ progenitor proliferation. J Neurosci Res [Internet] 78:770–83. Available from: http://www.ncbi.nlm.nih.gov/pubmed/15523635

Gao S, Alarcón C, Sapkota G, Rahman S, Chen P-Y, Goerner N, Macias MJ, Erdjument-Bromage H, Tempst P, Massagué J. 2009. Ubiquitin ligase Nedd4L targets activated Smad2/3 to limit TGF-beta signaling. Mol Cell [Internet]

36:457–68. Available from: http://www.ncbi.nlm.nih.gov/pubmed/19917253

Gassmann M, Bettler B. 2012. Regulation of neuronal GABA(B) receptor functions by subunit composition. Nat Rev Neurosci [Internet] 13:380–94. Available from: http://www.ncbi.nlm.nih.gov/pubmed/22595784

Gavrilovic J, Raff M, Cohen J. 1984. GABA uptake by purified rat schwann cells in culture. Brain Res [Internet] 303:183–5. Available from: http://www.ncbi.nlm.nih.gov/pubmed/6733523

Giovannini M, Robanus-Maandag E, Niwa-Kawakita M, van der Valk M, Woodruff JM, Goutebroze L, Mérel P, Berns A, Thomas G. 1999. Schwann cell hyperplasia and tumors in transgenic mice expressing a naturally occurring mutant NF2 protein. Genes Dev [Internet] 13:978–86. Available from: http://www.ncbi.nlm.nih.gov/pubmed/10215625

Giovannini M, Robanus-Maandag E, van der Valk M, Niwa-Kawakita M, Abramowski V, Goutebroze L, Woodruff JM, Berns A, Thomas G. 2000. Conditional biallelic Nf2 mutation in the mouse promotes manifestations of human neurofibromatosis type 2. Genes Dev [Internet] 14:1617–30. Available from: http://www.ncbi.nlm.nih.gov/pubmed/10887156

Glantschnig H, Rodan GA, Reszka AA. 2002. Mapping of MST1 kinase sites of phosphorylation. Activation and autophosphorylation. J Biol Chem [Internet] 277:42987–96. Available from: http://www.ncbi.nlm.nih.gov/pubmed/12223493

Glenn T, Talbot W. 2013. Can't wait to myelinate. Dev Cell 25:549–550.

Gokey NG, Srinivasan R, Lopez-Anido C, Krueger C, Svaren J. 2012. Developmental regulation of microRNA expression in Schwann cells. Mol Cell Biol [Internet] 32:558–68. Available from: http://www.pubmedcentral.nih.gov/articlerender.fcgi?artid=3255778&tool=pmcentrez&rendertype=abstract

Gonzalez-Agosti C, Wiederhold T, Herndon ME, Gusella J, Ramesh V. 1999. Interdomain interaction of merlin isoforms and its influence on intermolecular

binding to NHE-RF. J Biol Chem [Internet] 274:34438–42. Available from: http://www.ncbi.nlm.nih.gov/pubmed/10567424

Gonzalez-Burgos G, Fish KN, Lewis DA. 2011. GABA neuron alterations, cortical circuit dysfunction and cognitive deficits in schizophrenia. Neural Plast [Internet] 2011:723184. Available from: http://www.ncbi.nlm.nih.gov/pubmed/21904685

Gonzalez-Gomez P, Bello MJ, Alonso ME, Lomas J, Arjona D, Campos JM de, Vaquero J, Isla A, Lassaletta L, Gutierrez M, Sarasa JL, Rey JA. 2003. CpG island methylation in sporadic and neurofibromatis type 2-associated schwannomas. Clin Cancer Res [Internet] 9:5601–6. Available from: http://www.ncbi.nlm.nih.gov/pubmed/14654541

Goutagny S, Nault JC, Mallet M, Henin D, Rossi JZ, Kalamarides M. 2014. High incidence of activating TERT promoter mutations in meningiomas undergoing malignant progression. Brain Pathol [Internet] 24:184–9. Available from: http://www.ncbi.nlm.nih.gov/pubmed/24261697

Goutebroze L, Brault E, Muchardt C, Camonis J, Thomas G. 2000. Cloning and characterization of SCHIP-1, a novel protein interacting specifically with spliced isoforms and naturally occurring mutant NF2 proteins. Mol Cell Biol [Internet] 20:1699–712. Available from: http://www.ncbi.nlm.nih.gov/pubmed/10669747

Grinspan JB, Marchionni MA, Reeves M, Coulaloglou M, Scherer SS. 1996. Axonal interactions regulate Schwann cell apoptosis in developing peripheral nerve: neuregulin receptors and the role of neuregulins. J Neurosci [Internet] 16:6107–18. Available from: http://www.ncbi.nlm.nih.gov/pubmed/8815893

Grönholm M, Sainio M, Zhao F, Heiska L, Vaheri A, Carpén O. 1999. Homotypic and heterotypic interaction of the neurofibromatosis 2 tumor suppressor protein merlin and the ERM protein ezrin. J Cell Sci [Internet] 112 (Pt 6:895–904. Available from: http://www.ncbi.nlm.nih.gov/pubmed/10036239

Grove M, Brophy PJ. 2014. FAK is required for Schwann cell spreading on immature basal lamina to coordinate the radial sorting of peripheral axons with myelination. J Neurosci [Internet] 34:13422–34. Available from:

http://www.ncbi.nlm.nih.gov/pubmed/25274820

Grove M, Kim H, Santerre M, Krupka AJ, Han SB, Zhai J, Cho JY, Park R, Harris M, Kim S, Sawaya BE, Kang SH, Barbe MF, Cho S-H, Lemay MA, Son Y-J. 2017. YAP/TAZ initiate and maintain Schwann cell myelination. Elife [Internet] 6. Available from: http://www.ncbi.nlm.nih.gov/pubmed/28124973

Grove M, Komiyama NH, Nave K-AA, Grant SG, Sherman DL, Brophy PJ. 2007. FAK is required for axonal sorting by Schwann cells. J Cell Biol [Internet] 176:277–82. Available from: http://www.ncbi.nlm.nih.gov/pubmed/17242067

Gu Y, Chen C, Yi S, Wang S, Gong L, Liu J, Gu X, Zhao Q, Li S. 2015. miR-sc8 Inhibits Schwann Cell Proliferation and Migration by Targeting Egfr. PLoS One [Internet] 10:e0145185. Available from: http://www.ncbi.nlm.nih.gov/pubmed/26683191

Gürler HŞ, Bilgici B, Akar AK, Tomak L, Bedir A. 2014. Increased DNA oxidation (8-OHdG) and protein oxidation (AOPP) by low level electromagnetic field (2.45 GHz) in rat brain and protective effect of garlic. Int J Radiat Biol [Internet] 90:892–6. Available from: http://www.ncbi.nlm.nih.gov/pubmed/24844368

Gutmann DH, Giordano MJ, Fishback AS, Guha A. 1997. Loss of merlin expression in sporadic meningiomas, ependymomas and schwannomas. Neurology [Internet] 49:267–70. Available from: http://www.ncbi.nlm.nih.gov/pubmed/9222206

Halder S, Bhattacharyya D. 2012. Structural variations of single and tandem mismatches in RNA duplexes: a joint MD simulation and crystal structure database analysis. J Phys Chem B [Internet] 116:11845–56. Available from: http://www.ncbi.nlm.nih.gov/pubmed/22953716

Haller C, Casanova E, Müller M, Vacher CM, Vigot R, Doll T, Barbieri S, Gassmann M, Bettler B. 2004. Floxed allele for conditional inactivation of the GABAB(1) gene. Genesis 40:125–130.

Hanani M. 2005. Satellite glial cells in sensory ganglia: From form to function. Brain Res Rev 48:457–476.

Hannon GJ, Rivas F V, Murchison EP, Steitz JA. 2006. The expanding universe of noncoding RNAs. Cold Spring Harb Symp Quant Biol [Internet] 71:551–64. Available from: http://www.ncbi.nlm.nih.gov/pubmed/17381339

Hardell L, Carlberg M, Mild KH. 2006. Pooled analysis of two case-control studies on the use of cellular and cordless telephones and the risk of benign brain tumours diagnosed during 1997-2003. Int J Oncol 28:509–518.

Harding AE, Thomas PK. 1980a. The clinical features of hereditary motor and sensory neuropathy types I and II. Brain [Internet] 103:259–80. Available from: http://www.ncbi.nlm.nih.gov/pubmed/7397478

Harding AE, Thomas PK. 1980b. Autosomal recessive forms of hereditary motor and sensory neuropathy. J Neurol Neurosurg Psychiatry [Internet] 43:669–78. Available from: http://www.ncbi.nlm.nih.gov/pubmed/7431027

He J-F, Luo Y-M, Wan X-H, Jiang D. Biogenesis of MiRNA-195 and its role in biogenesis, the cell cycle, and apoptosis. J Biochem Mol Toxicol [Internet] 25:404–8. Available from: http://www.ncbi.nlm.nih.gov/pubmed/22190509

Hergovich A, Schmitz D, Hemmings BA. 2006. The human tumour suppressor LATS1 is activated by human MOB1 at the membrane. Biochem Biophys Res Commun [Internet] 345:50–8. Available from: http://www.ncbi.nlm.nih.gov/pubmed/16674920

Höke A. 2006. Mechanisms of Disease: what factors limit the success of peripheral nerve regeneration in humans? Nat Clin Pract Neurol [Internet] 2:448–54. Available from: http://www.ncbi.nlm.nih.gov/pubmed/16932603

Hossain S, Fragoso G, Mushynski WE, Almazan G. 2010. Regulation of peripheral myelination by Src-like kinases. Exp Neurol 226:47–57.

Hughes RAC. 2002. Peripheral neuropathy. BMJ [Internet] 324:466–9. Available from: http://www.ncbi.nlm.nih.gov/pubmed/11859051

INTERPHONE Study Group. 2011. Acoustic neuroma risk in relation to mobile telephone use: results of the INTERPHONE international case-control study.

Cancer Epidemiol [Internet] 35:453–64. Available from: http://www.ncbi.nlm.nih.gov/pubmed/21862434

Irby RB, Yeatman TJ. 2002. Increased Src activity disrupts cadherin/catenin-mediated homotypic adhesion in human colon cancer and transformed rodent cells. Cancer Res [Internet] 62:2669–74. Available from: http://www.ncbi.nlm.nih.gov/pubmed/11980666

Jagielska A, Norman AL, Whyte G, Vliet KJ Van, Guck J, Franklin RJM. 2012. Mechanical environment modulates biological properties of oligodendrocyte progenitor cells. Stem Cells Dev [Internet] 21:2905–14. Available from: http://www.ncbi.nlm.nih.gov/pubmed/22646081

James MF, Han S, Polizzano C, Plotkin SR, Manning BD, Stemmer-Rachamimov AO, Gusella JF, Ramesh V. 2009. NF2/merlin is a novel negative regulator of mTOR complex 1, and activation of mTORC1 is associated with meningioma and schwannoma growth. Mol Cell Biol [Internet] 29:4250–61. Available from: http://www.ncbi.nlm.nih.gov/pubmed/19451225

James MF, Manchanda N, Gonzalez-Agosti C, Hartwig JH, Ramesh V. 2001. The neurofibromatosis 2 protein product merlin selectively binds F-actin but not G-actin, and stabilizes the filaments through a lateral association. Biochem J [Internet] 356:377–86. Available from: http://www.ncbi.nlm.nih.gov/pubmed/11368764

Jessen KR, Mirsky R. 2005. The origin and development of glial cells in peripheral nerves. Nat Rev Neurosci [Internet] 6:671–82. Available from: http://www.ncbi.nlm.nih.gov/pubmed/16136171

Jessen KR, Mirsky R. 2008. Negative regulation of myelination: relevance for development, injury, and demyelinating disease. Glia [Internet] 56:1552–65. Available from: http://www.ncbi.nlm.nih.gov/pubmed/18803323

Jessen KR, Mirsky R, Lloyd AC. 2015. Schwann Cells: Development and Role in Nerve Repair. Cold Spring Harb Perspect Biol [Internet] 7:a020487. Available from: http://www.ncbi.nlm.nih.gov/pubmed/25957303

Jin H, Sperka T, Herrlich P, Morrison H. 2006. Tumorigenic transformation by CPI-17 through inhibition of a merlin phosphatase. Nature [Internet] 442:576–9. Available from: http://www.ncbi.nlm.nih.gov/pubmed/16885985

Jones BL, Henderson LP. 2007. Trafficking and potential assembly patterns of epsilon-containing GABAA receptors. J Neurochem [Internet] 103:1258–71. Available from: http://www.ncbi.nlm.nih.gov/pubmed/17714454

Jones KA, Borowsky B, Tamm JA, Craig DA, Durkin MM, Dai M, Yao WJ, Johnson M, Gunwaldsen C, Huang LY, Tang C, Shen Q, Salon JA, Morse K, Laz T, Smith KE, Nagarathnam D, Noble SA, Branchek TA, Gerald C. 1998. GABA(B) receptors function as a heteromeric assembly of the subunits GABA(B)R1 and GABA(B)R2. Nature [Internet] 396:674–9. Available from: http://www.ncbi.nlm.nih.gov/pubmed/9872315

Jow F, Chiu D, Lim H-K, Novak T, Lin S. Production of GABA by cultured hippocampal glial cells. Neurochem Int [Internet] 45:273–83. Available from: http://www.ncbi.nlm.nih.gov/pubmed/15145543

Kaempchen K, Mielke K, Utermark T, Langmesser S, Hanemann CO. 2003. Upregulation of the Rac1/JNK signaling pathway in primary human schwannoma cells. Hum Mol Genet [Internet] 12:1211–21. Available from: http://www.ncbi.nlm.nih.gov/pubmed/12761036

Kahle KT, Deeb TZ, Puskarjov M, Silayeva L, Liang B, Kaila K, Moss SJ. 2013. Modulation of neuronal activity by phosphorylation of the K-Cl cotransporter KCC2. Trends Neurosci [Internet] 36:726–737. Available from: http://www.ncbi.nlm.nih.gov/pubmed/24139641

Kalamarides M, Niwa-Kawakita M, Leblois H, Abramowski V, Perricaudet M, Janin A, Thomas G, Gutmann DH, Giovannini M. 2002. Nf2 gene inactivation in arachnoidal cells is rate-limiting for meningioma development in the mouse. Genes Dev [Internet] 16:1060–5. Available from: http://www.ncbi.nlm.nih.gov/pubmed/12000789

Kash SF, Johnson RS, Tecott LH, Noebels JL, Mayfield RD, Hanahan D, Baekkeskov

S. 1997. Epilepsy in mice deficient in the 65-kDa isoform of glutamic acid decarboxylase. Proc Natl Acad Sci U S A [Internet] 94:14060–5. Available from: http://www.ncbi.nlm.nih.gov/pubmed/9391152

Kaupmann K, Huggel K, Heid J, Flor PJ, Bischoff S, Mickel SJ, McMaster G, Angst C, Bittiger H, Froestl W, Bettler B. 1997. Expression cloning of GABA(B) receptors uncovers similarity to metabotropic glutamate receptors. Nature [Internet] 386:239–46. Available from: http://www.ncbi.nlm.nih.gov/pubmed/9069281

Kaupmann K, Malitschek B, Schuler V, Heid J, Froestl W, Beck P, Mosbacher J, Bischoff S, Kulik A, Shigemoto R, Karschin A, Bettler B. 1998. GABA(B)-receptor subtypes assemble into functional heteromeric complexes. Nature [Internet] 396:683–7. Available from: http://www.ncbi.nlm.nih.gov/pubmed/9872317

Kawase-Koga Y, Otaegi G, Sun T. 2009. Different timings of Dicer deletion affect neurogenesis and gliogenesis in the developing mouse central nervous system. Dev Dyn [Internet] 238:2800–12. Available from: http://www.ncbi.nlm.nih.gov/pubmed/19806666

Kim H, Laing M, Muller W. 2005. c-Src-null mice exhibit defects in normal mammary gland development and ERalpha signaling. Oncogene [Internet] 24:5629–5636. Available from: http://www.ncbi.nlm.nih.gov/pubmed/16007215

Kim VN, Han J, Siomi MC. 2009. Biogenesis of small RNAs in animals. Nat Rev Mol Cell Biol [Internet] 10:126–39. Available from: http://www.ncbi.nlm.nih.gov/pubmed/19165215

Kimura Y, Koga H, Araki N, Mugita N, Fujita N, Takeshima H, Nishi T, Yamashima T, Saido TC, Yamasaki T, Moritake K, Saya H, Nakao M. 1998. The involvement of calpain-dependent proteolysis of the tumor suppressor NF2 (merlin) in schwannomas and meningiomas. Nat Med [Internet] 4:915–22. Available from: http://www.ncbi.nlm.nih.gov/pubmed/9701243

Kino T, Takeshima H, Nakao M, Nishi T, Yamamoto K, Kimura T, Saito Y, Kochi M,

Kuratsu J, Saya H, Ushio Y. 2001. Identification of the cis-acting region in the NF2 gene promoter as a potential target for mutation and methylation-dependent silencing in schwannoma. Genes Cells [Internet] 6:441–54. Available from: http://www.ncbi.nlm.nih.gov/pubmed/11380622

Kluwe L, Mautner V, Heinrich B, Dezube R, Jacoby LB, Friedrich RE, MacCollin M. 2003. Molecular study of frequency of mosaicism in neurofibromatosis 2 patients with bilateral vestibular schwannomas. J Med Genet [Internet] 40:109–14. Available from: http://www.ncbi.nlm.nih.gov/pubmed/12566519

Koontz LM, Liu-Chittenden Y, Yin F, Zheng Y, Yu J, Huang B, Chen Q, Wu S, Pan D. 2013. The Hippo effector Yorkie controls normal tissue growth by antagonizing scalloped-mediated default repression. Dev Cell [Internet] 25:388–401. Available from: http://www.ncbi.nlm.nih.gov/pubmed/23725764

Koutsimpelas D, Ruerup G, Mann WJ, Brieger J. 2012. Lack of neurofibromatosis type 2 gene promoter methylation in sporadic vestibular schwannomas. ORL J Otorhinolaryngol Relat Spec [Internet] 74:33–7. Available from: http://www.ncbi.nlm.nih.gov/pubmed/22249120

Kozlov AS, Angulo MC, Audinat E, Charpak S. 2006. Target cell-specific modulation of neuronal activity by astrocytes. Proc Natl Acad Sci U S A [Internet] 103:10058–63. Available from: http://www.ncbi.nlm.nih.gov/pubmed/16782808

Kresak JL, Walsh M. 2016. Neurofibromatosis: A Review of NF1, NF2, and Schwannomatosis. J Pediatr Genet [Internet] 5:98–104. Available from: http://www.ncbi.nlm.nih.gov/pubmed/27617150

Kuhn SA, van Landeghem FKH, Zacharias R, Färber K, Rappert A, Pavlovic S, Hoffmann A, Nolte C, Kettenmann H. 2004. Microglia express GABA(B) receptors to modulate interleukin release. Mol Cell Neurosci [Internet] 25:312–22. Available from: http://www.ncbi.nlm.nih.gov/pubmed/15019947

Kuner R, Köhr G, Grünewald S, Eisenhardt G, Bach A, Kornau HC. 1999. Role of heteromer formation in GABAB receptor function. Science [Internet] 283:74–7. Available from: http://www.ncbi.nlm.nih.gov/pubmed/9872744

Lacy-Hulbert a, Metcalfe JC, Hesketh R. 1998. Biological responses to electromagnetic fields. FASEB J [Internet] 12:395–420. Available from: http://www.ncbi.nlm.nih.gov/pubmed/9535213

Lallemand D, Saint-Amaux AL, Giovannini M. 2009. Tumor-suppression functions of merlin are independent of its role as an organizer of the actin cytoskeleton in Schwann cells. J Cell Sci [Internet] 122:4141–4149. Available from: http://www.ncbi.nlm.nih.gov/pubmed/19910496

Lambert JJ, Belelli D, Hill-Venning C, Peters JA. 1995. Neurosteroids and GABAA receptor function. Trends Pharmacol Sci [Internet] 16:295–303. Available from: http://www.ncbi.nlm.nih.gov/pubmed/7482994

Lambert JJ, Belelli D, Peden DR, Vardy AW, Peters JA. 2003. Neurosteroid modulation of GABAA receptors. Prog Neurobiol [Internet] 71:67–80. Available from: http://www.ncbi.nlm.nih.gov/pubmed/14611869

Lau P, Verrier JD, Nielsen JA, Johnson KR, Notterpek L, Hudson LD. 2008. Identification of dynamically regulated microRNA and mRNA networks in developing oligodendrocytes. J Neurosci [Internet] 28:11720–30. Available from: http://www.jneurosci.org/content/28/45/11720.abstract?ijkey=b50631ebf7fb155fa39b2c37932207dab976fc92&keytype2=tf_ipsecsha

Laulajainen M, Muranen T, Carpén O, Grönholm M. 2008. Protein kinase A-mediated phosphorylation of the NF2 tumor suppressor protein merlin at serine 10 affects the actin cytoskeleton. Oncogene [Internet] 27:3233–43. Available from: http://www.ncbi.nlm.nih.gov/pubmed/18071304

Laycock-van Spyk S, Thomas N, Cooper DN, Upadhyaya M. 2011. Neurofibromatosis type 1-associated tumours: their somatic mutational spectrum and pathogenesis. Hum Genomics [Internet] 5:623–90. Available from: http://www.ncbi.nlm.nih.gov/pubmed/22155606

Lewis BP, Burge CB, Bartel DP. 2005. Conserved seed pairing, often flanked by adenosines, indicates that thousands of human genes are microRNA targets. Cell

[Internet] 120:15–20. Available from: http://www.ncbi.nlm.nih.gov/pubmed/15652477

Lewis BP, Shih I, Jones-Rhoades MW, Bartel DP, Burge CB. 2003. Prediction of mammalian microRNA targets. Cell [Internet] 115:787–98. Available from: http://www.ncbi.nlm.nih.gov/pubmed/14697198

Li W, You L, Cooper J, Schiavon G, Pepe-Caprio A, Zhou L, Ishii R, Giovannini M, Hanemann CO, Long SB, Erdjument-Bromage H, Zhou P, Tempst P, Giancotti FG. 2010. Merlin/NF2 suppresses tumorigenesis by inhibiting the E3 ubiquitin ligase CRL4(DCAF1) in the nucleus. Cell [Internet] 140:477–90. Available from: http://www.ncbi.nlm.nih.gov/pubmed/20178741

Li Y, Gonzalez MI, Meinkoth JL, Field J, Kazanietz MG, Tennekoon GI. 2003. Lysophosphatidic acid promotes survival and differentiation of rat Schwann cells. J Biol Chem [Internet] 278:9585–91. Available from: http://www.ncbi.nlm.nih.gov/pubmed/12524451

Liang N, Zhang C, Dill P, Panasyuk G, Pion D, Koka V, Gallazzini M, Olson EN, Lam H, Henske EP, Dong Z, Apte U, Pallet N, Johnson RL, Terzi F, Kwiatkowski DJ, Scoazec J-Y, Martignoni G, Pende M. 2014. Regulation of YAP by mTOR and autophagy reveals a therapeutic target of tuberous sclerosis complex. J Exp Med [Internet] 211:2249–63. Available from: http://www.ncbi.nlm.nih.gov/pubmed/25288394

Lin S-T, Fu Y-H. miR-23 regulation of lamin B1 is crucial for oligodendrocyte development and myelination. Dis Model Mech [Internet] 2:178–88. Available from: http://www.ncbi.nlm.nih.gov/pubmed/19259393

Liu C-Y, Zha Z-Y, Zhou X, Zhang H, Huang W, Zhao D, Li T, Chan SW, Lim CJ, Hong W, Zhao S, Xiong Y, Lei Q-Y, Guan K-L. 2010. The hippo tumor pathway promotes TAZ degradation by phosphorylating a phosphodegron and recruiting the SCF{beta}-TrCP E3 ligase. J Biol Chem [Internet] 285:37159–69. Available from: http://www.ncbi.nlm.nih.gov/pubmed/20858893

Liu QY, Schaffner AE, Chang YH, Maric D, Barker JL. 2000. Persistent activation of

GABA(A) receptor/Cl(-) channels by astrocyte-derived GABA in cultured embryonic rat hippocampal neurons. J Neurophysiol [Internet] 84:1392–403. Available from: http://www.ncbi.nlm.nih.gov/pubmed/10980012

Lomas J, Bello MJ, Arjona D, Alonso ME, Martinez-Glez V, Lopez-Marin I, Amiñoso C, de Campos JM, Isla A, Vaquero J, Rey JA. 2005. Genetic and epigenetic alteration of the NF2 gene in sporadic meningiomas. Genes Chromosomes Cancer [Internet] 42:314–9. Available from: http://www.ncbi.nlm.nih.gov/pubmed/15609345

Lopez-Anido C, Poitelon Y, Gopinath C, Moran JJ, Ma KH, Law WD, Antonellis A, Feltri ML, Svaren J. 2016. Tead1 regulates the expression of Peripheral Myelin Protein 22 during Schwann cell development. Hum Mol Genet [Internet] 25:3055–3069. Available from: http://www.ncbi.nlm.nih.gov/pubmed/27288457

López-Lago MA, Okada T, Murillo MM, Socci N, Giancotti FG. 2009. Loss of the tumor suppressor gene NF2, encoding merlin, constitutively activates integrin-dependent mTORC1 signaling. Mol Cell Biol [Internet] 29:4235–49. Available from: http://www.ncbi.nlm.nih.gov/pubmed/19451229

Loreti S, Ricordy R, Egle De Stefano M, Augusti-Tocco G, Maria Tata A. 2007. Acetylcholine inhibits cell cycle progression in rat Schwann cells by activation of the M2 receptor subtype. Neuron Glia Biol [Internet] 3:269–279. Available from: http://www.ncbi.nlm.nih.gov/entrez/query.fcgi?cmd=Retrieve&db=PubMed&dopt=Citation&list_uids=18634559

Lourenço T, Grãos M. 2016. Modulation of Oligodendrocyte Differentiation by Mechanotransduction. Front Cell Neurosci [Internet] 10:277. Available from: http://www.ncbi.nlm.nih.gov/pubmed/27965541

Luyt K, Slade TP, Dorward JJ, Durant CF, Wu Y, Shigemoto R, Mundell SJ, Váradi A, Molnár E. 2007. Developing oligodendrocytes express functional GABA(B) receptors that stimulate cell proliferation and migration. J Neurochem [Internet] 100:822–40. Available from: http://www.ncbi.nlm.nih.gov/pubmed/17144904

MacCollin M, Willett C, Heinrich B, Jacoby LB, Acierno JS, Perry A, Louis DN.

2003. Familial schwannomatosis: exclusion of the NF2 locus as the germline event. Neurology [Internet] 60:1968–74. Available from: http://www.ncbi.nlm.nih.gov/pubmed/12821741

Magnaghi V. 2007. GABA and neuroactive steroid interactions in glia: new roles for old players? Curr Neuropharmacol [Internet] 5:47–64. Available from: http://dx.doi.org/10.2174/157015907780077132

Magnaghi V, Ballabio M, Camozzi F, Colleoni M, Consoli A, Gassmann M, Lauria G, Motta M, Procacci P, Trovato AE, Bettler B. 2008a. Altered peripheral myelination in mice lacking GABAB receptors. Mol Cell Neurosci 37:599–609.

Magnaghi V, Ballabio M, Camozzi F, Colleoni M, Consoli A, Gassmann M, Lauria G, Motta M, Procacci P, Trovato AE, Bettler B. 2008b. Altered peripheral myelination in mice lacking GABAB receptors. Mol Cell Neurosci [Internet] 37:599–609. Available from: http://www.ncbi.nlm.nih.gov/pubmed/18206390

Magnaghi V, Ballabio M, Cavarretta ITR, Froestl W, Lambert JJ, Zucchi I, Melcangi RC. 2004a. GABAB receptors in Schwann cells influence proliferation and myelin protein expression. Eur J Neurosci [Internet] 19:2641–9. Available from: http://www.ncbi.nlm.nih.gov/pubmed/15147298

Magnaghi V, Ballabio M, Consoli A, Lambert JJ, Roglio I, Melcangi RC. 2006a. GABA receptor-mediated effects in the peripheral nervous system: A cross-interaction with neuroactive steroids. J Mol Neurosci [Internet] 28:89–102. Available from: http://www.ncbi.nlm.nih.gov/pubmed/16632878

Magnaghi V, Ballabio M, Consoli A, Lambert JJ, Roglio I, Melcangi RC. 2006b. GABA receptor-mediated effects in the peripheral nervous system: A cross-interaction with neuroactive steroids. J Mol Neurosci [Internet] 28:89–102. Available from: http://www.ncbi.nlm.nih.gov/pubmed/16632878

Magnaghi V, Ballabio M, Gonzalez LC, Leonelli E, Motta M, Melcangi RC. 2004b. The synthesis of glycoprotein Po and peripheral myelin protein 22 in sciatic nerve of male rats is modulated by testosterone metabolites. Mol Brain Res 126:67–73.

Magnaghi V, Ballabio M, Roglio I, Melcangi RC. 2007. Progesterone derivatives increase expression of Krox-20 and Sox-10 in rat Schwann cells. J Mol Neurosci 31:149–157.

Magnaghi V, Cavarretta I, Galbiati M, Martini L, Melcangi RC. 2001. Neuroactive steroids and peripheral myelin proteins. Brain Res Brain Res Rev [Internet] 37:360–71. Available from: http://www.ncbi.nlm.nih.gov/pubmed/11744100

Magnaghi V, Parducz A, Frasca A, Ballabio M, Procacci P, Racagni G, Bonanno G, Fumagalli F. 2010. GABA synthesis in Schwann cells is induced by the neuroactive steroid allopregnanolone. J Neurochem 112:980–990.

Magnaghi V, Veiga S, Ballabio M, Gonzalez LC, Garcia-Segura LM, Melcangi RC. 2006c. Sex-dimorphic effects of progesterone and its reduced metabolites on gene expression of myelin proteins by rat Schwann cells. J Peripher Nerv Syst 11:111–118.

Maguire J, Mody I. 2009. Steroid hormone fluctuations and GABA(A)R plasticity. Psychoneuroendocrinology [Internet] 34 Suppl 1:S84-90. Available from: http://www.ncbi.nlm.nih.gov/pubmed/19632051

Majewska MD, Harrison NL, Schwartz RD, Barker JL, Paul SM. 1986. Steroid hormone metabolites are barbiturate-like modulators of the GABA receptor. Science (80-) [Internet] 232:1004–1007. Available from: http://science.sciencemag.org/content/232/4753/1004.abstract

Mammoto T, Ingber DE. 2010. Mechanical control of tissue and organ development. Development [Internet] 137:1407–20. Available from: http://www.ncbi.nlm.nih.gov/pubmed/20388652

Margeta-Mitrovic M, Mitrovic I, Riley RC, Jan LY, Basbaum AI. 1999. Immunohistochemical localization of GABA(B) receptors in the rat central nervous system. J Comp Neurol [Internet] 405:299–321. Available from: http://www.ncbi.nlm.nih.gov/pubmed/10076927

Marieb EN, Hoehn K. 2007. Human Anatomy & Physiology.

Martinez J, Patkaniowska A, Urlaub H, Lührmann R, Tuschl T. 2002. Single-stranded antisense siRNAs guide target RNA cleavage in RNAi. Cell [Internet] 110:563–74. Available from: http://www.ncbi.nlm.nih.gov/pubmed/12230974

Martini L, Magnaghi V, Melcangi RC. 2003. Actions of progesterone and its 5alpha-reduced metabolites on the major proteins of the myelin of the peripheral nervous system. Steroids [Internet] 68:825–9. Available from: http://www.ncbi.nlm.nih.gov/pubmed/14667974

Martini R, Fischer S, López-Vales R, David S. 2008. Interactions between Schwann cells and macrophages in injury and inherited demyelinating disease. Glia [Internet] 56:1566–77. Available from: http://www.ncbi.nlm.nih.gov/pubmed/18803324

McCarthy MM, Amateau SK, Mong JA. 2002. Steroid modulation of astrocytes in the neonatal brain: implications for adult reproductive function. Biol Reprod [Internet] 67:691–8. Available from: http://www.ncbi.nlm.nih.gov/pubmed/12193373

McClatchey A, Giovannini M. 2005. Membrane organization and tumorigenesis--the NF2 tumor suppressor, Merlin. Genes Dev [Internet] 19:2265–2277. Available from: http://dx.doi.org/10.1101/gad.1335605

McClatchey AI, Fehon RG. 2009. Merlin and the ERM proteins--regulators of receptor distribution and signaling at the cell cortex. Trends Cell Biol [Internet] 19:198–206. Available from: http://www.ncbi.nlm.nih.gov/pubmed/19345106

McClatchey AI, Saotome I, Mercer K, Crowley D, Gusella JF, Bronson RT, Jacks T. 1998. Mice heterozygous for a mutation at the Nf2 tumor suppressor locus develop a range of highly metastatic tumors. Genes Dev [Internet] 12:1121–33. Available from: http://www.ncbi.nlm.nih.gov/pubmed/9553042

McLean GW, Carragher NO, Avizienyte E, Evans J, Brunton VG, Frame MC. 2005. The role of focal-adhesion kinase in cancer - a new therapeutic opportunity. Nat Rev Cancer [Internet] 5:505–15. Available from: http://www.ncbi.nlm.nih.gov/pubmed/16069815

Melcangi RC, Cavarretta ITR, Ballabio M, Leonelli E, Schenone A, Azcoitia I, Miguel Garcia-Segura L, Magnaghi V. 2005. Peripheral nerves: a target for the action of neuroactive steroids. Brain Res Brain Res Rev [Internet] 48:328–38. Available from: http://www.ncbi.nlm.nih.gov/pubmed/15850671

Melcangi RC, Celotti F, Ballabio M, Castano P, Poletti A, Milani S, Martini L. 1988. Ontogenetic development of the 5 alpha-reductase in the rat brain: cerebral cortex, hypothalamus, purified myelin and isolated oligodendrocytes. Brain Res Dev Brain Res [Internet] 44:181–8. Available from: http://www.ncbi.nlm.nih.gov/pubmed/3224423

Melcangi RC, Celotti F, Ballabio M, Poletti A, Martini L. 1990. Testosterone metabolism in peripheral nerves: presence of the 5 alpha-reductase-3 alpha-hydroxysteroid-dehydrogenase enzymatic system in the sciatic nerve of adult and aged rats. J Steroid Biochem [Internet] 35:145–8. Available from: http://www.ncbi.nlm.nih.gov/pubmed/2308325

Melcangi RC, Celotti F, Castano P, Martini L. 1992. Is the 5 alpha-reductase-3 alpha-hydroxysteroid dehydrogenase complex associated with the myelin in the peripheral nervous system of young and old male rats? Endocr Regul [Internet] 26:119–25. Available from: http://www.ncbi.nlm.nih.gov/pubmed/1308154

Melcangi RC, Magnaghi V, Galbiati M, Martini L. 2001. Formation and effects of neuroactive steroids in the central and peripheral nervous system. Int Rev Neurobiol [Internet] 46:145–76. Available from: http://www.ncbi.nlm.nih.gov/pubmed/11599299

Melcangi RC, Magnaghi V, Martini L. 1999. Steroid metabolism and effects in central and peripheral glial cells. J Neurobiol [Internet] 40:471–83. Available from: http://www.ncbi.nlm.nih.gov/pubmed/10453050

Melcangi RC, Magnaghi V, Martini L. 2000. Aging in peripheral nerves: Regulation of myelin protein genes by steroid hormones. Prog Neurobiol 60:291–308.

Melcangi RC, Panzica G. 2009. Neuroactive steroids: An update of their roles in central and peripheral nervous system. Psychoneuroendocrinology 34.

Mellon SH, Griffin LD, Compagnone NA. 2001. Biosynthesis and action of neurosteroids. Brain Res Brain Res Rev [Internet] 37:3–12. Available from: http://www.ncbi.nlm.nih.gov/pubmed/11744070

Melman YF, Shah R, Das S. 2014. MicroRNAs in heart failure: is the picture becoming less miRky? Circ Heart Fail [Internet] 7:203–14. Available from: http://www.ncbi.nlm.nih.gov/pubmed/24449811

Meng Z, Moroishi T, Guan K-L. 2016. Mechanisms of Hippo pathway regulation. Genes Dev [Internet] 30:1–17. Available from: http://www.ncbi.nlm.nih.gov/pubmed/26728553

Meng Z, Moroishi T, Mottier-Pavie V, Plouffe SW, Hansen CG, Hong AW, Park HW, Mo J-S, Lu W, Lu S, Flores F, Yu F-X, Halder G, Guan K-L. 2015. MAP4K family kinases act in parallel to MST1/2 to activate LATS1/2 in the Hippo pathway. Nat Commun [Internet] 6:8357. Available from: http://www.ncbi.nlm.nih.gov/pubmed/26437443

Michailov G V, Sereda MW, Brinkmann BG, Fischer TM, Haug B, Birchmeier C, Role L, Lai C, Schwab MH, Nave K-A. 2004. Axonal neuregulin-1 regulates myelin sheath thickness. Science [Internet] 304:700–3. Available from: http://www.ncbi.nlm.nih.gov/pubmed/15044753

Mirsky R, Woodhoo A, Parkinson DB, Arthur-Farraj P, Bhaskaran A, Jessen KR. 2008. Novel signals controlling embryonic Schwann cell development, myelination and dedifferentiation. In: Journal of the Peripheral Nervous System. Vol. 13. . p 122–135.

Mogha A, Benesh AE, Patra C, Engel FB, Schöneberg T, Liebscher I, Monk KR. 2013. Gpr126 functions in Schwann cells to control differentiation and myelination via G-protein activation. J Neurosci [Internet] 33:17976–85. Available from: http://www.ncbi.nlm.nih.gov/pubmed/24227709

Monk KR, Feltri ML, Taveggia C. 2015. New insights on schwann cell development. Glia 63:1376–1393.

Morris K V, Chan SW-L, Jacobsen SE, Looney DJ. 2004. Small interfering RNA-induced transcriptional gene silencing in human cells. Science [Internet] 305:1289–92. Available from: http://www.ncbi.nlm.nih.gov/pubmed/15297624

Morris ME, Di Costanzo GA, Fox S, Werman R. 1983. Depolarizing action of GABA (gamma-aminobutyric acid) on myelinated fibers of peripheral nerves. Brain Res [Internet] 278:117–26. Available from: http://www.ncbi.nlm.nih.gov/pubmed/6640304

Morrison H, Sherman LS, Legg J, Banine F, Isacke C, Haipek CA, Gutmann DH, Ponta H, Herrlich P. 2001. The NF2 tumor suppressor gene product, merlin, mediates contact inhibition of growth through interactions with CD44. Genes Dev [Internet] 15:968–80. Available from: http://www.ncbi.nlm.nih.gov/pubmed/11316791

Morrison H, Sperka T, Manent J, Giovannini M, Ponta H, Herrlich P. 2007. Merlin/neurofibromatosis type 2 suppresses growth by inhibiting the activation of Ras and Rac. Cancer Res 67:520–527.

Murthy A, Gonzalez-Agosti C, Cordero E, Pinney D, Candia C, Solomon F, Gusella J, Ramesh V. 1998. NHE-RF, a regulatory cofactor for Na(+)-H+ exchange, is a common interactor for merlin and ERM (MERM) proteins. J Biol Chem [Internet] 273:1273–6. Available from: http://www.ncbi.nlm.nih.gov/pubmed/9430655

Naef R, Suter U. 1998. Many facets of the peripheral myelin protein PMP22 in myelination and disease. Microsc Res Tech [Internet] 41:359–71. Available from: http://www.ncbi.nlm.nih.gov/pubmed/9672419

Namchuk M, Lindsay L, Turck CW, Kanaani J, Baekkeskov S. 1997. Phosphorylation of serine residues 3, 6, 10, and 13 distinguishes membrane anchored from soluble glutamic acid decarboxylase 65 and is restricted to glutamic acid decarboxylase 65alpha. J Biol Chem [Internet] 272:1548–57. Available from: http://www.ncbi.nlm.nih.gov/pubmed/8999827

Nave K-A, Salzer JL. 2006. Axonal regulation of myelination by neuregulin 1. Curr

Opin Neurobiol [Internet] 16:492–500. Available from: http://www.ncbi.nlm.nih.gov/pubmed/16962312

Ness JK, Snyder KM, Tapinos N. 2013. Lck tyrosine kinase mediates β1-integrin signalling to regulate Schwann cell migration and myelination. Nat Commun [Internet] 4:1912. Available from: http://www.pubmedcentral.nih.gov/articlerender.fcgi?artid=3674276&tool=pmcentrez&rendertype=abstract

Obremski VJ, Hall AM, Fernandez-Valle C. 1998. Merlin, the neurofibromatosis type 2 gene product, and beta1 integrin associate in isolated and differentiating Schwann cells. J Neurobiol [Internet] 37:487–501. Available from: http://www.ncbi.nlm.nih.gov/pubmed/9858254

Oguievetskaia K, Goutebroze L. 2006. [Cellular contacts in myelinated fibers of the peripheral nervous system]. J Soc Biol [Internet] 200:281–92. Available from: http://www.ncbi.nlm.nih.gov/pubmed/17652965

Okada M. 2012. Regulation of the SRC family kinases by Csk. Int J Biol Sci [Internet] 8:1385–97. Available from: http://www.ncbi.nlm.nih.gov/pubmed/23139636

Okada T, Lopez-Lago M, Giancotti FG. 2005. Merlin/NF-2 mediates contact inhibition of growth by suppressing recruitment of Rac to the plasma membrane. J Cell Biol [Internet] 171:361–71. Available from: http://www.ncbi.nlm.nih.gov/pubmed/16247032

Olsen RW, Wong EH, Stauber GB, Murakami D, King RG, Fischer JB. 1984. Biochemical properties of the GABA/barbiturate/benzodiazepine receptor-chloride ion channel complex. Adv Exp Med Biol [Internet] 175:205–19. Available from: http://www.ncbi.nlm.nih.gov/pubmed/6149674

Owens DF, Kriegstein AR. 2002. Is there more to GABA than synaptic inhibition? Nat Rev Neurosci [Internet] 3:715–27. Available from: http://www.ncbi.nlm.nih.gov/pubmed/12209120

Parkinson DB, Dong Z, Bunting H, Whitfield J, Meier C, Marie H, Mirsky R, Jessen KR. 2001. Transforming growth factor beta (TGFbeta) mediates Schwann cell death in vitro and in vivo: examination of c-Jun activation, interactions with survival signals, and the relationship of TGFbeta-mediated death to Schwann cell differentiation. J Neurosci [Internet] 21:8572–85. Available from: http://www.ncbi.nlm.nih.gov/pubmed/11606645

Passage E, Norreel JC, Noack-Fraissignes P, Sanguedolce V, Pizant J, Thirion X, Robaglia-Schlupp A, Pellissier JF, Fontés M. 2004. Ascorbic acid treatment corrects the phenotype of a mouse model of Charcot-Marie-Tooth disease. Nat Med [Internet] 10:396–401. Available from: http://www.ncbi.nlm.nih.gov/pubmed/15034573

Patte-Mensah C, Meyer L, Taleb O, Mensah-Nyagan AG. 2014. Potential role of allopregnanolone for a safe and effective therapy of neuropathic pain. Prog Neurobiol 113:70–78.

Pećina-Šlaus N. 2013. Merlin, the NF2 gene product. Pathol Oncol Res 19:365–373.

Pelton PD, Sherman LS, Rizvi TA, Marchionni MA, Wood P, Friedman RA, Ratner N. 1998. Ruffling membrane, stress fiber, cell spreading and proliferation abnormalities in human Schwannoma cells. Oncogene [Internet] 17:2195–209. Available from: http://www.ncbi.nlm.nih.gov/pubmed/9811451

Peltonen S, Alanne M, Peltonen J. 2013. Barriers of the peripheral nerve. Tissue barriers [Internet] 1:e24956. Available from: http://www.ncbi.nlm.nih.gov/pubmed/24665400

Perego C, di Cairano ES, Ballabio M, Magnaghi V. 2012. Neurosteroid allopregnanolone regulates EAAC1-mediated glutamate uptake and triggers actin changes in Schwann cells. J Cell Physiol 227:1740–1751.

Pereira JA, Baumann R, Norrmén C, Somandin C, Miehe M, Jacob C, Lühmann T, Hall-Bozic H, Mantei N, Meijer D, Suter U. 2010. Dicer in Schwann cells is required for myelination and axonal integrity. J Neurosci [Internet] 30:6763–75. Available from: http://www.ncbi.nlm.nih.gov/pubmed/20463238

Petrilli AM, Fernández-Valle C. 2016. Role of Merlin/NF2 inactivation in tumor biology. Oncogene [Internet] 35:537–48. Available from: http://www.ncbi.nlm.nih.gov/pubmed/25893302

Pinal CS, Tobin AJ. 1998. Uniqueness and redundancy in GABA production. Perspect Dev Neurobiol [Internet] 5:109–18. Available from: http://www.ncbi.nlm.nih.gov/pubmed/9777629

Plotkin SR, O'Donnell CC, Curry WT, Bove CM, MacCollin M, Nunes FP. 2011. Spinal ependymomas in neurofibromatosis Type 2: a retrospective analysis of 55 patients. J Neurosurg Spine [Internet] 14:543–7. Available from: http://www.ncbi.nlm.nih.gov/pubmed/21294614

Plouffe SW, Hong AW, Guan KL. 2015. Disease implications of the Hippo/YAP pathway. Trends Mol Med 21:212–222.

Poitelon Y, Lopez-Anido C, Catignas K, Berti C, Palmisano M, Williamson C, Ameroso D, Abiko K, Hwang Y, Gregorieff A, Wrana JL, Asmani M, Zhao R, Sim FJ, Wrabetz L, Svaren J, Feltri ML. 2016. YAP and TAZ control peripheral myelination and the expression of laminin receptors in Schwann cells. Nat Neurosci [Internet] 19:879–87. Available from: http://www.ncbi.nlm.nih.gov/pubmed/27273766

Poitelon Y, Nunes GD-F, Feltri ML. 2017. Myelinating cells can feel disturbances in the force. Oncotarget [Internet] 8:5680–5681. Available from: http://www.ncbi.nlm.nih.gov/pubmed/28031544

Poon CLC, Lin JI, Zhang X, Harvey KF. 2011. The sterile 20-like kinase Tao-1 controls tissue growth by regulating the Salvador-Warts-Hippo pathway. Dev Cell [Internet] 21:896–906. Available from: http://www.ncbi.nlm.nih.gov/pubmed/22075148

Poulikakos PI, Xiao G-H, Gallagher R, Jablonski S, Jhanwar SC, Testa JR. 2006. Re-expression of the tumor suppressor NF2/merlin inhibits invasiveness in mesothelioma cells and negatively regulates FAK. Oncogene [Internet] 25:5960–8. Available from: http://www.ncbi.nlm.nih.gov/pubmed/16652148

Praskova M, Khoklatchev A, Ortiz-Vega S, Avruch J. 2004. Regulation of the MST1 kinase by autophosphorylation, by the growth inhibitory proteins, RASSF1 and NORE1, and by Ras. Biochem J [Internet] 381:453–62. Available from: http://www.ncbi.nlm.nih.gov/pubmed/15109305

Praskova M, Xia F, Avruch J. 2008. MOBKL1A/MOBKL1B phosphorylation by MST1 and MST2 inhibits cell proliferation. Curr Biol [Internet] 18:311–21. Available from: http://www.ncbi.nlm.nih.gov/pubmed/18328708

Price GW, Kelly JS, Bowery NG. 1987. The location of GABAB receptor binding sites in mammalian spinal cord. Synapse [Internet] 1:530–8. Available from: http://www.ncbi.nlm.nih.gov/pubmed/2843995

Procacci P, Ballabio M, Castelnovo LF, Mantovani C, Magnaghi V, Landry M, Segalen B. 2012. GABA-B receptors in the PNS have a role in Schwann cells differentiation? Front Cell Neurosci [Internet] 6:68. Available from: http://www.ncbi.nlm.nih.gov/pubmed/23335881

Puia G, Ravazzini F, Castelnovo LF, Magnaghi V. 2015. PKCε and allopregnanolone: functional cross-talk at the GABAA receptor level. Front Cell Neurosci [Internet] 9:83. Available from: http://www.pubmedcentral.nih.gov/articlerender.fcgi?artid=4365694&tool=pmcentrez&rendertype=abstract

Puia G, Santi M, Vicini S, Pritchett DB, Purdy RH, Paul SM, Seeburg PH, Costa E. 1990. Neurosteroids act on recombinant human GABAA receptors. Neuron 4:759–765.

Quarles RH. 1997. Glycoproteins of myelin sheaths. J Mol Neurosci [Internet] 8:1–12. Available from: http://www.ncbi.nlm.nih.gov/pubmed/9061610

Quintes S, Brinkmann BG, Ebert M, Fröb F, Kungl T, Arlt FA, Tarabykin V, Huylebroeck D, Meijer D, Suter U, Wegner M, Sereda MW, Nave K-A. 2016. Zeb2 is essential for Schwann cell differentiation, myelination and nerve repair. Nat Neurosci [Internet] 19:1050–1059. Available from: http://www.ncbi.nlm.nih.gov/pubmed/27294512

Reddy DS. 2011. Role of anticonvulsant and antiepileptogenic neurosteroids in the pathophysiology and treatment of epilepsy. Front Endocrinol (Lausanne) [Internet] 2:38. Available from: http://www.ncbi.nlm.nih.gov/pubmed/22654805

Ridley AJ, Davis JB, Stroobant P, Land H. 1989. Transforming growth factors-beta 1 and beta 2 are mitogens for rat Schwann cells. J Cell Biol [Internet] 109:3419–24. Available from: http://www.ncbi.nlm.nih.gov/pubmed/2557356

Riemenschneider MJ, Perry A, Reifenberger G. 2006. Histological classification and molecular genetics of meningiomas. Lancet Neurol [Internet] 5:1045–54. Available from: http://www.ncbi.nlm.nih.gov/pubmed/17110285

Rivera C, Voipio J, Payne JA, Ruusuvuori E, Lahtinen H, Lamsa K, Pirvola U, Saarma M, Kaila K. 1999. The K+/Cl- co-transporter KCC2 renders GABA hyperpolarizing during neuronal maturation. Nature [Internet] 397:251–5. Available from: http://www.ncbi.nlm.nih.gov/pubmed/9930699

Roberts SA, Lloyd AC. 2012. Aspects of cell growth control illustrated by the Schwann cell. Curr Opin Cell Biol 24:852–857.

Rong R, Tang X, Gutmann DH, Ye K. 2004. Neurofibromatosis 2 (NF2) tumor suppressor merlin inhibits phosphatidylinositol 3-kinase through binding to PIKE-L. Proc Natl Acad Sci U S A [Internet] 101:18200–5. Available from: http://www.ncbi.nlm.nih.gov/pubmed/15598747

Roskoski R. 2005. Src kinase regulation by phosphorylation and dephosphorylation. Biochem Biophys Res Commun [Internet] 331:1–14. Available from: http://www.ncbi.nlm.nih.gov/pubmed/15845350

Roth FC, Draguhn A. 2012. GABA metabolism and transport: effects on synaptic efficacy. Neural Plast [Internet] 2012:805830. Available from: http://www.ncbi.nlm.nih.gov/pubmed/22530158

Rouleau GA, Merel P, Lutchman M, Sanson M, Zucman J, Marineau C, Hoang-Xuan K, Demczuk S, Desmaze C, Plougastel B. 1993. Alteration in a new gene encoding a putative membrane-organizing protein causes neuro-fibromatosis type

2. Nature [Internet] 363:515–21. Available from: http://www.ncbi.nlm.nih.gov/pubmed/8379998

Rowe JG, Radatz M, Walton L, Kemeny AA. 2002. Stereotactic radiosurgery for type 2 neurofibromatosis acoustic neuromas: patient selection and tumour size. Stereotact Funct Neurosurg [Internet] 79:107–16. Available from: http://www.ncbi.nlm.nih.gov/pubmed/12743432

Rupprecht R, Holsboer F. 1999. Neuroactive steroids: Mechanisms of action and neuropsychopharmacological perspectives. Trends Neurosci 22:410–416.

Sainz J, Huynh DP, Figueroa K, Ragge NK, Baser ME, Pulst SM. 1994. Mutations of the neurofibromatosis type 2 gene and lack of the gene product in vestibular schwannomas. Hum Mol Genet [Internet] 3:885–91. Available from: http://www.ncbi.nlm.nih.gov/pubmed/7951231

Saliev T, Mustapova Z, Kulsharova G, Bulanin D, Mikhalovsky S. 2014. Therapeutic potential of electromagnetic fields for tissue engineering and wound healing. Cell Prolif 47:485–493.

Salzer JL. 2015. Schwann cell myelination. Cold Spring Harb Perspect Biol 7.

Sanchez AM, Flamini MI, Genazzani AR, Simoncini T. 2013. Effects of progesterone and medroxyprogesterone on actin remodeling and neuronal spine formation. Mol Endocrinol [Internet] 27:693–702. Available from: http://www.ncbi.nlm.nih.gov/pubmed/23487486

Sanchez AM, Flamini MI, Zullino S, Gopal S, Genazzani AR, Simoncini T. 2011. Estrogen receptor-{alpha} promotes endothelial cell motility through focal adhesion kinase. Mol Hum Reprod [Internet] 17:219–26. Available from: http://www.ncbi.nlm.nih.gov/pubmed/21127007

Schaller MD, Hildebrand JD, Shannon JD, Fox JW, Vines RR, Parsons JT. 1994. Autophosphorylation of the focal adhesion kinase, pp125FAK, directs SH2-dependent binding of pp60src. Mol Cell Biol [Internet] 14:1680–8. Available from: http://www.ncbi.nlm.nih.gov/pubmed/7509446

Schulz A, Baader SL, Niwa-Kawakita M, Jung MJ, Bauer R, Garcia C, Zoch A, Schacke S, Hagel C, Mautner V-F, Hanemann CO, Dun X-P, Parkinson DB, Weis J, Schröder JM, Gutmann DH, Giovannini M, Morrison H. 2013. Merlin isoform 2 in neurofibromatosis type 2-associated polyneuropathy. Nat Neurosci [Internet] 16:426–33. Available from: http://www.ncbi.nlm.nih.gov/pubmed/23455610

Schulz A, Kyselyova A, Baader SL, Jung MJ, Zoch A, Mautner V-F, Hagel C, Morrison H. 2014a. Neuronal merlin influences ERBB2 receptor expression on Schwann cells through neuregulin 1 type III signalling. Brain [Internet] 137:420–32. Available from: http://www.ncbi.nlm.nih.gov/pubmed/24309211

Schulz A, Zoch A, Morrison H. 2014b. A neuronal function of the tumor suppressor protein merlin. Acta Neuropathol Commun [Internet] 2:82. Available from: http://www.ncbi.nlm.nih.gov/pubmed/25012216

Scoles DR, Huynh DP, Chen MS, Burke SP, Gutmann DH, Pulst SM. 2000. The neurofibromatosis 2 tumor suppressor protein interacts with hepatocyte growth factor-regulated tyrosine kinase substrate. Hum Mol Genet [Internet] 9:1567–74. Available from: http://www.ncbi.nlm.nih.gov/pubmed/10861283

Scoles DR, Huynh DP, Morcos PA, Coulsell ER, Robinson NG, Tamanoi F, Pulst SM. 1998. Neurofibromatosis 2 tumour suppressor schwannomin interacts with betaII-spectrin. Nat Genet [Internet] 18:354–9. Available from: http://www.ncbi.nlm.nih.gov/pubmed/9537418

Seddon HJ. 1942. A Classification of Nerve Injuries. Br Med J [Internet] 2:237–9. Available from: http://www.ncbi.nlm.nih.gov/pubmed/20784403

Sernagor E, Chabrol F, Bony G, Cancedda L. 2010. GABAergic control of neurite outgrowth and remodeling during development and adult neurogenesis: general rules and differences in diverse systems. Front Cell Neurosci [Internet] 4:11. Available from: http://www.ncbi.nlm.nih.gov/pubmed/20428495

Serrano A, Haddjeri N, Lacaille J-C, Robitaille R. 2006. GABAergic network activation of glial cells underlies hippocampal heterosynaptic depression. J

Neurosci [Internet] 26:5370–82. Available from: http://www.ncbi.nlm.nih.gov/pubmed/16707789

Shaw RJ, Paez JG, Curto M, Yaktine A, Pruitt WM, Saotome I, O'Bryan JP, Gupta V, Ratner N, Der CJ, Jacks T, McClatchey AI. 2001. The Nf2 tumor suppressor, merlin, functions in Rac-dependent signaling. Dev Cell [Internet] 1:63–72. Available from: http://www.ncbi.nlm.nih.gov/pubmed/11703924

Sher I, Hanemann CO, Karplus PA, Bretscher A. 2012. The tumor suppressor merlin controls growth in its open state, and phosphorylation converts it to a less-active more-closed state. Dev Cell [Internet] 22:703–5. Available from: http://www.ncbi.nlm.nih.gov/pubmed/22516197

Sherafat MA, Heibatollahi M, Mongabadi S, Moradi F, Javan M, Ahmadiani A. 2012. Electromagnetic field stimulation potentiates endogenous myelin repair by recruiting subventricular neural stem cells in an experimental model of white matter demyelination. J Mol Neurosci 48:144–153.

Sherman L, Xu HM, Geist RT, Saporito-Irwin S, Howells N, Ponta H, Herrlich P, Gutmann DH. 1997. Interdomain binding mediates tumor growth suppression by the NF2 gene product. Oncogene [Internet] 15:2505–9. Available from: http://www.ncbi.nlm.nih.gov/pubmed/9395247

Shin D, Shin J-Y, McManus MT, Ptácek LJ, Fu Y-H. 2009. Dicer ablation in oligodendrocytes provokes neuronal impairment in mice. Ann Neurol [Internet] 66:843–57. Available from: http://www.ncbi.nlm.nih.gov/pubmed/20035504

Sisken BF, Kanje M, Lundborg G, Herbst E, Kurtz W. 1989. Stimulation of rat sciatic nerve regeneration with pulsed electromagnetic fields. Brain Res 485:309–316.

Sorge LK, Levy BT, Maness PF. 1984. pp60c-src is developmentally regulated in the neural retina. Cell [Internet] 36:249–57. Available from: http://www.ncbi.nlm.nih.gov/pubmed/6198092

Sperfeld AD, Hein C, Schröder JM, Ludolph AC, Hanemann CO. 2002. Occurrence and characterization of peripheral nerve involvement in neurofibromatosis type

2. Brain [Internet] 125:996–1004. Available from: http://www.ncbi.nlm.nih.gov/pubmed/11960890

Steckelbroeck S, Watzka M, Reichelt R, Hans VH, Stoffel-Wagner B, Heidrich DD, Schramm J, Bidlingmaier F, Klingmüller D. 2001. Characterization of the 5alpha-reductase-3alpha-hydroxysteroid dehydrogenase complex in the human brain. J Clin Endocrinol Metab [Internet] 86:1324–31. Available from: http://www.ncbi.nlm.nih.gov/pubmed/11238528

Steiger JL, Bandyopadhyay S, Farb DH, Russek SJ. 2004. cAMP response element-binding protein, activating transcription factor-4, and upstream stimulatory factor differentially control hippocampal GABABR1a and GABABR1b subunit gene expression through alternative promoters. J Neurosci [Internet] 24:6115–26. Available from: http://www.ncbi.nlm.nih.gov/pubmed/15240803

Stemmer-Rachamimov AO, Xu L, Gonzalez-Agosti C, Burwick JA, Pinney D, Beauchamp R, Jacoby LB, Gusella JF, Ramesh V, Louis DN. 1997. Universal absence of merlin, but not other ERM family members, in schwannomas. Am J Pathol [Internet] 151:1649–54. Available from: http://www.ncbi.nlm.nih.gov/pubmed/9403715

Stewart HJ, Morgan L, Jessen KR, Mirsky R. 1993. Changes in DNA synthesis rate in the Schwann cell lineage in vivo are correlated with the precursor--Schwann cell transition and myelination. Eur J Neurosci [Internet] 5:1136–44. Available from: http://www.ncbi.nlm.nih.gov/pubmed/7506619

Sulaiman OAR, Gordon T. 2009. Role of chronic Schwann cell denervation in poor functional recovery after nerve injuries and experimental strategies to combat it. Neurosurgery [Internet] 65:A105-14. Available from: http://www.ncbi.nlm.nih.gov/pubmed/19927054

Sun C-X, Robb VA, Gutmann DH. 2002. Protein 4.1 tumor suppressors: getting a FERM grip on growth regulation. J Cell Sci [Internet] 115:3991–4000. Available from: http://www.ncbi.nlm.nih.gov/pubmed/12356905

Svaren J. 2014. MicroRNA and transcriptional crosstalk in myelinating glia.

Neurochem Int [Internet] 77:50–7. Available from: http://www.ncbi.nlm.nih.gov/pubmed/24979526

Syroid DE, Maycox PJ, Soilu-Hänninen M, Petratos S, Bucci T, Burrola P, Murray S, Cheema S, Lee KF, Lemke G, Kilpatrick TJ. 2000. Induction of postnatal schwann cell death by the low-affinity neurotrophin receptor in vitro and after axotomy. J Neurosci [Internet] 20:5741–7. Available from: http://www.ncbi.nlm.nih.gov/pubmed/10908614

Tabara H, Sarkissian M, Kelly WG, Fleenor J, Grishok A, Timmons L, Fire A, Mello CC. 1999. The rde-1 gene, RNA interference, and transposon silencing in C. elegans. Cell [Internet] 99:123–32. Available from: http://www.ncbi.nlm.nih.gov/pubmed/10535731

Taveggia C. 2016. Schwann cells-axon interaction in myelination. Curr Opin Neurobiol 39:24–29.

Taveggia C, Zanazzi G, Petrylak A, Yano H, Rosenbluth J, Einheber S, Xu X, Esper RM, Loeb JA, Shrager P, Chao M V, Falls DL, Role L, Salzer JL. 2005. Neuregulin-1 type III determines the ensheathment fate of axons. Neuron [Internet] 47:681–94. Available from: http://www.ncbi.nlm.nih.gov/pubmed/16129398

Tawk M, Makoukji J, Belle M, Fonte C, Trousson A, Hawkins T, Li H, Ghandour S, Schumacher M, Massaad C. 2011. Wnt/β-catenin signaling is an essential and direct driver of myelin gene expression and myelinogenesis. J Neurosci 31:3729–3742.

Thomas SM, Brugge JS. 1997. Cellular functions regulated by Src family kinases. Annu Rev Cell Dev Biol [Internet] 13:513–609. Available from: http://www.ncbi.nlm.nih.gov/pubmed/9442882

Todd AJ, Lochhead V. 1990. GABA-like immunoreactivity in type I glomeruli of rat substantia gelatinosa. Brain Res [Internet] 514:171–4. Available from: http://www.ncbi.nlm.nih.gov/pubmed/2357525

Topilko P, Schneider-Maunoury S, Levi G, Baron-Van Evercooren A, Chennoufi AB, Seitanidou T, Babinet C, Charnay P. 1994. Krox-20 controls myelination in the peripheral nervous system. Nature [Internet] 371:796–9. Available from: http://www.ncbi.nlm.nih.gov/pubmed/7935840

Torpy JM, Kincaid JL, Glass RM. 2008. JAMA patient page. Peripheral neuropathy. JAMA [Internet] 299:1096. Available from: http://www.ncbi.nlm.nih.gov/pubmed/18319421

Towers S, Princivalle A, Billinton A, Edmunds M, Bettler B, Urban L, Castro-Lopes J, Bowery NG. 2000. GABAB receptor protein and mRNA distribution in rat spinal cord and dorsal root ganglia. Eur J Neurosci [Internet] 12:3201–10. Available from: http://www.ncbi.nlm.nih.gov/pubmed/10998104

Trofatter JA, MacCollin MM, Rutter JL, Murrell JR, Duyao MP, Parry DM, Eldridge R, Kley N, Menon AG, Pulaski K. 1993. A novel moesin-, ezrin-, radixin-like gene is a candidate for the neurofibromatosis 2 tumor suppressor. Cell [Internet] 72:791–800. Available from: http://www.ncbi.nlm.nih.gov/pubmed/8453669

Vergnano AM, Schlichter R, Poisbeau P. 2007. PKC activation sets an upper limit to the functional plasticity of GABAergic transmission induced by endogenous neurosteroids. Eur J Neurosci [Internet] 26:1173–82. Available from: http://www.ncbi.nlm.nih.gov/pubmed/17767496

Viader A, Chang L-W, Fahrner T, Nagarajan R, Milbrandt J. 2011a. MicroRNAs modulate Schwann cell response to nerve injury by reinforcing transcriptional silencing of dedifferentiation-related genes. J Neurosci [Internet] 31:17358–69. Available from: http://www.ncbi.nlm.nih.gov/pubmed/22131398

Viader A, Chang L-WW, Fahrner T, Nagarajan R, Milbrandt J. 2011b. MicroRNAs modulate Schwann cell response to nerve injury by reinforcing transcriptional silencing of dedifferentiation-related genes. J Neurosci [Internet] 31:17358–17369. Available from: http://www.jneurosci.org/content/31/48/17358.full.pdf

Vogel KS, Klesse LJ, Velasco-Miguel S, Meyers K, Rushing EJ, Parada LF. 1999. Mouse tumor model for neurofibromatosis type 1. Science [Internet] 286:2176–9.

Available from: http://www.ncbi.nlm.nih.gov/pubmed/10591653

Waldvogel HJ, Faull RL, Jansen KL, Dragunow M, Richards JG, Mohler H, Streit P. 1990. GABA, GABA receptors and benzodiazepine receptors in the human spinal cord: an autoradiographic and immunohistochemical study at the light and electron microscopic levels. Neuroscience [Internet] 39:361–85. Available from: http://www.ncbi.nlm.nih.gov/pubmed/1965016

Wang J, Ren K-Y, Wang Y-H, Kou Y-H, Zhang P-X, Peng J-P, Deng L, Zhang H-B, Jiang B-G. 2015. Effect of active Notch signaling system on the early repair of rat sciatic nerve injury. Artif cells, nanomedicine, Biotechnol [Internet] 43:383–9. Available from: http://www.ncbi.nlm.nih.gov/pubmed/24866722

Wanner IB, Mahoney J, Jessen KR, Wood PM, Bates M, Bunge MB. 2006. Invariant mantling of growth cones by Schwann cell precursors characterize growing peripheral nerve fronts. Glia [Internet] 54:424–38. Available from: http://www.ncbi.nlm.nih.gov/pubmed/16886207

Webber C, Zochodne D. 2010. The nerve regenerative microenvironment: early behavior and partnership of axons and Schwann cells. Exp Neurol [Internet] 223:51–9. Available from: http://www.ncbi.nlm.nih.gov/pubmed/19501085

Webster HD, Martin R, O'Connell MF. 1973. The relationships between interphase Schwann cells and axons before myelination: a quantitative electron microscopic study. Dev Biol [Internet] 32:401–16. Available from: http://www.ncbi.nlm.nih.gov/pubmed/4789698

White JH, Wise A, Main MJ, Green A, Fraser NJ, Disney GH, Barnes AA, Emson P, Foord SM, Marshall FH. 1998. Heterodimerization is required for the formation of a functional GABA(B) receptor. Nature [Internet] 396:679–82. Available from: http://www.ncbi.nlm.nih.gov/pubmed/9872316

Wiszniewski W. [Neurofibromatosis type 2 (NF2)--classical example of a rare familial cancer syndrome]. Med Wieku Rozwoj [Internet] 3:47–54. Available from: http://www.ncbi.nlm.nih.gov/pubmed/10910638

Witzel C, Rohde C, Brushart TM. 2005. Pathway sampling by regenerating peripheral axons. J Comp Neurol [Internet] 485:183–90. Available from: http://www.ncbi.nlm.nih.gov/pubmed/15791642

Woodhoo A, Alonso MBD, Droggiti A, Turmaine M, D'Antonio M, Parkinson DB, Wilton DK, Al-Shawi R, Simons P, Shen J, Guillemot F, Radtke F, Meijer D, Feltri ML, Wrabetz L, Mirsky R, Jessen KR. 2009. Notch controls embryonic Schwann cell differentiation, postnatal myelination and adult plasticity. Nat Neurosci [Internet] 12:839–47. Available from: http://www.ncbi.nlm.nih.gov/pubmed/19525946

Woodhoo A, Sommer L. 2008. Development of the Schwann cell lineage: from the neural crest to the myelinated nerve. Glia [Internet] 56:1481–90. Available from: http://www.ncbi.nlm.nih.gov/pubmed/18803317

Wu LMN, Williams A, Delaney A, Sherman DL, Brophy PJ. 2012. Increasing internodal distance in myelinated nerves accelerates nerve conduction to a flat maximum. Curr Biol 22:1957–1961.

Xing Z, Chen HC, Nowlen JK, Taylor SJ, Shalloway D, Guan JL. 1994. Direct interaction of v-Src with the focal adhesion kinase mediated by the Src SH2 domain. Mol Biol Cell [Internet] 5:413–21. Available from: http://www.ncbi.nlm.nih.gov/pubmed/8054685

Xu HM, Gutmann DH. 1998. Merlin differentially associates with the microtubule and actin cytoskeleton. J Neurosci Res [Internet] 51:403–15. Available from: http://www.ncbi.nlm.nih.gov/pubmed/9486775

Yan JL, Zhou J, Ma HP, Ma XN, Gao YH, Shi WG, Fang QQ, Ren Q, Xian CJ, Chen KM. 2015. Pulsed electromagnetic fields promote osteoblast mineralization and maturation needing the existence of primary cilia. Mol Cell Endocrinol 404:132–140.

Yi C, Troutman S, Fera D, Stemmer-Rachamimov A, Avila JL, Christian N, Persson NL, Shimono A, Speicher DW, Marmorstein R, Holmgren L, Kissil JL. 2011. A tight junction-associated Merlin-angiomotin complex mediates Merlin's

regulation of mitogenic signaling and tumor suppressive functions. Cancer Cell [Internet] 19:527–40. Available from: http://www.ncbi.nlm.nih.gov/pubmed/21481793

Yin F, Yu J, Zheng Y, Chen Q, Zhang N, Pan D. 2013. Spatial organization of Hippo signaling at the plasma membrane mediated by the tumor suppressor Merlin/NF2. Cell [Internet] 154:1342–55. Available from: http://www.ncbi.nlm.nih.gov/pubmed/24012335

Yogesha SD, Sharff AJ, Giovannini M, Bricogne G, Izard T. 2011. Unfurling of the band 4.1, ezrin, radixin, moesin (FERM) domain of the merlin tumor suppressor. Protein Sci [Internet] 20:2113–20. Available from: http://www.ncbi.nlm.nih.gov/pubmed/22012890

Yokoyama T, Osada H, Murakami H, Tatematsu Y, Taniguchi T, Kondo Y, Yatabe Y, Hasegawa Y, Shimokata K, Horio Y, Hida T, Sekido Y. 2008. YAP1 is involved in mesothelioma development and negatively regulated by Merlin through phosphorylation. Carcinogenesis [Internet] 29:2139–46. Available from: http://www.ncbi.nlm.nih.gov/pubmed/18725387

Yoo NJ, Park SW, Lee SH. 2012. Mutational analysis of tumour suppressor gene NF2 in common solid cancers and acute leukaemias. Pathology [Internet] 44:29–32. Available from: http://www.ncbi.nlm.nih.gov/pubmed/22081132

Yu B, Zhou S, Wang Y, Qian T, Ding G, Ding F, Gu X. 2012. miR-221 and miR-222 promote Schwann cell proliferation and migration by targeting LASS2 after sciatic nerve injury. J Cell Sci 125:2675–2683.

Yun B, Anderegg A, Menichella D, Wrabetz L, Feltri ML, Awatramani R. 2010. MicroRNA-deficient Schwann cells display congenital hypomyelination. J Neurosci [Internet] 30:7722–8. Available from: http://www.ncbi.nlm.nih.gov/pubmed/20519547

Zagorodnyuk VP, D'Antona G, Brookes SJH, Costa M. 2002. Functional GABAB receptors are present in guinea pig nodose ganglion cell bodies but not in peripheral mechanosensitive endings. Auton Neurosci [Internet] 102:20–9.

Available from: http://www.ncbi.nlm.nih.gov/pubmed/12492132

Zhang J, Ji J-Y, Yu M, Overholtzer M, Smolen GA, Wang R, Brugge JS, Dyson NJ, Haber DA. 2009. YAP-dependent induction of amphiregulin identifies a non-cell-autonomous component of the Hippo pathway. Nat Cell Biol [Internet] 11:1444–50. Available from: http://www.ncbi.nlm.nih.gov/pubmed/19935651

Zhang N, Bai H, David KK, Dong J, Zheng Y, Cai J, Giovannini M, Liu P, Anders RA, Pan D. 2010. The Merlin/NF2 tumor suppressor functions through the YAP oncoprotein to regulate tissue homeostasis in mammals. Dev Cell [Internet] 19:27–38. Available from: http://www.ncbi.nlm.nih.gov/pubmed/20643348

Zhao B, Li L, Tumaneng K, Wang C-Y, Guan K-L. 2010a. A coordinated phosphorylation by Lats and CK1 regulates YAP stability through SCF(beta-TRCP). Genes Dev [Internet] 24:72–85. Available from: http://www.ncbi.nlm.nih.gov/pubmed/20048001

Zhao B, Wei X, Li W, Udan RS, Yang Q, Kim J, Xie J, Ikenoue T, Yu J, Li L, Zheng P, Ye K, Chinnaiyan A, Halder G, Lai Z-C, Guan K-L. 2007. Inactivation of YAP oncoprotein by the Hippo pathway is involved in cell contact inhibition and tissue growth control. Genes Dev [Internet] 21:2747–61. Available from: http://www.ncbi.nlm.nih.gov/pubmed/17974916

Zhao B, Ye X, Yu J, Li L, Li W, Li S, Yu J, Lin JD, Wang C-Y, Chinnaiyan AM, Lai Z-C, Guan K-L. 2008. TEAD mediates YAP-dependent gene induction and growth control. Genes Dev [Internet] 22:1962–71. Available from: http://www.ncbi.nlm.nih.gov/pubmed/18579750

Zhao X, He X, Han X, Yu Y, Ye F, Chen Y, Hoang T, Xu X, Mi Q-SS, Xin M, Wang F, Appel B, Lu QR. 2010b. MicroRNA-mediated control of oligodendrocyte differentiation. Neuron [Internet] 65:612–26. Available from: http://www.ncbi.nlm.nih.gov/pubmed/20223198

Zhao YL, Takagawa K, Oya T, Yang HF, Gao ZY, Kawaguchi M, Ishii Y, Sasaoka T, Owada K, Furuta I, Sasahara M. 2003. Active Src expression is induced after rat peripheral nerve injury. Glia [Internet] 42:184–193. Available from:

http://www.ncbi.nlm.nih.gov/pubmed/12655602

Zheng S, Huang J, Zhou K, Xiang Q, Zhang Y, Tan Z, Simoncini T, Fu X, Wang T. 2012. Progesterone enhances vascular endothelial cell migration via activation of focal adhesion kinase. J Cell Mol Med 16:296–305.

Zhou D, Conrad C, Xia F, Park J-S, Payer B, Yin Y, Lauwers GY, Thasler W, Lee JT, Avruch J, Bardeesy N. 2009. Mst1 and Mst2 maintain hepatocyte quiescence and suppress hepatocellular carcinoma development through inactivation of the Yap1 oncogene. Cancer Cell [Internet] 16:425–38. Available from: http://www.ncbi.nlm.nih.gov/pubmed/19878874